

**5<sup>th</sup>**  
EDITION

Enhanced  
**DIGITAL  
VERSION**  
Included

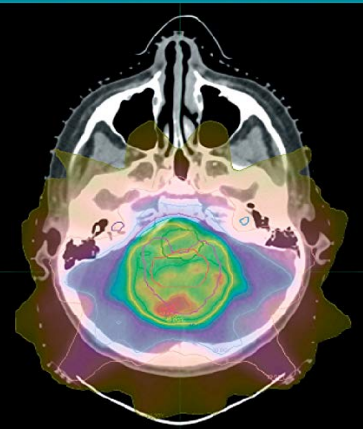
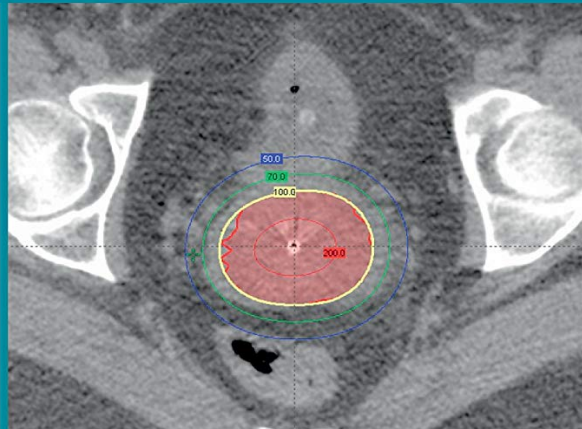
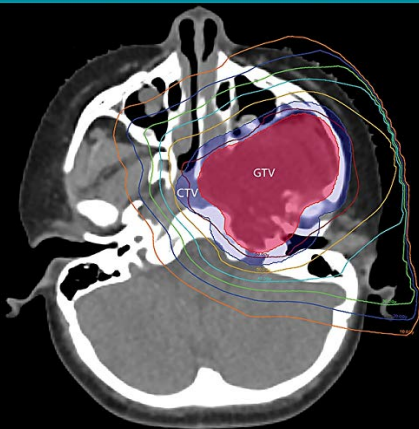
*Gunderson & Tepper's*

# CLINICAL RADIATION ONCOLOGY

JOEL E. **TEPPER**

ROBERT L. **FOOTE**

JEFF M. **MICHALSKI**



---

## ASSOCIATE EDITORS

### **Jeffrey A. Bogart, MD**

Professor and Chair  
Department of Radiation Oncology  
SUNY Upstate Medical University  
Syracuse, New York

### **Minesh P. Mehta, MBChB, FASTRO**

Professor and Chair  
Department of Radiation Oncology  
FIU Herbert Wertheim College of Medicine  
Deputy Director and Chief  
Miami Cancer Institute  
Baptist Health South Florida  
Miami, Florida

### **Andrea K. Ng, MD, MPH**

Professor  
Department of Radiation Oncology  
Harvard Medical School  
Dana-Farber Cancer Institute  
Brigham and Women's Hospital  
Boston, Massachusetts

### **Abram Recht, MD**

Professor  
Department of Radiation Oncology  
Harvard Medical School  
Vice Chair  
Department of Radiation Oncology  
Beth Israel Deaconess Medical Center  
Boston, Massachusetts

### **Christopher L. Tinkle, MD, PhD**

Assistant Member  
Department of Radiation Oncology  
St. Jude Children's Research Hospital  
Memphis, Tennessee

### **Akila N. Viswanathan, MD, MPH**

Professor  
Department of Radiation Oncology and Molecular Radiation Sciences  
Johns Hopkins University School of Medicine  
Baltimore, Maryland

**5<sup>th</sup>**  
EDITION

***Gunderson & Tepper's***

# CLINICAL RADIATION ONCOLOGY

---

## SENIOR EDITORS

**Joel E. Tepper, MD, FASTRO**

Hector MacLean Distinguished Professor of Cancer Research  
Department of Radiation Oncology  
University of North Carolina Lineberger Comprehensive Cancer Center  
University of North Carolina School of Medicine  
Chapel Hill, North Carolina

**Robert L. Foote, MD, FACR, FASTRO**

Hitachi Professor of Radiation Oncology Research  
Department of Radiation Oncology  
Mayo Clinic College of Medicine and Science, Mayo Clinic  
Rochester, Minnesota

**Jeff M. Michalski, MD, MBA, FACR, FASTRO**

Carlos A. Perez Distinguished Professor  
Vice Chair of Radiation Oncology  
Washington University School of Medicine in St. Louis  
St. Louis, Missouri



Elsevier  
1600 John F. Kennedy Blvd.  
Ste. 1600  
Philadelphia, PA 19103-2899

GUNDERSON & TEPPER'S CLINICAL RADIATION ONCOLOGY,  
FIFTH EDITION  
Copyright © 2021 by Elsevier Inc. All rights reserved.

ISBN: 978-0-323-67246-7

No part of this publication may be reproduced or transmitted in any form or by any means, electronic or mechanical, including photocopying, recording, or any information storage and retrieval system, without permission in writing from the publisher. Details on how to seek permission, further information about the Publisher's permissions policies, and our arrangements with organizations such as the Copyright Clearance Center and the Copyright Licensing Agency can be found at our website: [www.elsevier.com/permissions](http://www.elsevier.com/permissions).

This book and the individual contributions contained in it are protected under copyright by the Publisher (other than as may be noted herein).

#### Notices

Knowledge and best practice in this field are constantly changing. As new research and experience broaden our understanding, changes in research methods, professional practices, or medical treatment may become necessary. Practitioners and researchers must always rely on their own experience and knowledge in evaluating and using any information, methods, compounds, or experiments described herein. In using such information or methods they should be mindful of their own safety and the safety of others, including parties for whom they have a professional responsibility. With respect to any drug or pharmaceutical products identified, readers are advised to check the most current information provided (i) on procedures featured or (ii) by the manufacturer of each product to be administered, to verify the recommended dose or formula, the method and duration of administration, and contraindications. It is the responsibility of practitioners, relying on their own experience and knowledge of their patients, to make diagnoses, to determine dosages and the best treatment for each individual patient, and to take all appropriate safety precautions. To the fullest extent of the law, neither the Publisher nor the authors, contributors, or editors, assume any liability for any injury and/or damage to persons or property as a matter of products liability, negligence or otherwise, or from any use or operation of any methods, products, instructions, or ideas contained in the material herein.

*The Publisher*

Previous editions copyrighted © 2014, 2008, 2001, 1995, 1988, 1983 by Saunders and Churchill Livingstone, imprints of Elsevier Inc.

Library of Congress Control Number: 2019949699

Executive Content Strategist: Robin Carter  
Senior Content Development Specialist: Anne Snyder  
Publishing Services Manager: Catherine Jackson  
Senior Project Manager: John Casey  
Book Designer: Patrick Ferguson

Printed in China

9 8 7 6 5 4 3 2 1



To my wife Laurie, for her support and for teaching me what is important in life, and who has made me a better person;  
and to my family, including Miriam, Adam, Abigail, Agustin, Zekariah, Zohar, Sammy, Marcelo, Jonah, and Aurelio for the love and support they have given me for many years.  
To my parents, who taught me the importance of education, learning, and doing that which should be done.  
To my many mentors who taught me in the past and those who continue to teach me.  
To my professional colleagues, both at the University of North Carolina and around the country, who have made me a better physician.

### **JET**

To Kally, who, during our 40 years of marriage, has made innumerable, selfless, personal sacrifices for my patients and for my professional career.  
To my father, Leonard, who introduced me to the art, science, and practice of medicine.  
To John Earle, Len Gunderson and John Noseworthy. Their mentorship has enriched my professional life with experiences, opportunities, and growth beyond my wildest dreams.  
To the Mayo Clinic for providing a patient-centered, collegial, cooperative, compassionate, respectful, scholarly, integrated, professional, innovative, and healing environment in which to work and serve.

### **RLF**

To Sheila, my loving wife of 31 years, for her steadfast support of my career and academic endeavors while also encouraging me to enjoy life with our family.  
To our children, Basia, Sophie, and Jeffrey, who have enriched my life with their love and support.  
To my parents, Richard and Rita, who both faced their own challenges of cancer therapy and taught me perspectives of care that you don't get in medical school.  
To my mentors, especially Drs. Jim Cox and Larry Kun, who we lost this past year during the development of this new edition. They inspired me to reach higher.  
And finally, to my colleagues at Washington University in St. Louis who have patiently given me the time and support to contribute to this work.

### **JMM**

# CONTRIBUTORS

**Christopher D. Abraham, MD**

Assistant Professor  
Department of Radiation Oncology  
Washington University School of Medicine  
in St. Louis  
St. Louis, Missouri

**Ross A. Abrams, MD**

Department of Radiation Oncology  
Rush University Medical Center  
Chicago, Illinois

**Ayda Al-Awadhi, MBBS**

Department of Cancer Medicine  
University of Texas MD Anderson Cancer  
Center  
Houston, Texas

**Kaled M. Alektiar, MD**

Member  
Department of Radiation Oncology  
Memorial Sloan Kettering Cancer Center  
New York, New York

**Jan Alsner, PhD**

Professor  
Department of Experimental Clinical  
Oncology  
Aarhus University Hospital  
Aarhus, Denmark

**K. Kian Ang, MD, PhD<sup>†</sup>**

Professor and Gilbert H. Fletcher Endowed  
Chair  
Department of Radiation Oncology  
University of Texas MD Anderson Cancer  
Center  
Houston, Texas

**Lilyana Angelov, MD, FAANS, FRCS(C)**

The Kerscher Family Chair for Spine Tumor  
Excellence  
Head, Section of Spine Tumors  
Professor, Department of Neurological  
Surgery  
Cleveland Clinic Lerner College of Medicine  
at Case Western Reserve University  
Rose Ella Burkhart Brain Tumor and Neuro-  
Oncology Center  
Department of Neurosurgery  
Neurological Institute and Taussig Cancer  
Institute  
Cleveland Clinic  
Cleveland, Ohio

**Jonathan B. Ashman, MD, PhD**

Assistant Professor  
Department of Radiation Oncology  
Mayo Clinic College of Medicine and Science  
Phoenix, Arizona

**Matthew T. Ballo, MD**

Professor  
Radiation Oncology  
West Cancer Center and Research Institute  
Memphis, Tennessee

**Lucia Baratto, MD**

Research Fellow  
Department of Radiology  
Division of Nuclear Medicine and Molecular  
Imaging  
Stanford University  
Stanford, California

**Christopher Andrew Barker, MD**

Radiation Oncologist  
Director of Clinical Investigation  
Department of Radiation Oncology  
Memorial Sloan Kettering Cancer Center  
New York, New York

**Adam Bass, MD**

Associate Professor of Medicine  
Dana-Farber Cancer Institute  
Harvard Medical School  
Boston, Massachusetts

**Brian C. Baumann, MD**

Assistant Professor  
Department of Radiation Oncology  
Washington University School of Medicine  
in St. Louis  
St. Louis, Missouri

**Beth M. Beadle MD, PhD**

Associate Professor  
Department of Radiation Oncology  
Stanford University  
Stanford, California

**Staci Beamer, MD**

Assistant Professor  
Division of Cardiovascular and Thoracic  
Surgery  
Mayo Clinic College of Medicine and Science  
Phoenix, Arizona

**Philippe L. Bedard, MD, FRCPC**

Medical Oncologist  
Princess Margaret Cancer Centre  
Associate Professor  
Department of Medicine  
University of Toronto  
Toronto, Ontario, Canada

**Jonathan J. Beitler, MD, MBA, FACR, FASTRO**

Professor  
Departments of Radiation Oncology,  
Otolaryngology, and Hematology and  
Medical Oncology  
Emory University School of Medicine  
Georgia Research Alliance Clinical Scientist  
Winship Cancer Institute of Emory  
University  
NRG Institutional Principal Investigator  
Atlanta, Georgia

**Sushil Beriwal, MD, MBA**

Professor  
Department of Radiation Oncology  
UPMC Hillman Cancer Center  
University of Pittsburgh School of Medicine  
Pittsburgh, Pennsylvania

**Ranjit S. Bindra, MD, PhD**

Associate Professor  
Therapeutic Radiology  
Yale Medical School  
New Haven, Connecticut

**Michael W. Bishop, MD**

Assistant Member  
Department of Oncology  
St. Jude Children's Research Hospital  
Memphis, Tennessee

**Rachel Blitzblau, MD, PhD**

Associate Professor  
Department of Radiation Oncology  
Duke University Medical Center  
Durham, North Carolina

**Jeffrey A. Bogart, MD**

Professor and Chair  
Department of Radiation Oncology  
SUNY Upstate Medical University  
Syracuse, New York

**James A. Bonner, MD**

Chairman and Merle M. Salter Professor  
Department of Radiation Oncology  
The University of Alabama at Birmingham  
Birmingham, Alabama

<sup>†</sup>Deceased



**J. Daniel Bourland, PhD, MSPH**

Professor  
Radiation Oncology, Biomedical  
Engineering, and Physics  
Wake Forest School of Medicine  
Winston-Salem, North Carolina

**Joseph A. Bovi, MD**

Department of Radiation Oncology  
Medical College of Wisconsin  
Froedtert Memorial Lutheran Hospital  
Milwaukee, Wisconsin

**Andrew G. Brandmaier, MD, PhD**

Assistant Professor  
Department of Radiation Oncology  
Weill Cornell Medical College  
New York, New York

**John Breneman, MD**

Professor  
Department of Radiation Oncology  
University of Cincinnati  
Cincinnati Children's Hospital Medical  
Center  
Cincinnati, Ohio

**Juan P. Brito, MD**

Assistant Professor of Medicine  
Division of Endocrinology, Diabetes,  
Metabolism, and Nutrition  
Mayo Clinic College of Medicine and  
Science, Mayo Clinic  
Rochester, Minnesota

**Michael D. Brundage, MD, MSc, FRCPC**

Professor  
Oncology and Public Health Sciences  
Queen's University  
Radiation Oncologist  
Cancer Centre of Southeastern Ontario  
Kingston, Ontario, Canada

**Matthew R. Callstrom, MD, PhD**

Professor of Radiology  
Mayo Clinic College of Medicine and  
Science, Mayo Clinic  
Rochester, Minnesota

**Felipe A. Calvo, MD, PhD**

Professor and Chairman  
Department of Oncology  
Clinica Universidad de Navarra  
Madrid, Spain

**George M. Cannon, MD**

Adjunct Assistant Professor  
Radiation Oncology  
University of Utah  
Salt Lake City, Utah

**Bruce A. Chabner, MD**

Clinical Director, Emeritus  
Massachusetts General Hospital Cancer  
Center  
Massachusetts General Hospital  
Professor of Medicine  
Harvard Medical School  
Boston, Massachusetts

**Michael D. Chan, MD**

Associate Professor and Vice Chairman  
Department of Radiation Oncology  
Wake Forest School of Medicine  
Winston-Salem, North Carolina

**Samuel T. Chao, MD**

Associate Professor  
Department of Radiation Oncology  
Rose Ella Burkhardt Brain Tumor and  
Neuro-Oncology Center  
Cleveland Clinic  
Cleveland, Ohio

**Anne-Marie Charpentier, MD, FRCPC**

Radiation Oncologist  
Centre Hospitalier de l'Université de  
Montréal  
Clinical Assistant Professor  
Université de Montréal  
Montréal, Quebec, Canada

**Aadel A. Chaudhuri, MD**

Assistant Professor  
Department of Radiation Oncology  
Washington University School of Medicine  
in St. Louis  
St. Louis, Missouri

**Nathan I. Cherny, MBBS, FRACP, FRCP**

Norman Levan Chair of Humanistic  
Medicine  
Cancer Pain and Palliative Medicine Service  
Shaare Zedek Medical Center  
Jerusalem, Israel

**Fumiko Chino, MD**

Assistant Professor  
Department of Radiation Oncology  
Memorial Sloan Kettering Cancer Center  
New York, New York

**John P. Christodouleas, MD, MPH**

Attending Physician  
Department of Radiation Oncology  
University of Pennsylvania  
Philadelphia, Pennsylvania

**Stephen G. Chun, MD**

Assistant Professor  
Department of Radiation Oncology  
The University of Texas MD Anderson  
Cancer Center  
Houston, Texas

**Christine H. Chung, MD**

Chair, Department of Head and Neck–  
Endocrine Oncology  
Moffitt Cancer Center  
Tampa, Florida

**Peter W. M. Chung, MBChB, MRCP, FRCR, FRCPC**

Radiation Oncologist  
Princess Margaret Cancer Centre  
Associate Professor  
Department of Radiation Oncology  
University of Toronto  
Toronto, Ontario, Canada

**Jeffrey M. Clarke, MD**

Assistant Professor  
Department of Medicine  
Division of Medical Oncology  
Duke University School of Medicine  
Durham, North Carolina

**Louis S. Constine, MD, FASTRO, FACR**

The Philip Rubin Professor of Radiation  
Oncology and Pediatrics  
Vice Chair, Department of Radiation  
Oncology  
James P. Wilmot Cancer Center  
University of Rochester Medical Center  
The Judy DiMarzo Cancer Survivorship  
Program  
James P. Wilmot Cancer Institute  
University of Rochester Medical Center  
Rochester, New York

**Benjamin W. Corn, MD**

Chairman  
Department of Radiation Medicine  
Shaare Zedek Medical Center  
Jerusalem, Israel;  
Professor  
Tel Aviv University School of Medicine  
Tel Aviv, Israel

**Allan Covens, MD, FRCSC**

Professor  
Department of Obstetrics and Gynecology  
Division of Gynecologic Oncology  
Sunnybrook Health Sciences Centre  
University of Toronto  
Toronto, Ontario, Canada

**Christopher H. Crane, MD**

Department of Radiation Oncology  
Memorial Sloan Kettering Cancer Center  
New York, New York

**Carien L. Creutzberg, MD, PhD**

Professor  
Department of Radiation Oncology  
Leiden University Medical Center  
Leiden, Netherlands

**Juanita M. Crook, MD, FRCP**

Professor  
Department of Radiation Oncology  
University of British Columbia  
Radiation Oncologist  
Center for the Southern Interior  
British Columbia Cancer Agency  
Kelowna, British Columbia, Canada

**Brian G. Czito, MD**

Professor  
Department of Radiation Oncology  
Duke Cancer Institute  
Duke University  
Durham, North Carolina

**Bouthaina S. Dabaja, MD**

Professor  
Section Chief, Hematology  
Department of Radiation Oncology  
University of Texas MD Anderson Cancer  
Center  
Houston, Texas

**Thomas B. Daniels, MD**

Department of Radiation Oncology  
Mayo Clinic Arizona  
Assistant Professor of Radiation Oncology  
Mayo Clinic College of Medicine and Science  
Phoenix, Arizona

**Marc David, MD**

Assistant Professor  
Department of Radiation Oncology  
McGill University Health Centre  
Montreal, Quebec, Canada

**Laura A. Dawson, MD**

Professor  
Department of Radiation Oncology  
Princess Margaret Cancer Centre  
University of Toronto  
Toronto, Ontario, Canada

**Ryan W. Day, MD**

Instructor of Surgery  
Mayo Clinic  
Scottsdale, Arizona;  
Senior Fellow  
Department of Surgical Oncology  
University of Texas MD Anderson Cancer  
Center  
Houston, Texas

**Amanda J. Deisher, PhD**

Instructor  
Department of Radiation Oncology  
Mayo Clinic College of Medicine and  
Science, Mayo Clinic  
Rochester, Minnesota

**Thomas F. DeLaney, MD**

Andres Soriano Professor of Radiation  
Oncology  
Harvard Medical School  
Associate Medical Director  
Francis H. Burr Proton Therapy Center  
Massachusetts General Hospital  
Boston, Massachusetts

**Phillip M. Devlin, BPhil, MTS, EdM, MD, FACR, FASTRO, FFRSOCI (Hon)**

Chief, Division of Brachytherapy  
Dana-Farber/Brigham and Women's Cancer  
Center  
Associate Professor of Radiation Oncology  
Harvard Medical School  
Institute Physician  
Dana-Farber Cancer Institute  
Boston, Massachusetts

**James J. Dignam, PhD**

Professor  
Department of Public Health Sciences  
University of Chicago  
Chicago, Illinois  
Statistics and Data Management Center  
NRG Oncology

**Don S. Dizon, MD**

Associate Professor  
Warren Alpert Medical School of Brown  
University  
Head of Women's Cancers at Lifespan  
Cancer Institute  
Director of Medical Oncology  
Rhode Island Hospital  
Providence, Rhode Island

**Jeffrey S. Dome, MD, PhD**

Chief  
Hematology and Oncology  
Children's National Health System  
Washington, DC

**Hugues Duffau, MD, PhD**

Professor and Chairman  
Montpellier University Medical Center  
Institute for Neurosciences of Montpellier  
Hôpital Gui de Chauliac  
Montpellier, France

**Thierry Duprez, MD**

Medical Imaging and Radiology  
Universite Catholique de Louvain  
Head of Neurology/Head and Neck Section  
Cliniques Universitaires Saint-Luc  
Brussels, Belgium

**Peter T. Dziegielewski, MD, FRCS(C)**

Associate Professor  
Chief, Division of Head and Neck Oncologic  
Surgery  
Microvascular Reconstructive Surgery  
Kenneth W. Grader Professor  
University of Florida College of Medicine  
Gainesville, Florida

**Charles Eberhart, MD, PhD**

Professor  
Pathology, Ophthalmology, and Oncology  
Johns Hopkins University School of  
Medicine  
Baltimore, Maryland

**David W. Eisele, MD, FACS**

Andelot Professor and Director  
Department of Otolaryngology—Head and  
Neck Surgery  
Johns Hopkins University School of  
Medicine  
Baltimore, Maryland

**Suzanne B. Evans, MD, MPH**

Associate Professor, Therapeutic Radiology  
Associate Director, Residency Program  
Yale University School of Medicine  
New Haven, Connecticut

**Michael Farris, MD**

Assistant Professor  
Department of Radiation Oncology  
Wake Forest Baptist Health  
Winston-Salem, North Carolina

**Mary Feng, MD**

Professor  
Department of Radiation Oncology  
University of California, San Francisco  
San Francisco, California

**Rui P. Fernandes, MD, DMD, FACS, FRCS(Ed)**

Associate Professor  
OMS, Neurosurgery, Orthopedics, Surgery  
University of Florida College of Medicine  
Jacksonville, Florida



**Gini F. Fleming, MD**

Professor  
Department of Medicine  
University of Chicago Medical Center  
Chicago, Illinois

**John C. Flickinger, MD**

Professor  
Department of Radiation Oncology  
University of Pittsburgh  
Radiation Oncologist  
Department of Radiation Oncology  
UPMC Presbyterian-Shadyside  
Pittsburgh, Pennsylvania

**Robert L. Foote, MD, FACR, FASTRO**

Hitachi Professor of Radiation Oncology  
Research  
Department of Radiation Oncology  
Mayo Clinic College of Medicine and  
Science, Mayo Clinic  
Rochester, Minnesota

**Silvia C. Formenti, MD**

Sandra and Edward Meyer Professor of  
Cancer Research  
Chairman, Department of Radiation  
Oncology  
Associate Director, Meyer Cancer Institute  
Weill Cornell Medical College  
Radiation Oncologist in Chief  
New York Presbyterian Hospital  
New York, New York

**Benedick A. Fraass, PhD, FAAPM, FASTRO, FACR**

Vice Chair for Research, Professor and  
Director of Medical Physics  
Department of Radiation Oncology  
Cedars-Sinai Medical Center  
Health Sciences Professor  
Department of Radiation Oncology  
University of California, Los Angeles  
Los Angeles, California;  
Professor Emeritus  
Department of Radiation Oncology  
University of Michigan  
Ann Arbor, Michigan

**Carolyn R. Freeman, MBBS, FRCPC, FASTRO**

Professor of Oncology and Pediatrics  
Mike Rosenbloom Chair of Radiation  
Oncology  
McGill University  
Montreal, Quebec, Canada

**Adam S. Garden, MD**

Professor  
Department of Radiation Oncology  
University of Texas MD Anderson Cancer  
Center  
Houston, Texas

**Lilian T. Gien, MD**

Associate Professor  
Division of Gynecologic Oncology  
Odette Cancer Center  
Sunnybrook Health Sciences Centre  
Toronto, Ontario, Canada

**Mary K. Gospodarowicz, MD, FRCPC, FRCR (Hon)**

Professor and Chair  
Department of Radiation Oncology  
University of Toronto  
Princess Margaret Hospital  
Toronto, Ontario, Canada

**Cai Grau, MD, DMSc**

Professor  
Department of Oncology and Danish Centre  
for Particle Therapy  
Aarhus University Hospital  
Aarhus, Denmark

**Vincent Grégoire, MD, PhD, FRCR**

Radiation Oncology Department  
Centre Léon Bérard  
Lyon, France

**Chul S. Ha, MD**

Professor  
Department of Radiation Oncology  
University of Texas Health Science Center at  
San Antonio  
San Antonio, Texas

**Michael G. Haddock, MD**

Professor of Radiation Oncology  
Mayo Clinic College of Medicine and  
Science, Mayo Clinic  
Rochester, Minnesota

**Ezra Hahn, MD, FRCPC**

Radiation Oncologist  
Department of Radiation Oncology  
Princess Margaret Cancer Centre  
Sunnybrook Health Sciences Centre of the  
University of Toronto  
Toronto, Ontario, Canada

**Matthew D. Hall, MD, MBA**

Radiation Oncology  
Miami Cancer Institute  
Baptist Health South Florida  
Miami, Florida

**Dennis E. Hallahan, MD**

Elizabeth H. and James S. McDonnell  
Distinguished Professor of Medicine  
Chair, Department of Radiation Oncology  
Washington University School of Medicine  
in St. Louis  
Barnes Jewish Hospital  
St. Louis, Missouri

**Christopher L. Hallemeier, MD**

Associate Professor  
Department of Radiation Oncology  
Mayo Clinic College of Medicine and  
Science, Mayo Clinic  
Rochester, Minnesota

**Michele Y. Halyard, MD**

Professor  
Department of Radiation Oncology  
Mayo Clinic College of Medicine and  
Science, Mayo Clinic  
Phoenix, Arizona

**Marc Hamoir, MD**

Head and Neck Surgery  
Chairman of the Executive Board of the  
Cancer Center  
Saint-Luc University Hospital Cancer Center  
Brussels, Belgium

**Timothy P. Hanna, MD, MSc, PhD, FRCPC**

Clinician Scientist  
Cancer Care and Epidemiology  
Cancer Research Institute at Queen's  
University  
Radiation Oncologist  
Cancer Centre of Southeastern Ontario  
Kingston General Hospital  
Kingston, Ontario, Canada

**Paul M. Harari, MD**

Jack Fowler Professor and Chairman  
Human Oncology  
University of Wisconsin School of Medicine  
and Public Health  
Madison, Wisconsin

**Joseph M. Herman, MD, MSc, MSHCM**

Professor  
Department of Radiation Oncology  
The University of Texas MD Anderson  
Cancer Center  
Houston, Texas

**Michael G. Herman, PhD**

Professor  
Department of Radiation Oncology  
Mayo Clinic College of Medicine and  
Science, Mayo Clinic  
Rochester, Minnesota

**Caroline L. Holloway, MD, FRCPC**  
 Clinical Assistant Professor  
 Department of Radiation Oncology  
 BC Cancer Agency, Vancouver Island Centre  
 Victoria, British Columbia, Canada

**Bradford S. Hoppe, MD, MPH**  
 Associate Professor  
 Department of Radiation Oncology  
 Mayo Clinic College of Medicine and  
 Science, Mayo Clinic  
 Jacksonville, Florida

**Michael R. Horsman, PhD, DMSc**  
 Professor  
 Department of Experimental Clinical  
 Oncology  
 Aarhus University Hospital  
 Aarhus, Denmark

**Janet K. Horton, MD**  
 Adjunct Associate Professor  
 Duke University Medical Center  
 Durham, North Carolina

**Julie Howle, MBBS, MS, FRACS, FACS**  
 Surgical Oncologist  
 Westmead Private Hospital  
 Westmead, New South Wales, Australia;  
 Clinical Senior Lecturer  
 Department of Surgery  
 The University of Sydney  
 Sydney, New South Wales, Australia

**Brian A. Hrycushko, PhD**  
 Assistant Professor  
 Department of Radiation Oncology  
 UT Southwestern Medical Center  
 Dallas, Texas

**David Hsu, MD, PhD**  
 William Dalton Family Assistant Professor  
 Division of Medical Oncology  
 Department of Internal Medicine  
 Duke Cancer Institute  
 Duke University  
 Durham, North Carolina

**Chen Hu, PhD**  
 Assistant Professor of Oncology  
 Division of Biostatistics and Bioinformatics  
 Sidney Kimmel Comprehensive Cancer  
 Center  
 Johns Hopkins University  
 Baltimore, Maryland  
 Statistics and Data Management Center  
 NRG Oncology

**Patricia A. Hudgins, MD**  
 Professor  
 Department of Radiology and Imaging  
 Sciences  
 Emory University School of Medicine  
 Atlanta, Georgia

**Christine A. Iacobuzio-Donahue, MD, PhD**  
 Director, David M. Rubenstein Center for  
 Pancreatic Cancer Research  
 Department of Radiation Oncology  
 Memorial Sloan Kettering Cancer Center  
 New York, New York

**Andrei Iagaru, MD**  
 Assistant Professor  
 Department of Radiology  
 Division of Nuclear Medicine and Molecular  
 Imaging  
 Stanford University  
 Stanford, California

**Nicole M. Iñiguez-Ariza, MD**  
 Division of Endocrinology, Diabetes,  
 Metabolism, and Nutrition  
 Mayo Clinic College of Medicine and  
 Science, Mayo Clinic  
 Rochester, Minnesota;  
 Department of Endocrinology and  
 Metabolism  
 Instituto Nacional de Ciencias Médicas y  
 Nutrición Salvador Zubirán  
 Mexico City, Mexico

**Jedediah E. Johnson, PhD**  
 Assistant Professor  
 Department of Radiation Oncology  
 Mayo Clinic College of Medicine and  
 Science, Mayo Clinic  
 Rochester, Minnesota

**Joseph G. Jurcic, MD**  
 Professor of Medicine  
 Director, Hematologic Malignancies Section  
 Department of Medicine  
 Columbia University Irving Medical Center  
 Attending Physician  
 New York-Presbyterian Hospital/Columbia  
 University Irving Medical Center  
 New York, New York

**John A. Kalapurakal, MD, FACR, FASTRO**  
 Professor  
 Department of Radiation Oncology  
 Northwestern University  
 Chicago, Illinois

**Brian D. Kavanagh, MD**  
 Professor and Chair  
 Department of Radiation Oncology  
 University of Colorado School of Medicine  
 University of Colorado Comprehensive  
 Cancer Center  
 Aurora, Colorado

**Kara M. Kelly, MD**  
 Waldemar J. Kaminski Endowed Chair of  
 Pediatrics  
 Department of Pediatric Oncology  
 Roswell Park Cancer Institute  
 Division Chief, Pediatric Hematology/  
 Oncology and Research Professor  
 Department of Pediatrics  
 University of Buffalo School of Medicine  
 and Biomedical Sciences  
 Buffalo, New York

**Amir H. Khandani, MD**  
 Associate Professor of Radiology  
 Chief, Division of Nuclear Medicine  
 Department of Radiology  
 University of North Carolina at Chapel Hill  
 Chapel Hill, North Carolina

**Deepak Khuntia, MD**  
 Vice President, Medical Affairs  
 Oncology Systems  
 Varian Medical Systems, Inc.  
 Palo Alto, California;  
 Radiation Oncologist  
 Valley Medical Oncology Consultants  
 Pleasanton, California

**Ana Ponce Kiess, MD, PhD**  
 Assistant Professor  
 Departments of Radiation Oncology and  
 Molecular Radiation Sciences  
 Johns Hopkins University School of  
 Medicine  
 Baltimore, Maryland

**Joseph K. Kim, MD**  
 Resident Physician  
 Department of Radiation Oncology  
 New York University  
 New York, New York

**Susan J. Knox, MD, PhD**  
 Associate Professor  
 Department of Radiation Oncology  
 Stanford University  
 Stanford, California

**Wui-Jin Koh, MD**  
 Senior Vice President and Chief Medical  
 Officer  
 National Comprehensive Cancer Network  
 (NCCN)  
 Philadelphia, Pennsylvania

**Rupesh R. Kotecha, MD**

Department of Radiation Oncology  
Miami Cancer Institute  
Baptist Health South Florida  
Department of Radiation Oncology  
FIU Herbert Wertheim College of Medicine  
Miami, Florida

**Matthew W. Krasin, MD**

Member  
Department of Radiation Oncology  
St. Jude Children's Research Hospital  
Memphis, Tennessee

**Larry E. Kun, MD<sup>†</sup>**

Professor and Director of Educational  
Programs  
Department of Radiation Oncology  
Professor, Department of Pediatrics  
UT Southwestern Medical Center  
Dallas, Texas

**A. Nicholas Kurup, MD**

Associate Professor of Radiology  
Mayo Clinic College of Medicine and  
Science, Mayo Clinic  
Rochester, Minnesota

**Nadia N. Issa Laack, MD**

Professor  
Chair, Department of Radiation Oncology  
Mayo Clinic College of Medicine and  
Science, Mayo Clinic  
Rochester, Minnesota

**Ann S. LaCasce, MD, MMSc**

Associate Professor of Medicine  
Harvard Medical School  
Dana-Farber Cancer Institute  
Boston, Massachusetts

**Michael J. LaRiviere, MD**

Resident Physician  
Department of Radiation Oncology  
University of Pennsylvania  
Philadelphia, Pennsylvania

**Andrew B. Lassman, MD**

Chief, Neuro-Oncology Division  
Columbia University Irving Medical Center  
Medical Director  
Clinical Protocol and Data Management Office  
Herbert Irving Comprehensive Cancer Center  
New York, New York

**Colleen A. Lawton, MD**

Vice Chair and Professor  
Department of Radiation Oncology  
Medical College of Wisconsin  
Milwaukee, Wisconsin

**Nancy Lee, MD**

Radiation Oncologist  
Department of Radiation Oncology  
Memorial Sloan Kettering Cancer Center  
New York, New York

**Percy Lee, MD**

Associate Professor  
Vice Chair of Education  
UCLA Department of Radiation Oncology  
University of California, Los Angeles  
Los Angeles, California

**Benoît Lengelé, MD, PhD, FRCS, KB**

Head of Department  
Plastic and Reconstructive Surgery  
Cliniques Universitaires Saint-Luc  
Brussels, Belgium

**William P. Levin, MD**

Associate Professor  
Department of Radiation Oncology  
Abramson Cancer Center of the University  
of Pennsylvania  
Philadelphia, Pennsylvania

**Jeremy H. Lewin, MBBS, FRACP**

Medical Oncologist  
Peter MacCallum Cancer Centre  
Clinical Senior Lecturer  
Sir Peter MacCallum Department of  
Oncology  
University of Melbourne  
Melbourne, Victoria, Australia

**Dror Limon, MD**

Head of CNS Radiotherapy Service  
Radiotherapy Institute  
Tel-Aviv Sourasky Medical Center  
Tel-Aviv, Israel

**Jacob C. Lindegaard, MD, DMSc**

Associate Professor  
Department of Oncology  
Aarhus University Hospital  
Aarhus, Denmark

**Daniel J. Ma, MD**

Associate Professor  
Department of Radiation Oncology  
Mayo Clinic College of Medicine and  
Science, Mayo Clinic  
Rochester, Minnesota

**Shannon M. MacDonald, MD**

Associate Professor  
Department of Radiation Oncology  
Massachusetts General Hospital/Harvard  
Medical School  
Boston, Massachusetts

**William J. Mackillop, MBChB, FRCR, FRCPC**

Professor  
Oncology and Public Health Sciences  
Queen's University  
Kingston, Ontario, Canada

**Kelly R. Magliocca, DDS, MPH**

Assistant Professor  
Department of Pathology and Laboratory  
Medicine  
Emory University School of Medicine  
Atlanta, Georgia

**Anuj Mahindra, MBBS**

Director, Malignant Hematology  
Division of Hematology/Oncology  
Scripps Clinic  
La Jolla, California

**Anthony A. Mancuso, MD**

Professor and Chair  
Department of Radiology  
Professor of Otolaryngology  
University of Florida College of Medicine  
Gainesville, Florida

**Bindu Manyam, MD**

Department of Radiation Oncology  
Allegheny Health Network  
Pittsburgh, Pennsylvania

**Karen J. Marcus, MD, FACR**

Associate Professor and Division Chief  
Pediatric Radiation Oncology  
Dana-Farber/Boston Children's Cancer and  
Blood Disorders Center  
Brigham and Women's Hospital  
Harvard Medical School  
Boston, Massachusetts

**Stephanie Markovina, MD, PhD**

Assistant Professor  
Department of Radiation Oncology  
Washington University School of Medicine  
in St. Louis  
St. Louis, Missouri

**Lawrence B. Marks, MD, FASTRO**

Dr. Sidney K. Simon Distinguished Professor  
of Oncology Research  
Chair, Department of Radiation Oncology  
University of North Carolina School of  
Medicine  
Chapel Hill, North Carolina

**Martha M. Matuszak, PhD**

Associate Professor  
Department of Radiation Oncology  
University of Michigan  
Ann Arbor, Michigan

<sup>†</sup>Deceased

**Mark W. McDonald, MD**

Associate Professor  
Department of Radiation Oncology  
Emory University School of Medicine  
Atlanta, Georgia

**Lisa A. McGee, MD**

Assistant Professor  
Department of Radiation Oncology  
Mayo Clinic College of Medicine and  
Science, Mayo Clinic  
Phoenix, Arizona

**Paul M. Medin, PhD**

Professor  
Department of Radiation Oncology  
UT Southwestern Medical Center  
Dallas, Texas

**Minesh P. Mehta, MBChB, FASTRO**

Professor and Chair  
FIU Herbert Wertheim College of Medicine  
Deputy Director and Chief  
Department of Radiation Oncology  
Miami Cancer Institute  
Baptist Health South Florida  
Miami, Florida

**William M. Mendenhall, MD, FASTRO**

Professor  
Department of Radiation Oncology  
University of Florida College of Medicine  
Gainesville, Florida

**Ruby F. Meredith, MD, PhD**

Professor  
Department of Radiation Oncology  
University of Alabama at Birmingham  
Senior Scientist  
UAB Comprehensive Cancer Center  
University of Alabama at Birmingham  
Birmingham, Alabama

**Jeff M. Michalski, MD, MBA, FACR, FASTRO**

Carlos A. Perez Distinguished Professor  
Vice Chair of Radiation Oncology  
Washington University School of Medicine  
in St. Louis  
St. Louis, Missouri

**Michael T. Milano, MD, PhD**

Professor  
Department of Radiation Oncology  
University of Rochester  
Rochester, New York

**Bruce D. Minsky, MD**

Professor of Radiation Oncology  
Frank T. McGraw Memorial Chair  
The University of Texas MD Anderson  
Cancer Center  
Houston, Texas

**Michael Mix, MD**

Assistant Professor  
Department of Radiation Oncology  
SUNY Upstate Medical University  
Syracuse, New York

**Amy C. Moreno, MD**

Assistant Professor  
Department of Radiation Oncology  
The University of Texas MD Anderson  
Cancer Center  
Houston, Texas

**William H. Morrison, MD**

Professor  
Department of Radiation Oncology  
University of Texas MD Anderson Cancer  
Center  
Houston, Texas

**Erin S. Murphy, MD**

Assistant Professor  
Department of Radiation Oncology  
Rose Ella Burkhardt Brain Tumor and  
Neuro-Oncology Center  
Cleveland Clinic  
Cleveland, Ohio

**Rashmi K. Murthy, MD, MBE**

Assistant Professor  
Department of Breast Medical Oncology  
University of Texas MD Anderson Cancer  
Center  
Houston, Texas

**Andrea K. Ng, MD, MPH**

Professor of Radiation Oncology  
Dana-Farber Cancer Institute  
Brigham and Women's Hospital  
Harvard Medical School  
Boston, Massachusetts

**Marianne Nordmark, MD, PhD**

Senior Staff Specialist  
Department of Oncology  
Aarhus University Hospital  
Aarhus, Denmark

**Yazmin Odia, MD, MS**

Lead Physician of Medical Neuro-Oncology  
Miami Cancer Institute  
Baptist Health South Florida  
Miami, Florida

**Desmond A. O'Farrell, MSc, CMD**

Teaching Associate in Radiation Oncology  
Harvard Medical School  
Clinical Physicist  
Department of Radiation Oncology  
Dana-Farber/Brigham and Women's Cancer  
Center  
Boston, Massachusetts

**Paul Okunieff, MD**

Professor and Chair  
Department of Radiation Oncology  
University of Florida  
Gainesville, Florida

**Hilary L.P. Orlowski, MD**

Assistant Professor of Radiology  
Mallinckrodt Institute of Radiology  
Washington University School of Medicine  
in St. Louis  
St. Louis, Missouri

**Sophie J. Otter, MD(Res), MRCP, FRCR**

Consultant Clinical Oncologist  
Department of Oncology  
Royal Surrey County Hospital  
Guildford, Surrey, United Kingdom

**Roger Ove, MD, PhD**

Clinical Associate Professor  
Department of Radiation Oncology  
University Hospitals Case Medical Center  
Seidman Cancer Center  
Cleveland, Ohio

**Jens Overgaard, MD, DMSc**

Professor  
Department of Experimental Clinical  
Oncology  
Aarhus University Hospital  
Aarhus, Denmark

**Manisha Palta, MD**

Associate Professor  
Department of Radiation Oncology  
Duke Cancer Institute  
Duke University  
Durham, North Carolina

**Luke E. Pater, MD**

Associate Professor  
Department of Radiation Oncology  
University of Cincinnati  
Cincinnati, Ohio

**Todd Pawlicki, PhD, FAAPM, FASTRO**

Professor and Vice-Chair  
Department of Radiation Medicine and  
Applied Sciences  
Director, Division of Medical Physics and  
Technology  
University of California, San Diego  
La Jolla, California

**Jennifer L. Peterson, MD**

Department of Radiation Oncology  
Mayo Clinic Florida  
Associate Professor of Radiation Oncology  
Mayo Clinic College of Medicine and Science  
Jacksonville, Florida

**Thomas M. Pisansky, MD**

Professor  
Department of Radiation Oncology  
Mayo Clinic College of Medicine and  
Science, Mayo Clinic  
Rochester, Minnesota

**Erqi Pollom, MD, MS**

Department of Radiation Oncology  
Stanford University  
Stanford, California

**Louis Potters, MD, FACR, FASTRO, FABS**

Professor and Chairperson  
Department of Radiation Medicine  
Northwell Health and the Zucker School of  
Medicine at Hofstra/Northwell  
Deputy Physician-in-Chief  
Northwell Health Cancer Institute  
Lake Success, New York

**Harry Quon, MD, MS**

Associate of Radiation Oncology and  
Molecular Radiation Sciences  
Johns Hopkins University School of  
Medicine  
Baltimore, Maryland

**David Raben, MD**

Professor  
Department of Radiation Oncology  
University of Colorado  
Aurora, Colorado

**Ezequiel Ramirez, MS, CMD RT(R)(T)**

Chief Medical Dosimetrist  
University of California, San Francisco  
San Francisco, California

**Demetrios Raptis, MD**

Assistant Professor of Radiology  
Mallinckrodt Institute of Radiology  
Washington University School of Medicine  
in St. Louis  
St. Louis, Missouri

**Michal Raz, MD**

Neuropathologist  
Pathology Department  
Tel-Aviv Sourasky Medical Center  
Tel-Aviv, Israel

**Abram Recht, MD**

Professor  
Department of Radiation Oncology  
Harvard Medical School  
Vice Chair  
Department of Radiation Oncology  
Beth Israel Deaconess Medical Center  
Boston, Massachusetts

**Pablo F. Recinos, MD**

Assistant Professor  
Department of Neurological Surgery  
Cleveland Clinic  
Cleveland, Ohio

**Marsha Reyngold, MD, PhD**

Radiation Oncologist  
Department of Radiation Oncology  
Memorial Sloan Kettering Cancer Center  
New York, New York

**Nadeem Riaz, MD**

Assistant Attending  
Department of Radiation Oncology  
Memorial Sloan Kettering Cancer Center  
New York, New York

**Kenneth B. Roberts, MD**

Professor  
Department of Therapeutic Radiology  
Yale University School of Medicine  
New Haven, Connecticut

**Stephen S. Roberts, MD**

Associate Attending Physician  
Department of Pediatrics  
Memorial Sloan Kettering Cancer Center  
New York, New York

**Claus M. Rödel, MD**

Professor and Chairman  
Radiotherapy and Oncology  
University Hospital Frankfurt, Goethe  
University  
Frankfurt, Germany

**Carlos Rodriguez-Galindo, MD**

Member and Chair  
Department of Global Pediatric Medicine  
Member, Department of Oncology  
St. Jude Children's Research Hospital  
Memphis, Tennessee

**C. Leland Rogers, MD**

Professor  
Department of Radiation Oncology  
Barrow Neurological Institute  
Phoenix, Arizona

**Todd L. Rosenblat, MD**

Assistant Professor of Medicine  
Columbia University Irving Medical Center  
New York, New York

**William G. Rule, MD**

Assistant Professor  
Department of Radiation Oncology  
Mayo Clinic College of Medicine and  
Science, Mayo Clinic  
Phoenix, Arizona

**David P. Ryan, MD**

Clinical Director and Chief of Hematology/  
Oncology  
Massachusetts General Hospital Cancer  
Center  
Professor of Medicine  
Harvard Medical School  
Boston, Massachusetts

**Nabil F. Saba, MD**

Professor  
Departments of Hematology and Medical  
Oncology and Otolaryngology  
Emory University School of Medicine  
Atlanta, Georgia

**Joseph K. Salama, MD**

Professor  
Department of Radiation Oncology  
Duke University School of Medicine  
Durham, North Carolina

**John T. Sandlund Jr, MD**

Member, Department of Oncology  
St. Jude Children's Research Hospital  
Professor  
Department of Pediatrics  
University of Tennessee College of Medicine  
Memphis, Tennessee

**Michael Heinrich Seegenschmiedt, MD**

Professor  
Strahlentherapie Osnabrück  
Osnabrück, Germany

**Amy Sexauer, MD, PhD**

Dana-Farber Cancer Institute  
Division of Pediatrics  
Hematology/Oncology/Stem Cell Transplant  
Department of Pediatrics  
Boston Children's Hospital  
Boston, Massachusetts

**Jacob E. Shabason, MD**

Assistant Professor  
Department of Radiation Oncology  
Perelman School of Medicine at the  
University of Pennsylvania  
Philadelphia, Pennsylvania

**Chirag Shah, MD**

Department of Radiation Oncology  
Taussig Cancer Institute  
Cleveland Clinic  
Cleveland, Ohio

**Jason P. Sheehan, MD**

Harrison Distinguished Professor  
Neurological Surgery  
University of Virginia  
Charlottesville, Virginia



**Arif Sheikh, MD**

Mount Sinai Health System  
New York, New York

**Anup S. Shetty, MD**

Assistant Professor of Radiology  
Mallinckrodt Institute of Radiology  
Washington University School of Medicine  
in St. Louis  
St. Louis, Missouri

**Arun D. Singh MD**

Professor of Ophthalmology  
Department of Ophthalmic Oncology  
Cleveland Clinic  
Cleveland, Ohio

**William Small Jr, MD, FACRO, FACR, FASTRO**

Professor and Chairman  
Department of Radiation Oncology  
Loyola University Chicago  
Stritch School of Medicine  
Chicago, Illinois

**Mike Soike, MD**

Department of Radiation Oncology  
Wake Forest Baptist Health  
Winston-Salem, North Carolina

**C. Arturo Solares, MD**

Professor  
Department of Otolaryngology  
Emory University School of Medicine  
Atlanta, Georgia

**Timothy D. Solberg, PhD**

Professor and Director, Medical Physics  
Department of Radiation Oncology  
University of California, San Francisco  
San Francisco, California

**Alexandra J. Stewart, DM, MRCP, FRCR**

Consultant Clinical Oncologist  
St. Luke's Cancer Centre  
Royal Surrey County Hospital  
Senior Lecturer  
University of Surrey  
Guildford, United Kingdom

**Rebecca L. Stone, MD, MS**

Assistant Professor  
Department of Gynecology and Obstetrics  
Johns Hopkins Hospital  
Baltimore, Maryland

**John H. Suh, MD**

Professor and Chairman  
Department of Radiation Oncology  
Rose Ella Burkhardt Brain Tumor and  
Neuro-Oncology Center  
Cleveland Clinic  
Cleveland, Ohio

**Winston W. Tan, MD**

Division of Hematology and Oncology  
Mayo Clinic Florida  
Associate Professor of Medicine  
Mayo Clinic College of Medicine and Science  
Jacksonville, Florida

**Joel E. Tepper, MD, FASTRO**

Hector MacLean Distinguished Professor of  
Cancer Research  
Department of Radiation Oncology  
University of North Carolina Lineberger  
Comprehensive Cancer Center  
University of North Carolina School of  
Medicine  
Chapel Hill, North Carolina

**Charles R. Thomas Jr, MD**

Professor and Chair  
Radiation Medicine  
Knight Cancer Institute  
Oregon Health & Science University  
Portland, Oregon

**Robert D. Timmerman, MD**

Professor and Vice-Chair  
Department of Radiation Oncology  
UT Southwestern Medical Center  
Dallas, Texas

**Christopher L. Tinkle, MD, PhD**

Assistant Member  
Department of Radiation Oncology  
St. Jude Children's Research Hospital  
Memphis, Tennessee

**Betty C. Tong, MD**

Associate Professor  
Department of Surgery  
Division of Cardiovascular and Thoracic  
Surgery  
Duke University School of Medicine  
Durham, North Carolina

**Jordan A. Torok, MD**

Assistant Professor  
Department of Radiation Oncology  
Duke University School of Medicine  
Durham, North Carolina

**Chiaojung Jillian Tsai, MD, PhD**

Radiation Oncologist  
Department of Radiation Oncology  
Memorial Sloan Kettering Cancer Center  
New York, New York

**Richard W. Tsang, MD, FRCPC**

Professor  
Department of Radiation Oncology  
University of Toronto  
Princess Margaret Hospital  
Toronto, Ontario, Canada

**Mark D. Tyson, MD**

Department of Urology  
Mayo Clinic Arizona  
Assistant Professor of Urology  
Mayo Clinic College of Medicine and Science  
Phoenix, Arizona

**Kenneth Y. Usuki, MS, MD**

Associate Professor  
Department of Radiation Oncology  
University of Rochester  
Rochester, Minnesota

**Vincenzo Valentini, MD**

Professor and Chairman  
Radiation Oncology  
Policlinico Gemelli-Università Cattolica del  
Sacro Cuore  
Rome, Italy

**Julie My Van Nguyen, MD, MSc, FRCSC**

Fellow  
Division of Gynecologic Oncology  
University of Toronto  
Toronto, Ontario, Canada

**Noam VanderWalde, MD, MS**

Assistant Professor  
Department of Radiation Oncology  
West Cancer Center and Research Institute  
Memphis, Tennessee

**Ralph Vatner, MD, PhD**

Assistant Professor  
Department of Radiation Oncology  
University of Cincinnati  
Cincinnati Children's Hospital Medical  
Center  
Cincinnati, Ohio

**Michael J. Veness, MD, MMed, FRANZCR**

Clinical Professor  
Department of Radiation Oncology  
Westmead Hospital  
The University of Sydney  
Sydney, New South Wales, Australia

**Vivek Verma, MD**

Attending Physician  
Department of Radiation Oncology  
Allegheny General Hospital  
Pittsburgh, Pennsylvania

**Frank A. Vicini, MD**

Department of Radiation Oncology  
21st Century Oncology  
Michigan Healthcare Professionals  
Farmington Hills, Michigan

**Akila N. Viswanathan, MD, MPH**

Professor  
Department of Radiation Oncology and  
Molecular Radiation Sciences  
Johns Hopkins University School of  
Medicine  
Baltimore, Maryland

**Daniel R. Wahl, MD, PhD**

Assistant Professor  
Department of Radiation Oncology  
University of Michigan  
Ann Arbor, Michigan

**Padraig R. Warde, MBBCh, FRCPC**

Radiation Oncologist  
Princess Margaret Cancer Centre  
Professor  
Department of Radiation Oncology  
University of Toronto  
Toronto, Ontario, Canada

**Christopher G. Willett, MD**

Professor and Chair  
Department of Radiation Oncology  
Duke Cancer Institute  
Duke University  
Durham, North Carolina

**Christopher D. Willey, MD, PhD**

Associate Professor  
Department of Radiation Oncology  
The University of Alabama at Birmingham  
Birmingham, Alabama

**Grant Williams, MD**

Assistant Professor  
Division of Hematology and Oncology and  
Gerontology, Geriatrics, and Palliative  
Care  
University of Alabama at Birmingham  
Birmingham, Alabama

**Lynn D. Wilson, MD, MPH, FASTRO**

Professor, Executive Vice Chairman, Clinical  
Director  
Department of Therapeutic Radiology  
Professor, Department of Dermatology  
Staff Attending, Yale–New Haven Hospital  
Yale University School of Medicine  
Smilow Cancer Hospital  
New Haven, Connecticut

**Karen M. Winkfield, MD, PhD**

Associate Professor  
Department of Radiation Oncology  
Wake Forest Baptist Health  
Winston-Salem, North Carolina

**Suzanne L. Wolden, MD**

Attending Physician  
Department of Radiation Oncology  
Memorial Sloan Kettering Cancer Center  
New York, New York

**Jeffrey Y.C. Wong, MD, FASTRO**

Professor and Chair  
Department of Radiation Oncology  
City of Hope National Medical Center  
Duarte, California

**Terence Z. Wong, MD, PhD**

Professor of Radiology  
Chief, Division of Nuclear Medicine  
Department of Radiology  
Duke Cancer Institute  
Duke University Health System  
Durham, North Carolina

**William W. Wong, MD**

Vice Chair, Department of Radiation  
Oncology  
Mayo Clinic Arizona  
Professor of Radiation Oncology  
Mayo Clinic College of Medicine and Science  
Phoenix, Arizona

**Zhong Wu, MD, PhD**

Research Fellow in Medicine  
Dana-Farber Cancer Institute  
Harvard Medical School  
Boston, Massachusetts

**Joachim Yahalom, MD, FACR**

Professor  
Department of Radiation Oncology  
Memorial Sloan Kettering Cancer Center  
New York, New York

**Eddy S. Yang, MD, PhD**

Professor  
Department of Radiation Oncology  
The University of Alabama at Birmingham  
Birmingham, Alabama

**Y. Nancy You, MD, MHSc**

Associate Professor  
Department of Surgical Oncology  
Associate Medical Director  
Clinical Cancer Genetics Program  
The University of Texas MD Anderson  
Cancer Center  
Houston, Texas

**Ye Yuan, MD, PhD**

Resident Physician  
UCLA Department of Radiation Oncology  
University of California, Los Angeles  
Los Angeles, California

**Elaine M. Zeman, PhD**

Associate Professor  
Department of Radiation Oncology  
University of North Carolina School of  
Medicine  
Chapel Hill, North Carolina

**Peixin Zhang, PhD**

Statistics and Data Management Center  
NRG Oncology

**Tiffany C. Zigras, MD, MSc, MEng,  
FRCSC**

Fellow  
Division of Gynecologic Oncology  
University of Toronto  
Toronto, Ontario, Canada

Joel Tepper and I were approached by the senior medical editor of Churchill Livingstone in late 1995 about co-editing a textbook on clinical radiation oncology as a counterpart to the multidisciplinary textbook *Clinical Oncology*, edited by Abeloff, Armitage, Lichter, and Niederhuber. By May 1996, the decision had been made to proceed and a contract was signed in July. We were interested in producing a new radiation oncology textbook that was easily readable and useful to both residents and experienced radiation oncologists. As such, we introduced “Key Points” for each disease-site chapter, as well as algorithms for workup and treatment for each disease. We thought that, along with careful editing and organization, this would provide a new and valuable resource to the radiation oncology community. While providing a thorough coverage of all the topics, we made no attempt to cover all issues but rather emphasized what was important to the clinician.

Since Joel and I had similar disease-site interests, the decision was made to select associate editors for eight other disease-site sections/chapters “to enhance the scientific content and comprehensiveness of the textbook” (breast, central nervous system, childhood, gynecologic, genitourinary, head and neck, lymphoma/hematologic, thoracic). Associate editors were involved in helping select appropriate senior authors for each of the disease-site chapters, in editing the chapters for scientific content and accuracy, and in writing a section overview for their respective disease-sites.

The first edition of *Clinical Radiation Oncology* (CRO), published in 2000 by Churchill Livingstone/Harcourt Science, was a 1300-page, black and white textbook containing 63 chapters in three major sections—Scientific Foundations of Radiation, Techniques and Modalities, Disease Sites. Subsequent editions (CRO2, CRO3, CRO4) were published in 2007 (Churchill Livingstone, Elsevier), 2012 (Saunders/Elsevier) and 2016 (Elsevier), with Joel and I as the co-senior editors, plus section editors for gastrointestinal and sarcoma, while continuing to involve associate editors for the other eight disease-site sections. CRO2 was a full-color textbook and expanded to 76 chapters with approximately 1800 pages. An exciting feature of CRO3 was the availability of an online version of the textbook that contained the entire print component of the textbook along with additional text, figures, tables, and a complete

set of cited references. This allowed a reduction in the length of the printed textbook by limiting the number of critical references in the print version of each chapter to 50. For CRO4 an exciting new feature was the periodic update of chapters in the online version of the textbook. Periodic changes were made in chapter senior authors and co-authors and in the associate editors for subsequent editions, as appropriate.

While I was heavily involved in the clinical/content updates for CRO4, I promised my wife, Katheryn, that I would not edit further editions of CRO. Therefore, when the decision was made to proceed with CRO5, I conferred with Joel in selecting two new senior editors (Drs. Robert Foote and Jeff Michalski), which resulted in a more diverse group of senior editors by virtue of their respective disease-site expertise. At Joel’s request, I was involved with the three of them in the planning process for CRO5. As a group we decided to add six new chapters while keeping the length of the hardcopy textbook similar to CRO4 by reducing the number of critical references in the hardcopy version from 50 to 25.

The intent of the first edition of CRO was “to be both comprehensive and authoritative, yet not exhaustive” by virtue of liberal use of tables, figures, and treatment algorithms as a supplement to the text. The comprehensive/authoritative intent of the print versions of the book persisted in subsequent editions, but the addition of an online version for CRO3 and subsequent editions has perhaps resulted in some “exhaustive” chapters online for those readers who found the additional information useful. *It has been both a privilege and a pleasure to be associated with Clinical Radiation Oncology planning and editing in conjunction with Joel and many other national and international experts for over 20 years!* The contributions of outstanding authors, associate editors, and senior editors will allow CRO5 to be a valuable resource for many readers in the coming years.

**Leonard L. Gunderson, MD, MS, FASTRO**  
*Professor Emeritus and Consultant*  
*Department of Radiation Oncology*  
*Mayo Clinic Rochester/Arizona*  
*Mayo Clinic College of Medicine and Science*

# PREFACE

The radiation oncology community has received the four previous editions of *Clinical Radiation Oncology* very well, and it has become the standard radiation oncology textbook for many physicians. For the fifth edition of *Clinical Radiation Oncology*, the major change that has been made is that Len Gunderson has decided to step down as a senior editor, a position he has held since the inception of this textbook. His insight and efforts have been essential over the years in making this book successful. Drs. Gunderson and Tepper thought carefully about who could replace Dr. Gunderson as a senior editor and decided that two people were needed to fill that role. We have been fortunate to have recruited Robert Foote and Jeff Michalski to be senior editors. As the field of radiation oncology has expanded in its scope, having a third senior editor allows us to have broader expertise.

Despite this major change, our intent is to maintain the many excellent features of the previous editions while adding some new features, new chapters and chapter authors, and new associate editors.

The fifth edition has maintained three separate sections—Scientific Foundations of Radiation Oncology, Techniques and Modalities, and Disease Sites. Within Scientific Foundations of Radiation Oncology, four new chapters have been added: “Radiation Physics: Charged Particle Therapy,” “Tumor Ablation in Interventional Radiology,” “Radiation Therapy in the Elderly,” and “Palliative Radiation Medicine,” reflecting the increasing clinical interest in all of these issues within the oncologic community. In the section on Techniques and Modalities, two new chapters have been added: “Quality and Safety in Radiation Oncology” and “Immunotherapy with Radiotherapy.”

The associate editors for Disease Sites chapters were an important component of the success of the four previous editions and have been retained. Three associate editor positions have changed—Dr. Michalski has taken the lead on genitourinary diseases, Akila Viswanathan has become the associate editor for gynecologic tumors, and Abram Recht is the associate editor for breast tumors. Larry Kun functioned as the associate editor for pediatric tumors until his untimely death, and the remainder of his responsibilities were taken over by Christopher Tinkle and Jeff Michalski. Associate editors are involved in the selec-

tion of chapter authors and in editing the chapters for scientific content and accuracy. For most disease sites, the associate editors also wrote an overview in which they discuss issues common to various disease sites within the section and give their unique perspective on important issues.

Features that are retained within Disease Sites section include an opening page format summarizing the most important issues, a full-color format throughout each chapter, liberal use of tables and figures, and a closing section with a discussion of controversies and problems and a treatment algorithm that reflects the treatment approach of the authors. Chapters have been edited not only for scientific accuracy, but also for organization, format, and adequacy of outcome data (disease control, survival, and treatment tolerance).

We are again indebted to the many national and international experts who contributed to the fifth edition of *Clinical Radiation Oncology* as associate editors, senior authors, or co-authors. Their outstanding efforts combined with ours will hopefully make this new edition a valuable contribution and resource in the field in the coming years.

## ACKNOWLEDGMENTS

We wish to thank our wives, Laurie, Kally, and Sheila, and Dr. Tepper’s secretary, Betty Bush, for their patience and assistance during the many months we were involved in the preparation of the fifth edition of *Clinical Radiation Oncology*.

We also thank the associate editors and the many senior authors and co-authors for their time, efforts, and outstanding contributions to this edition.

We acknowledge the editors and production staff at Elsevier, especially Anne Snyder, Tara Delaney, and Robin Carter, who have done an outstanding job in collating and producing the fifth edition of *Clinical Radiation Oncology*.

**Joel E. Tepper**  
**Robert L. Foote**  
**Jeff M. Michalski**

# VIDEO CONTENTS

- Video 20.1** Prostate Brachytherapy
- Video 22.1** Intraoperative Radiation
- Video 36.1** Ocular Melanoma
- Video 65.1** Penile Brachytherapy



# The Biological Basis of Radiation Oncology

Elaine M. Zeman

## WHAT IS RADIATION BIOLOGY?

In the most general sense, radiation biology is the study of the effects of electromagnetic radiation on biological systems. Three aspects of this definition deserve special mention. First, *effects* may include everything from DNA damage to genetic mutations, chromosome aberrations, cell killing, disturbances in cell cycle transit and cell proliferation, neoplastic transformation, early and late effects in normal tissues, teratogenesis, cataractogenesis, and carcinogenesis, to name but a few. *Electromagnetic radiation* refers to any type of radiant energy in motion with wave and/or particulate characteristics that has the capacity to impart some or all of its energy to the medium through which it passes. The amount of energy deposited can vary over some 25 orders of magnitude, depending on the type of electromagnetic radiation. For example, 1 kHz radio waves have energies in the range of  $10^{-11}$  to  $10^{-12}$  eV, whereas x-rays or  $\gamma$ -rays may have energies upwards of 10 MeV or more. The more energetic forms of electromagnetic radiation, the ionizing radiations, deposit energy as they traverse the medium by setting secondary particles in motion that can go on to produce further ionizations. Finally, *biological systems* may be, for example, quite simple cell-free extracts of biomolecules, or increasingly complex, from prokaryotes to single-celled eukaryotes, to mammalian cells in culture, to tissues and tumors in laboratory animals or humans, to entire ecosystems.

Radiotherapy-oriented radiobiology focuses on that portion of the electromagnetic spectrum energetic enough to cause ionization of atoms. This ultimately results in the breaking of chemical bonds, which can lead to damage to important biomolecules. The most significant effect of ionizing radiation in this context is cell killing, which directly or indirectly is at the root of nearly all of the normal tissue and tumor responses noted in patients.

Cytotoxicity is not the only significant biological effect caused by radiation exposure, although it will be the main focus of this chapter. Other important radiation effects—carcinogenesis, for example—will also be discussed, although the reader should be aware that radiation carcinogenesis is a large discipline in and of itself, involving investigators from fields as diverse as biochemistry, toxicology, epidemiology, environmental sciences, molecular biology, tumor biology, health and medical physics, as well as radiobiology. Most radiation protection standards are based on minimizing the risks associated with mutagenic and carcinogenic events. Therefore radiological health professionals are de facto educators of and advocates for the general

public when it comes to ionizing radiation, who need to be fully conversant in the potential risks and benefits of medical procedures involving radiation.

The majority of this chapter will be devoted to so-called “foundational” radiobiology, that is, studies that largely predate the revolution in molecular biology and biotechnology during the 1980s and 1990s. While the reader might be tempted to view this body of knowledge as rather primitive by today’s standards, relying too heavily on phenomenology, empiricism, and descriptive models and theories, the real challenge is to integrate the new biology into the already-existing framework of foundational radiobiology. Chapter 2 endeavors to do this.

## RADIOTHERAPY-ORIENTED RADIOBIOLOGY: A CONCEPTUAL FRAMEWORK

Before examining any one aspect of radiobiology in depth, it is important to introduce several general concepts to provide a framework for putting the information in its proper perspective.

### The Therapeutic Ratio

The most fundamental of these concepts is what is termed the therapeutic ratio—in essence, a risk-versus-benefit approach to planning a radiotherapy treatment regimen. Many of the radiobiological phenomena to be discussed in this chapter are thought to play important roles in optimizing, or at least “fine tuning,” the therapeutic ratio. In theory, it should be possible to eradicate any malignant tumor simply by delivering a sufficiently high dose of radiation. Of course, in practice, the biological consequences for normal tissues that are necessarily irradiated along with the tumor limit the total dose that can be safely administered. As such, a balance must be struck between what is deemed an acceptable probability of a radiation-induced complication in a normal tissue and the probability of tumor control. Ideally, one would hope to achieve the maximum likelihood of tumor control that does not produce unacceptable normal tissue damage.

The concept of therapeutic ratio is best illustrated graphically, by comparing dose-response curves for both tumor control and normal tissue complication rates plotted as a function of dose. Examples of this approach are shown in Fig. 1.1 for cases in which the therapeutic ratio is either “unfavorable,” “favorable,” or “optimal,” bearing in mind that these are theoretical curves. Actual dose-response curves derived from experimental or clinical data are much more variable, particularly for tumors, which tend to show much shallower dose responses.<sup>1</sup> This

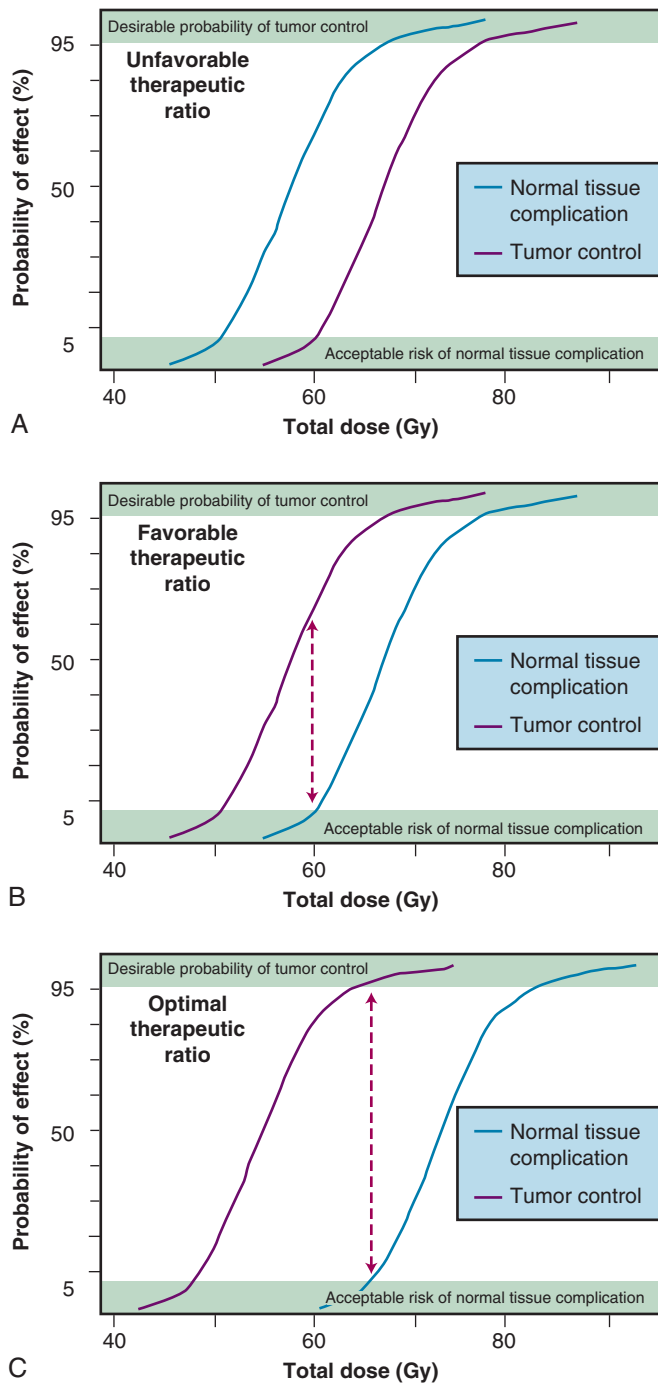


**Fig. 1.1** Illustrating the concept of therapeutic ratio under conditions in which the relationship between the normal tissue tolerance and tumor control dose-response curves is unfavorable (A), favorable (B), and optimal (C).

serves to underscore how difficult it can be in practice to assign a single numerical value to the therapeutic ratio in any given situation.

Many of the radiobiological properties of cells and tissues can have a favorable or adverse effect on the therapeutic ratio. Therefore, in planning a course of radiation therapy, the goal should be to optimize the therapeutic ratio as much as possible; in other words, using our graphical approach, increase the separation between the tumor control and normal tissue complication curves. This can be accomplished either by shifting the tumor control curve to the left with respect to the dose

axis (toward lower doses, i.e., radiosensitization) or shifting the normal tissue complication curve to the right (toward higher doses, i.e., radioprotection) or, perhaps, some combination of both. The key, however, is to shift these curves differentially, not necessarily an easy task given that there are not that many exploitable differences in the radiobiology of cells derived from tumors and those derived from normal tissues.

### The Radiation Biology Continuum

There is a surprising continuity between the physical events that occur in the first few femtoseconds after ionizing radiation interacts with the atoms of a biomolecule and the ultimate consequences of that interaction on tissues. The consequences themselves may not become apparent until days, weeks, months, or even years after the radiation exposure. Some of the important steps in this radiobiology continuum are listed in Table 1.1. The orderly progression from one stage of the continuum to the next—from physical to physicochemical to biochemical to biological—is particularly noteworthy not only because of the vastly different time scales over which the critical events occur but also because of the increasing biological complexity associated with each of the endpoints or outcomes. Each stage of the continuum also offers a unique radiobiological window of opportunity: the potential to intervene in the process and thereby modify all of the events and outcomes that follow.

### Levels of Complexity in Radiobiological Systems

Another important consideration in all radiobiological studies is the nature of the experimental system used to study a particular phenomenon, the assay(s) used, and the endpoint(s) assessed. For example, one investigator might be interested in studying DNA damage caused by ionizing radiation, in particular, the frequency of DNA double-strand breaks (DSBs) produced per unit dose. As an experimental system, the investigator might choose DNA extracted from irradiated mammalian cells and, as an endpoint, use pulsed field gel electrophoresis to measure the distance and rate at which irradiated DNA migrates through the gel compared with unirradiated DNA. The DNA containing more DSBs migrates farther than DNA containing fewer breaks, allowing a calibration curve to be generated that relates migration to the dose received. A second investigator, meanwhile, may be interested in improving the control rate of head and neck cancers with radiation therapy by employing a nonstandard fractionation schedule. In this case, the type of experiment would be a clinical trial. The experimental system would be a cohort of patients, some of whom are randomized to receive nonstandard fractionation and the rest receiving standard fractionation. The endpoints assessed could be one or more of the following: locoregional control, long-term survival, disease-free survival, normal tissue complication frequency, and so forth, evaluated at specific times after completion of the radiation therapy.

In considering both the strengths and weaknesses of these two investigators' studies, any number of pertinent questions may be asked. Which is the more complex or heterogeneous system? Which is the more easily manipulated and controlled system? Which is more relevant for the day-to-day practice of radiation oncology? What kinds of results are gleaned from each and can these results be obtained in a timely manner? In this example, it is clear that human patients with spontaneously arising tumors represent a far more heterogeneous and complex experimental system than extracted mammalian DNA. However, the DNA system is much more easily manipulated, possible confounding factors can be more easily controlled, and the measurement of the desired endpoint (migration distance/rate) plus the data analysis can be completed within a day or two. Obviously, this is not the case with the human studies, in which numerous confounding factors can and do influence results,

TABLE 1.1 Stages in the Radiobiology Continuum

Time Scale of Events ("Stage")	Initial Event	Final Event	Response Modifiers/Possible Interventions
10 <sup>-16</sup> to 10 <sup>-12</sup> second ("Physical")	Ionization of atoms	Free radicals formed in biomolecules	Type of ionizing radiation; shielding
10 <sup>-12</sup> to 10 <sup>-2</sup> second ("Physicochemical")	Free radicals formed in biomolecules	DNA damage	Presence or absence of free radical scavengers, molecular oxygen and/or oxygen-mimetic radiosensitizers
1.0 second to several hours ("Biochemical")	DNA damage	Unrepaired or misrejoined DNA damage	Presence or absence of functioning DNA damage recognition and repair systems; repair-inhibiting drugs; altering the time required to complete repair processes
Hours to years ("Biological")	Unrepaired or misrejoined DNA damage	Clonogenic cell death, apoptosis, mutagenesis, transformation, carcinogenesis, "early and late effects" normal tissues, whole body radiation syndromes, tumor control, etc.	Cell-cell interactions, biological response modifiers, adaptive mechanisms, structural and functional organization of tissues, cell kinetics, etc.

manipulation of the system can be difficult, if not impossible, and the experimental results typically take years to obtain.

The issue of relevance is an even thornier one. Arguably, both studies are relevant to radiation oncology in so far as the killing of cells is at the root of radiation's normal tissue and tumor toxicity, and that cell killing usually is, directly or indirectly, a consequence of irreparable damage to DNA. As such, any laboratory findings that contribute to the knowledge base of radiation-induced DNA damage are relevant. Clearly, however, clinical trials with human patients not only are a more familiar experimental system to radiation oncologists but also, efficacy in conducting trials with cancer patients is ultimately what leads to new standards of care in clinical practice and becomes the gold standard against which all newer therapeutic strategies are judged.

There is a time and place both for relatively simple systems and more complex ones. The relatively simple, homogeneous, and easily manipulated systems are best suited for the study of the mechanisms of radiation action, such as measuring DNA or chromosomal damage, changes in gene expression, activation of cell cycle checkpoints, or the survival of irradiated cells *in vitro*. The more complicated and heterogeneous systems, with their unique endpoints, are more clinically relevant, such as assays of tumor control or normal tissue complication rates. Both types of assay systems have inherent strengths and weaknesses, yet both are critically important if we hope to improve the practice of radiation therapy based on sound biological principles.

## Heterogeneity

Why is radiation therapy successful at controlling one patient's tumor but not another's when the two tumors in all other clinical respects seem identical? Why are we generally more successful at controlling certain types of cancers than others? The short answer to such questions is that, although the tumors may appear identical "macroscopically," their component cells may be quite different genotypically and phenotypically. Also, there could be important differences between the two patients' normal tissues.

Because normal tissues by definition are composed of more than one type of cell, they are necessarily heterogeneous. However, tumors, owing both to the genomic instability of individual cells and to micro-environmental differences, are much more so. Different subpopulations of cells isolated from human and experimental cancers can differ with respect to differentiation, invasive and metastatic potential, immunogenicity, and sensitivity to radiation and chemotherapy, to name but a few. (For reviews, see Heppner and Miller<sup>2</sup> and Suit et al.<sup>3</sup>) This heterogeneity is manifest both within a particular patient and, to a much greater extent, between patients with otherwise similar tumors. Both intrinsic and extrinsic factors contribute to this heterogeneity. Intrinsic factors

can include inherent radiosensitivity, genomic instability, gene expression patterns, DNA repair fidelity, mode(s) of cell death, cell cycle regulation, and how the tissue is structurally and functionally arranged. Extrinsic factors, on the other hand, are related to microenvironmental differences between tissues, such as the functionality of the vasculature, availability of oxygen and nutrients, pH, presence or absence of reactive oxygen species, cytokines and immune cells, energy charge, and cell-cell and cell-extracellular matrix interactions.

What are the practical implications of normal tissue and tumor heterogeneity? First, if one assumes that normal tissues are the more uniform and predictable in behavior of the two, then tumor heterogeneity is responsible, either directly or indirectly, for most radiotherapy failures. If so, this suggests that a valid clinical strategy might be to identify the radioresistant subpopulation(s) of tumor cells and then tailor therapy specifically to cope with them—although, admittedly, this approach is much easier said than done. Some clinical studies—both prospective and retrospective—now include one or more determinations of, for example, extent of tumor hypoxia<sup>4,5</sup> or potential doubling time of tumor clonogens<sup>6</sup> or specific tumor molecular/genetic factors. The hope is that these and other biomarkers can identify subsets of patients bearing tumors with different biological characteristics and that, accordingly, patients with particular characteristics can be assigned prospectively to different treatment groups.

Another consequence of tissue heterogeneity is that any radiobiological endpoint measured in an intact tissue necessarily reflects the sum total of the individual radiosensitivities of all of the subsets of cells, plus all other intrinsic and extrinsic factors that contribute to the overall response of the tissue. Since data on normal tissue tolerances and tumor control probabilities are also averaged across large numbers of patients, heterogeneity is even more pronounced.

## Powers of Ten

Tumor control is achieved only when all clonogenic cells are killed or otherwise rendered unable to sustain tumor growth indefinitely. In order to estimate the likelihood of cure, it is necessary to know, or at least have an appreciation for, approximately how many clonogenic cells the tumor contains, how radiosensitive these cells are (i.e., some measure of killing efficiency per unit radiation dose), and what the relationship is between the number of clonogenic cells remaining after treatment and the probability of recurrence. The latter is perhaps the easiest to ascertain given our knowledge of both the random and discrete nature of radiation damage and the general shape of dose-response curves for mammalian cells and tissues. For a given number of surviving cells per tumor, the probability of local control can be derived from Poisson statistics using the equation  $P = e^{-n}$ , where  $P$  is the tumor

control probability and  $n$  is the average number of surviving clonogenic tumor cells. For example, when an average of one clonogenic cell per tumor remains at the end of radiation therapy, the tumor control rate will be about 37%. This means that about 6 out of 10 tumors of the same size and relative radiosensitivity will recur. Should the treatment reduce clonogenic cell numbers to an average of 0.1 per tumor, the tumor control probability would increase to 90%; 0.05 per tumor, 95%; and 0.01 per tumor, 99%, respectively.

The tumor control probability for a given fraction of surviving cells is not particularly helpful when the total number of cells at risk is unknown; this is where an understanding of logarithmic relationships and exponential cell killing is useful. For example, estimates are that a 1-cm<sup>3</sup> (1-g) tumor mass contains approximately 10<sup>9</sup> cells,<sup>7</sup> admittedly a theoretical (and incorrect) value that assumes that all cells are perfectly packed and uniformly sized and that the tumor contains no stroma. A further assumption, that all such cells are clonogenic (rarely, if ever, the case), suggests that at least 9 logs of cell killing would be necessary before any appreciable tumor control (about 37%) would be achieved, and 10 logs of cell killing would be required for a high degree of tumor control (i.e., 90%).

After the first log or two of cell killing, however, some tumors respond by shrinking, a so-called partial response. After two to three logs of cell killing, the tumor may shrink to a size below the current limits of clinical detection, that is, a complete response. While partial and complete responses are valid clinical endpoints, a complete response does not necessarily equal a tumor cure. At least six more logs of cell killing would still be required before any significant probability of cure would be expected. This explains why radiation therapy is not halted if the tumor disappears during the course of treatment; this concept is illustrated graphically in Fig. 1.2.

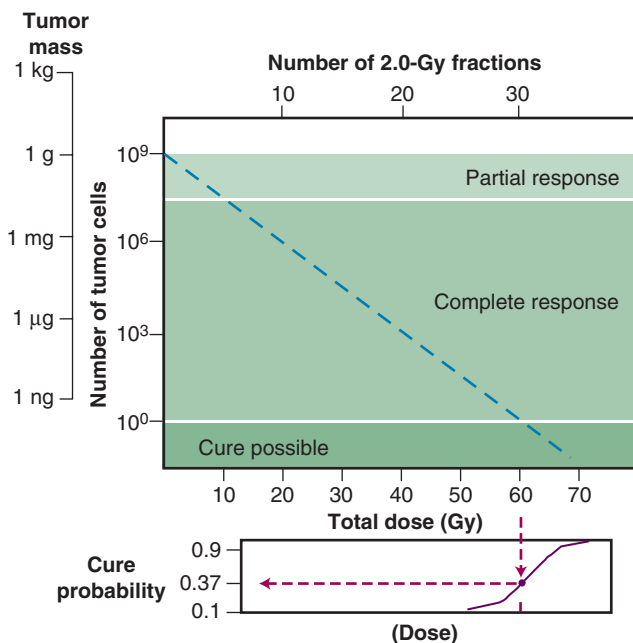


**Fig. 1.2** The relationship between radiation dose and tumor cell survival during fractionated radiotherapy of a hypothetical 1-g tumor containing 10<sup>9</sup> clonogenic cells. Although a modest decrease in cell-surviving fraction can cause the tumor to shrink (partial response) or disappear below the limits of clinical detection (complete response), few if any cures would be expected until at least 9 logs of clonogenic cells have been killed. In this example, a total dose of at least 60 Gy delivered as daily 2-Gy fractions would be required to produce a tumor control probability of 0.37, assuming that each dose reduced the surviving fraction to 0.5. (Modified from Steel G, Adams G, Peckham M, eds. *The Biological Basis of Radiotherapy*. New York: Elsevier, 1983.)

Finally, it should be noted that while the goal of curative radiation therapy is to reduce tumor cell survival by at least nine logs, even for the smallest tumor likely to be encountered, it is much less clear how many logs of cell killing a particular normal tissue can tolerate before it loses its structural and/or functional integrity. This would depend on how the tissue is organized structurally, functionally, and proliferatively, which constituent cells are the most and least radiosensitive, and which cells are the most important to the integrity of the tissue. It is unlikely, however, that many normal tissues could tolerate a depletion of two logs (99%) of their cells, let alone nine or more logs.

## RADIATION BIOLOGY AND THERAPY: THE FIRST 50 YEARS

In fewer than 4 years after the discovery of x-rays by Roentgen,<sup>8</sup> radioactivity by Becquerel,<sup>9</sup> and radium by the Curies,<sup>10</sup> the new modality of cancer treatment known as radiation therapy claimed its first cure of skin cancer.<sup>11</sup> Today, more than 120 years later, radiotherapy is most commonly given as a series of small daily dose fractions of approximately 1.8 to 2.0 Gy each, 5 days per week, over a period of 5 to 7 weeks to total doses of 50 to 75 Gy. While it is true that the historical development of this conventional radiotherapy schedule was empirically based, there were a number of early radiobiological experiments that suggested this approach.

In the earliest days of radiotherapy, both x-rays and radium were used for cancer treatment. Due to the greater availability and convenience of using x-ray tubes and the higher intensities of radiation output achievable, it was fairly easy to deliver one or a few large doses in short overall treatment times. Thus, from about 1900 into the 1920s, this “massive dose technique”<sup>12</sup> was a common way of administering radiation therapy. Normal tissue complications were often quite severe and, to make matters worse, the rate of local tumor recurrence was still unacceptably high.

Radium therapy was used more extensively in France. Because of the low activities available, radium applications necessarily involved longer overall treatment times in order to reach comparable total doses. Although extended treatments were less convenient, clinical results were often superior. Perceiving that the change in overall time was the critical factor, physicians began to experiment with the use of multiple, smaller x-ray doses delivered over extended periods. By that time, there was already a radiobiological precedent for expecting improvement in tumor control when radiation treatments were protracted.

As early as 1906, Bergonié and Tribondeau observed histologically that the immature, dividing cells of the rat testis showed evidence of damage at lower radiation doses than the mature, nondividing cells of the stroma.<sup>13</sup> Based on these observations, they put forth some basic “laws” stating that x-rays were more effective on cells that were (1) actively dividing, (2) likely to continue to divide indefinitely, and (3) undifferentiated.<sup>13</sup> Since tumors were already known to contain cells that were not only less differentiated but also exhibited greater mitotic activity, they reasoned that several radiation exposures might preferentially kill these tumor cells but not their slowly proliferating, differentiated counterparts in the surrounding normal tissues.

The end of common usage of the massive dose technique in favor of fractionated treatment came during the 1920s as a consequence of the pioneering experiments of Claude Regaud.<sup>14</sup> Using the testes of the rabbit as a model tumor system (since the rapid and unlimited proliferation of spermatogenic cells simulated to some extent the pattern of cell proliferation in malignant tumors), Regaud showed that only through the use of multiple, smaller radiation doses could animals be completely sterilized without producing severe injury to the scrotum.<sup>15</sup> Regaud suggested that the superior results afforded the multifraction irradiation scheme were related to alternating periods of relative radioresistance and sensitivity in the rapidly proliferating germ cells.<sup>16</sup> These principles



were soon tested in the clinic by Henri Coutard, who first used fractionated radiotherapy for the treatment of head and neck cancers, with spectacularly improved results, comparatively speaking.<sup>17,18</sup> Largely as a result of these and related experiments, fractionated treatment subsequently became the standard form of radiation therapy.

Time-dose equivalents for skin erythema published by Reisner,<sup>19</sup> Quimby and MacComb,<sup>20</sup> and others<sup>21,22</sup> formed the basis for the calculation of equivalents for other tissue and tumor responses. By plotting the total doses required for each of these “equivalents” for a given level of effect in a particular tissue, as a function of a treatment parameter—such as overall treatment time, number of fractions, dose per fraction, and so forth—an isoeffect curve could be derived. All time-dose combinations that fell along such a curve theoretically would produce tissue responses of equal magnitude. Isoeffect curves, relating the total dose to the overall treatment time, derived in later years from some of these data,<sup>23</sup> are shown in Fig. 1.3.

The first published isoeffect curves were produced by Strandqvist in 1944<sup>24</sup> and are also shown in Fig. 1.3. When transformed on log-log coordinates, isoeffect curves for a variety of skin reactions and the cure of skin cancer were drawn as parallel lines, with common slopes of 0.33. These results implied that there would be no therapeutic advantage to using prolonged treatment times (i.e., multiple small fractions versus

one, or a few, large doses) for the preferential eradication of tumors while simultaneously sparing normal tissues.<sup>25</sup> It was somewhat ironic that the Strandqvist curves were so popular in the years that followed, when it was already known that the therapeutic ratio did increase (at least to a point) with prolonged, as opposed to very short, overall treatment times. However, the overarching advantage was that these isoeffect curves were quite reliable at predicting skin reactions, which were the dose-limiting factors at that time.

## THE “GOLDEN AGE” OF RADIATION BIOLOGY AND THERAPY: THE SECOND 50 YEARS

Perhaps the defining event that ushered in the golden age of radiation biology was the publication of the first survival curve for mammalian cells exposed to graded doses of x-rays. This first report of a quantitative measure of intrinsic radiosensitivity of a human cell line (HeLa, derived from a cervical carcinoma<sup>26</sup>) was published by Puck and Marcus in 1956.<sup>27</sup> In order to put this seminal work in the proper perspective, it is first necessary to review the physicochemical basis for why ionizing radiation is toxic to biological materials.

### The Interaction of Ionizing Radiation With Biological Materials

As mentioned in the introductory section of this chapter, ionizing radiation deposits energy as it traverses the absorbing medium through which it passes. The most important feature of the interaction of ionizing radiation with biological materials is the random and discrete nature of the energy deposition. Energy is deposited in increasingly energetic packets referred to as *spurs* ( $\leq 100$  eV deposited), *blobs* (100–500 eV), or *short tracks* (500–5000 eV), each of which can leave from approximately three to several dozen ionized atoms in its wake. This is illustrated in Fig. 1.4, along with a segment of (interphase) chromatin shown to scale. The frequency distribution and density of the different types of energy deposition events along the track of the incident photon or particle are measures of the radiation’s linear energy transfer (LET; see also the “Relative Biological Effectiveness” section to come). Because these energy deposition events are discrete, it follows that while the average energy deposited in a macroscopic volume of biological material is small, the distribution of this energy on a microscopic scale may be quite large. This explains why ionizing radiation is so efficient at producing biological damage; the total amount of energy deposited in a 70-kg human that

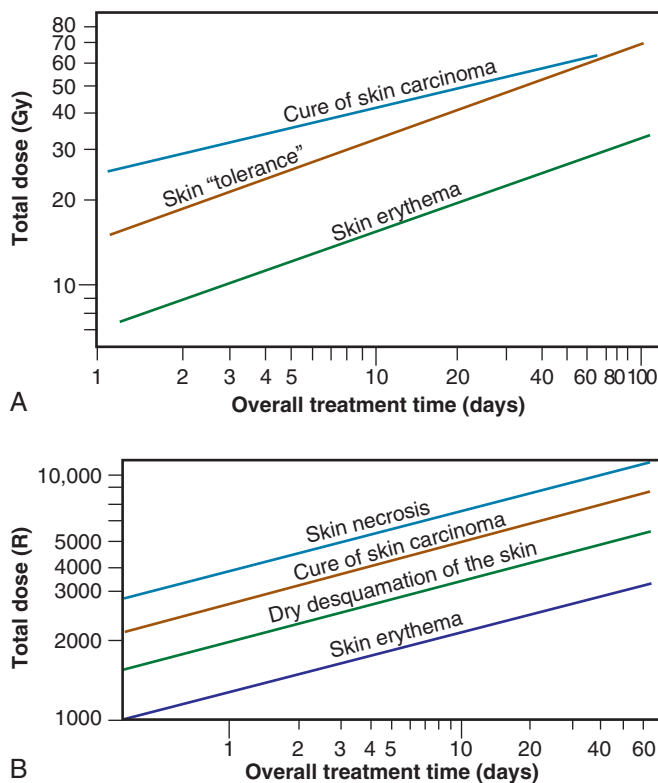


**Fig. 1.3** Isoeffect curves relating the log of the total dose to the log of the overall treatment time for various levels of skin reaction, and the cure of skin cancer. (A) Isoeffect curves constructed by Cohen in 1966, based on a survey of earlier published data on radiotherapy “equivalents.”<sup>19–22</sup> See text for details. The slope of the curves for skin complications was 0.33 and that for tumor control, 0.22. (B) Strandqvist’s isoeffect curves, first published in 1944. All lines were drawn parallel and had a common slope of 0.33. (A, Modified from Cohen L. Radiation response and recovery: Radiobiological principles and their relation to clinical practice. In: Schwartz E, ed. *The Biological Basis of Radiation Therapy*. Philadelphia: J.B. Lippincott; 1966:208; B, modified from Strandqvist M. Studien über die kumulative Wirkung der Roentgenstrahlen bei Fraktionierung. *Acta Radiol Suppl.* 1944;55:1.)

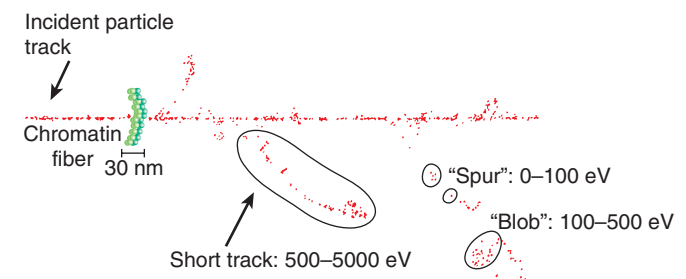


**Fig. 1.4** Hypothetical  $\alpha$ -particle track through an absorbing medium, illustrating the random and discrete energy deposition “events” along the track. Each event can be classified according to the amount of energy deposited locally, which, in turn, determines how many ionized atoms will be produced. A segment of chromatin is also shown, approximately to scale. (Modified from Goodhead DT. Physics of radiation action: microscopic features that determine biological consequences. In: Hagen U, Harder D, Jung H, et al., eds. *Radiation Research 1895–1995, Proceedings of the 10th International Congress of Radiation Research*. Volume 2: Congress Lectures. Würzburg: Universitätsdruckerei H. Sturtz AG; 1995:43–48.)

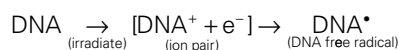


will result in a 50% probability of death is only about 70 calories, about as much energy as is absorbed by drinking one sip of hot coffee.<sup>28</sup> The key difference is that the energy contained in the sip of coffee is uniformly distributed, not random and discrete.

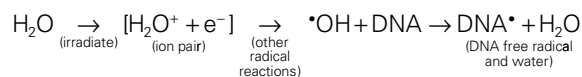
Those biomolecules receiving a direct hit from a spur or blob receive, relatively speaking, a huge radiation dose, that is, a large energy deposition in a very small volume. For photons and charged particles, this energy deposition results in the ejection of orbital electrons from atoms, causing the target molecule to be converted first into an ion pair and then into a free radical. Further, the ejected electrons—themselves energetic charged particles—can go on to produce additional ionizations. For uncharged particles such as neutrons, the interaction is between the incident particles and the nuclei of the atoms in the absorbing medium, causing the ejection of recoil protons (charged) and lower-energy neutrons. The cycle of ionization, free radical production, and release of secondary charged particles continues until all of the energy of the incident photon or particle is expended. These interactions are complete within a picosecond after the initial energy transfer. After that time, the chemical reactions of the resulting free radicals predominate the radiation response (see later discussion).

Any and all cellular molecules are potential targets for the localized energy deposition events that occur in spurs, blobs, or short tracks. Whether the ionization of a particular biomolecule results in a measurable biological effect depends on a number of factors, including how probable a target the molecule represents from the point of view of the ionizing particle, how important the molecule is to the continued health of the cell, how many copies of the molecule are normally present in the cell and to what extent the cell can react to the loss of working copies, how important the cell is to the structure or function of its corresponding tissue or organ, and so on. DNA, for example, is obviously an important cellular macromolecule, and one that is present only as a single, double-stranded copy. On the other hand, other molecules in the cell may be less crucial to survival, yet are much more abundant than DNA and, therefore, have a much higher probability of being hit and ionized. By far, the most abundant molecule in the cell is water, comprising at least 70% to 80% of the cell on a per weight basis. The highly reactive free radicals formed by the radiolysis of water are capable of augmenting the DNA damage resulting from direct energy absorption by migrating to the DNA and damaging it indirectly. This mechanism is referred to as *indirect radiation action* to distinguish it from the aforementioned *direct radiation action*.<sup>29</sup> The direct and indirect action pathways for ionizing radiation are illustrated below.

#### Direct Effect



#### Indirect Effect



The most highly reactive and damaging species produced by the radiolysis of water is the hydroxyl radical ( $\bullet\text{OH}$ ), although other free radical species are also produced in varying yields.<sup>30,31</sup> Cell killing by indirect action constitutes some 70% of the total damage produced in DNA for low LET radiation.

How do the free radicals produced by the direct and indirect action of ionizing radiation go on to cause the myriad lesions that have been identified in irradiated DNA? Since they contain unpaired electrons, free radicals are highly reactive chemically and will undergo multiple reactions in an attempt to either acquire new electrons or rid themselves of remaining unpaired ones. These reactions are considered quite slow

compared with the time scale of the initial ionization events but are still fast relative to normal enzymatic processes in a typical mammalian cell. For all intents and purposes, free radical reactions are complete within milliseconds of irradiation. The  $\bullet\text{OH}$  radical is capable of both abstraction of hydrogen atoms from other molecules and addition across carbon-carbon or other double bonds. More complex macromolecules that have been converted to free radicals can undergo a series of transmutations in an attempt to rid themselves of unpaired electrons, many of which result in the breakage of nearby chemical bonds. In the case of DNA, these broken bonds may result in the loss of a base or an entire nucleotide, or a frank scission of the sugar phosphate backbone, involving either one or both DNA strands. In some cases, chemical bonds are broken initially but then rearranged, exchanged, or rejoined in inappropriate ways. Bases in DNA may be modified by the addition of one or more hydroxyl groups (e.g., the base thymine converted to thymine glycol), pyrimidines may become dimerized, and/or the DNA may become cross-linked to itself or to associated proteins. Again, because the initial energy deposition events are discrete, the free radicals produced also are clustered and, therefore, undergo their multiple chemical reactions and produce multiple damages in a highly localized area. This has been termed the *locally multiply damaged site*<sup>32</sup> or *cluster*<sup>33</sup> hypothesis. Examples of the types of damage found in irradiated DNA are shown in Fig. 1.5.

### Biochemical Repair of DNA Damage

DNA is unique insofar as it is the only cellular macromolecule with its own repair system. Until as recently as 35 years ago, little was known about DNA repair processes in mammalian cells, particularly because of the complexities involved and the relative lack of spontaneously occurring mutants defective in genes involved with DNA repair. As a consequence, most studies of DNA repair were carried out either in bacteria or yeasts and usually employed UV radiation as the tool for producing DNA damage. Although these were rather simple and relatively clean systems in which to study DNA repair, their relevance to mammalian repair systems and to the broader spectrum of DNA damage produced by ionizing radiation ultimately limited their usefulness.

The study of DNA repair in mammalian cells received a significant boost during the late 1960s with publications by Cleaver<sup>34,35</sup> that identified the molecular defect responsible for the human disease xeroderma pigmentosum (XP). Patients with XP are exquisitely sensitive to sunlight and highly (skin) cancer prone. Cleaver showed that cells derived from such patients were likewise sensitive to UV radiation and defective in the nucleotide excision repair pathway (see later discussion). These cells were not especially sensitive to ionizing radiation, however. Several years later, Taylor et al.<sup>36</sup> reported that cells derived from patients with a second cancer-proneness disorder called ataxia telangiectasia (AT) were extremely sensitive to ionizing radiation and radiation-mimetic drugs, but not UV. In the years that followed, cell cultures derived from patients with these two conditions were used to help elucidate the complicated processes of DNA repair in mammalian cells. Today, dozens of other clinical syndromes associated with radiosensitivity, cancer proneness, or both have been identified.<sup>37,38</sup>

Today, many rodent and human genes involved in DNA repair have been cloned and extensively characterized.<sup>39</sup> Some 30 to 40 proteins participate in excision repair of base damage; about half that many are involved in the repair of strand breaks.<sup>37</sup> Many of these proteins function as component parts of larger repair complexes. Some are interchangeable and participate in other DNA repair and replication pathways as well. It is also noteworthy that some are not involved with the repair process per se, but rather link DNA repair to other cellular functions, including transcription, cell cycle arrest, chromatin remodeling, and apoptosis.<sup>40</sup>

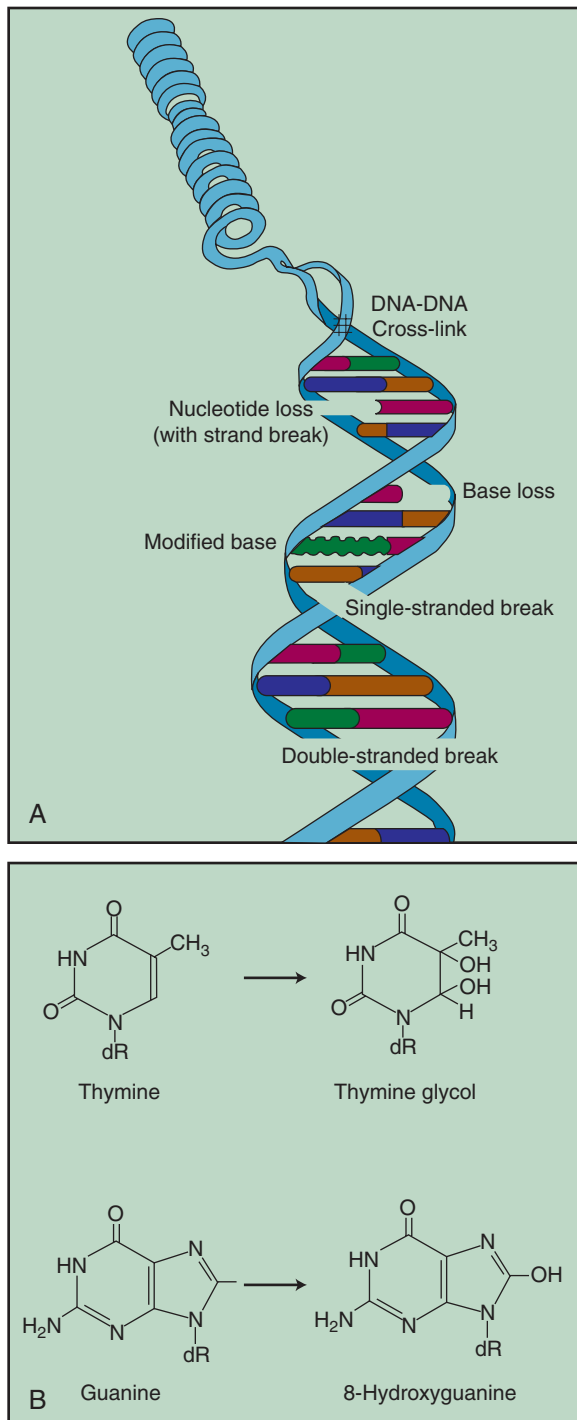


**Fig. 1.5** Types of DNA damage produced by ionizing radiation. (A) Segment of irradiated DNA containing single- and double-stranded breaks, cross-links, and base damage. (B) Two types of modified bases observed in irradiated DNA include thymine glycol, which results from the addition of two hydroxyl (OH) groups across the carbon-carbon double bond of thymine, and 8-hydroxyguanine, produced by  $\cdot\text{OH}$  radical addition to guanine.

This attests to the fact that the maintenance of genomic integrity results from a complex interplay between not only the repair proteins themselves but also others that serve as damage sensors, signaling mediators and transducers, and effectors. Collectively, this complex network of proteins that sense, initiate, and coordinate DNA damage signaling and repair

with other cellular activities is termed the *DNA Damage Response* (DDR).<sup>37,41</sup> For example, the defect responsible for the disease AT is not in a gene that codes for a repair protein but rather in a gene that acts in part as a damage sensor and signal transducer but also participates in a related pathway that normally prevents cells from entering S phase and beginning DNA synthesis while residual DNA damage is present. This is termed the  $G_1$  cell cycle checkpoint response.<sup>42</sup> Because of this genetic defect, AT cells do not experience the normal  $G_1$  arrest after irradiation and enter S phase with residual DNA damage. This accounts both for the exquisite radiosensitivity of AT cells and the resulting genomic instability that can lead to cancer.

The molecular and biochemical intricacies of DNA repair in mammalian cells are described in detail in Chapter 2. A brief overview is also presented next.

### Base Excision Repair

The repair of base damage is initiated by DNA repair enzymes called *glycosylases*, which recognize specific types of damaged bases and excise them without otherwise disturbing the DNA strand.<sup>43</sup> The action of the glycosylase results in the formation of another type of damage observed in irradiated DNA—an apurinic or apyrimidinic (AP) site. The AP site is then recognized by another repair enzyme, an endonuclease that nicks the DNA adjacent to the lesion, in effect creating a DNA single-stranded break. This break then becomes the substrate for an exonuclease, which removes the abasic site, along with a few additional bases. The small gap that results is patched by DNA polymerase using the opposite, hopefully undamaged, DNA strand as a template. Finally, DNA ligase seals the patch in place.

### Nucleotide Excision Repair

The DNA glycosylases that begin the process of base excision repair do not recognize all known forms of base damage, however, particularly bulky or complex lesions.<sup>43</sup> In such cases, another group of enzymes, termed *structure-specific endonucleases*, initiate the excision repair process. These repair proteins do not recognize the specific lesion but rather the structural distortions in DNA that necessarily accompany a complex base lesion. The structure-specific endonucleases incise the affected DNA strand on both sides of the lesion, releasing an oligonucleotide fragment made up of the damage site and several bases on either side of it. After this step, the remainder of the nucleotide excision repair process is similar to that of base excision repair. The gap is then filled by DNA polymerase and sealed by DNA ligase.

For both types of excision repair, active genes in the process of transcription are repaired preferentially and more quickly. This has been termed *transcription-coupled repair*.<sup>44</sup>

### Single-Strand Break Repair

Single-strand breaks (SSBs) in the DNA backbone are common lesions, produced in the tens of thousands per cell per day as part of normal metabolism and respiration<sup>45</sup> on top of any additional breaks introduced by radiation exposure. These are repaired using the machinery of excision repair, that is, gap filling by DNA polymerase and sealing by DNA ligase.

### Double-Strand Break Repair

Despite the fact that unrepaired or misrejoined double-strand breaks (DSBs) often have the most catastrophic consequences for the cell in terms of loss of reproductive integrity,<sup>46</sup> how mammalian cells repair these lesions has been more difficult to elucidate than how they repair base damage. Much of what was originally discovered about these repair processes is derived from studies of x-ray-sensitive rodent cells that were later discovered to harbor specific defects in strand break repair.<sup>47</sup> Since then, dozens of other rodent and human cells characterized

by DDR defects have been identified and are also used to help probe these fundamental processes.

With respect to the repair of DSBs, the situation is more complicated in that the damage on each strand of DNA may be different and, therefore, no intact template would be available to guide the repair process. Under these circumstances, cells must rely on a somewhat error-prone process that rejoins the break(s) regardless of the loss of intervening base pairs for which there is no template (nonhomologous end joining [NHEJ]) or depend on genetic recombination in which a template for presumably error-free repair is obtained from recently replicated DNA of a sister chromatid (homologous recombination [HR]<sup>48</sup>) to cope with the damage. NHEJ occurs throughout the cell cycle, but predominates in cells that have not yet replicated their DNA, that is, cells in the G<sub>1</sub> or G<sub>0</sub> phases of the cell cycle. NHEJ involves a heterodimeric enzyme complex consisting of the proteins Ku-70 and Ku-80, the catalytic subunit of DNA protein kinase (DNA-PK<sub>cs</sub>), and DNA ligase IV. Cells that have already replicated most or all of their DNA—in the late S or G<sub>2</sub> phases of the cell cycle—depend on HR to repair DSBs. HR involves the assembly of a nucleoprotein filament that contains, among others, the proteins Rad51 and Rad52. This filament then invades the homologous DNA sequence of a sister chromatid, which becomes the template for repair. The BRCA2 protein is also implicated in HR as it interacts with the Rad51 protein.<sup>38</sup> Defects in either the *BRCA1* (which helps determine which DSB repair pathway will be used in a particular situation) or *BRCA2* genes are associated with hereditary breast and ovarian cancer.<sup>49</sup>

### Mismatch Repair

The primary role of mismatch repair (MMR) is to eliminate from newly synthesized DNA errors such as base/base mismatches and insertion/deletion loops caused by DNA polymerase.<sup>50</sup> This process consists of three steps: mismatch recognition and assembly of the repair complex, degradation of the error-containing strand, and repair synthesis. In humans, MMR involves at least five proteins, including hMSH2 and hMLH1, as well as other members of the DNA repair and replication machinery.

Radiation-induced DNA lesions are not targets for mismatch repair per se. However, one manifestation of a defect in mismatch repair is germane to any study of oncogenesis: genomic instability,<sup>51</sup> which renders affected cells hypermutable. This “mutator phenotype” is associated with several cancer predisposition syndromes, in particular, hereditary non-polyposis colon cancer (HNPCC, a.k.a. Lynch syndrome).<sup>52,53</sup> Genomic instability is considered one of the main enablers of normal cells to accumulate cancer-causing mutations and also drives tumor progression to more aggressive and potentially treatment-resistant phenotypes.

### The DDR as a Clinical Target

Historically, attempts to inhibit the repair of radiation-induced DNA damage were of interest to researchers probing these fundamental processes. However, clinical translation was typically lacking, mostly out of concern that normal tissues would also be affected in an adverse way. More recently, it has become clear that the cells of many tumors harbor one or more defects in the DDR (as a consequence of genomic instability) that are not present in normal cells and that this difference might be exploitable clinically.

One approach along these lines is the use of inhibitors of the protein poly(ADP-ribose) polymerase (PARP).<sup>54,55</sup> As of 2018, dozens of trials were underway using PARP inhibitors in combination with chemo- and immunotherapies.<sup>56,57</sup> PARP is a damage sensor involved in both base excision and SSB repair that, if inhibited, leads to the persistence of SSBs. If left unrejoined, these breaks can cause the collapse of replication forks in DNA that then impede DNA replication, transcription, and HR repair,<sup>55</sup> leading to radiosensitization and, ultimately, cell death.<sup>58</sup>

In normal cells, little or no toxicity caused by PARP inhibition would be expected, as all DDR pathways are intact and salvage repair pathways to bypass PARP inhibition are active. In tumor cells already harboring defects in HR, however, PARP inhibition would be preferentially toxic. One clinical example is the targeting of breast cancers harboring cellular defects in the BRCA1/2 proteins—which either orchestrate or are directly involved in HR—for PARP inhibition. This overall approach of using the combined lethal effect of two genetic defects (one inherent HR defect plus one synthetic one induced by PARP inhibition) that are otherwise nonlethal singly is termed *synthetic lethality*.<sup>54,55,58</sup> Synthetic lethality approaches targeting DDR proteins (including those other than PARP) likely will play increasingly important roles in the future.

### Cytogenetic Effects of Ionizing Radiation

When cells divide following radiation exposure, chromosomes frequently contain visible structural aberrations that are the result of any unrepaired or misrejoined DNA damage that persists from the time of irradiation. Most chromosome aberrations are lethal to the cell. In some cases, these aberrations physically interfere with the processes of mitosis and cytokinesis, resulting in prompt cell death. In other cases, cell division can occur but the loss or uneven distribution of genetic material between the cell's progeny is ultimately lethal as well, although the affected cells may linger for several days before they die, with some even be able to go through a few more cell divisions in the interim.

Most chromosome aberrations result from an interaction between two damage sites; therefore, they can be grouped into three different types of “exchange” categories. A fourth category is reserved for those chromosome aberrations that are thought to result from a single damage site.<sup>59</sup> These categories are described here; representative types of aberrations from each category are shown in Fig. 1.6:

1. Intra-arm Exchanges: An interaction between lesions on the same arm of a single chromosome (example: interstitial deletion).
2. Inter-arm Exchanges: An interaction between lesions on opposite arms of the same chromosome (example: centric ring).
3. Interchanges: An interaction between lesions on different chromosomes (example: dicentric).
4. “Single Hit” Breaks: The complete severance of part of one arm of a single chromosome not obviously associated with any more than a single lesion (example: terminal deletion).

These four categories can be further subdivided according to whether the initial radiation damage occurred before or after the DNA is replicated (a chromosome- vs. chromatid-type aberration, respectively) and, for the three exchange categories, whether the lesion interaction is symmetrical or asymmetrical. Asymmetrical exchanges always lead to the formation of acentric fragments that are usually lost in subsequent cell divisions and, therefore, are nearly always fatal to the cell. These fragments may be retained transiently in the cell's progeny as extranuclear chromatin bodies called *micronuclei*. Symmetrical exchanges are more insidious in that they do not lead to the formation of acentric fragments and the accompanying loss of genetic material at the next cell division; thus, they do not always kill the cell. As such, they will be transmitted to all progeny of the original cell. Some types of symmetrical exchanges (e.g., a reciprocal translocation) have been implicated in radiation carcinogenesis insofar as they have the net effect of either bringing new combinations of genes together or separating preexisting groups of genes.<sup>28</sup> Depending on where in the genome the translocation takes place, genes normally active could be turned off or vice versa, potentially with adverse consequences.

Quantitation of the types and frequencies of chromosome aberrations in irradiated cells can be used to probe dose-response relationships for ionizing radiation and, to a first approximation, also can serve as a radiation dosimeter. For example, the dose-response curve for the

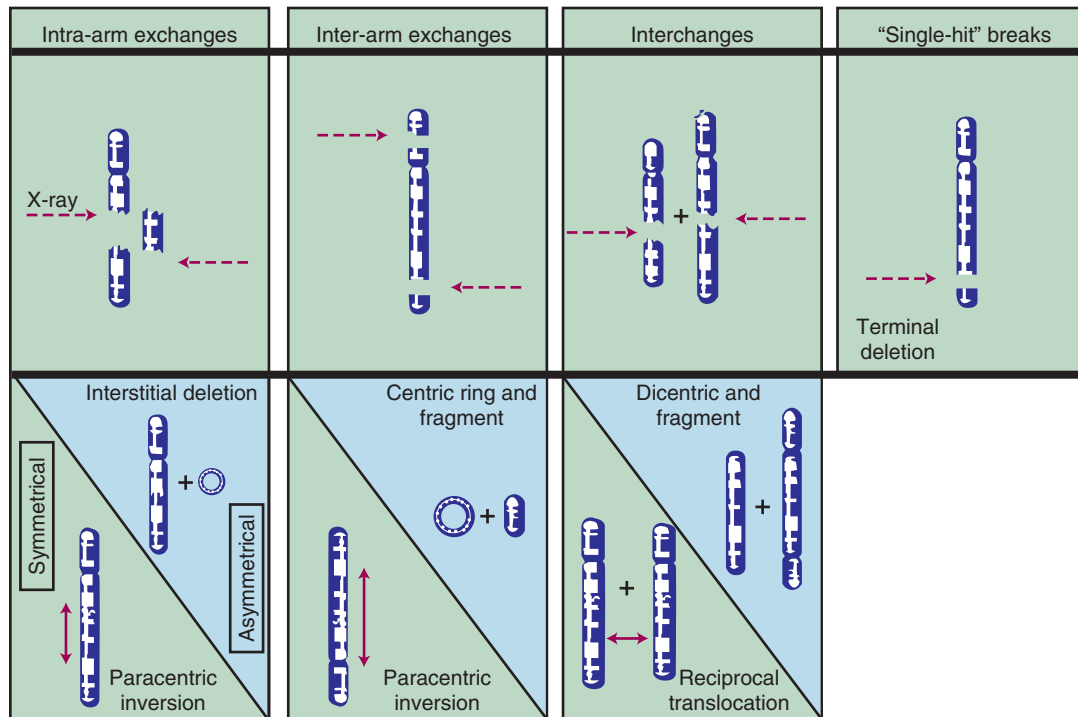


**Fig. 1.6** Types of radiation-induced chromosome aberrations that are the result of unrepaired or misrejoined DNA damage. Aberrations are classified according to whether they involve a single or multiple chromosomes, whether the damage is thought to be caused by the passage of a single charged particle track (“one-hit” aberration), or by the interaction of damages produced by two different tracks (“two-hit” aberration), and whether the irradiation occurred prior to or after the chromosomes had replicated (chromosome- vs. chromatid-type aberrations, respectively; only chromosome-type aberrations are shown). The aberrations can be further subdivided according to whether broken pieces of the chromosome rearrange themselves symmetrically (with no net loss of genetic material) or asymmetrically (acentric fragments produced).

induction of exchange-type aberrations after exposure to low-LET radiation tends to be linear-quadratic in shape, whereas that for single-hit aberrations tends to be linear. In mathematical terms, the incidence,  $I$ , of a particular aberration as a function of radiation dose,  $D$ , can be expressed as

$$I = \alpha D + \beta D^2 + c \quad \text{for exchange-type aberrations}$$

$$I = \alpha D + c \quad \text{for single-hit aberrations,}$$

where  $\alpha$  and  $\beta$  are proportionality constants related to the yields of the particular type of aberration and  $c$  is the spontaneous frequency of that aberration in unirradiated cells. For fractionated doses or continuous low dose rates of low-LET radiation, the yield of exchange-type aberrations decreases relative to that for acute doses, and the dose-response curve becomes more linear. For high-LET radiations, dose-response curves become steeper (higher aberration yields per unit dose) and more linear compared with those for low-LET radiations.

## Cell Survival Curves and Survival Curve Theory

### What Is Meant by “Cell Death”?

The traditional definition of death as a permanent, irreversible cessation of vital functions is not the same as what constitutes “death” to the radiation biologist or oncologist. For proliferating cells—including those maintained *in vitro*, the stem cells of normal tissues, and tumor clonogens—cell death in the radiobiological sense refers to a loss of reproductive integrity, that is, an inability to sustain proliferation indefinitely. This type of “reproductive” or “clonogenic” death does not

preclude the possibility that a cell may remain physically intact, metabolically active, and continue its tissue-specific functions for some time after irradiation.<sup>60</sup>

Compared with nearly 65 years ago, when the term *clonogenic death* was first coined and used as an endpoint in assays of cellular radiosensitivity,<sup>27,61</sup> by today’s standards it is clearly an operationally defined term that encompasses several distinct mechanisms by which cells die, all of which result in a cell losing its ability to divide indefinitely. These modes of cell death include mitotic catastrophe, apoptosis, necrosis, senescence, and autophagy. Strictly speaking, differentiation is included as well, because differentiated cells lose their ability to divide.<sup>62,63</sup>

Mitotic catastrophe is the major mode of radiation-induced death for most mammalian cells, occurring secondary to chromosome aberrations and/or spindle defects that interfere with the cell division process.<sup>64,65</sup> Accordingly, this type of cell death occurs during or soon after an attempted cell division postirradiation (although not necessarily during the very first division attempt), leaving in its wake large, flattened, and multinucleated cells that are typically aneuploid. Apoptosis, or programmed cell death, is a type of nonmitotic or interphase death commonly associated with embryonic development and normal tissue remodeling and homeostasis.<sup>66</sup> However, certain normal tissue and tumor cells also undergo apoptosis following irradiation, including normal cells of hematopoietic or lymphoid origin, crypt cells of the small intestine, salivary gland cells, plus a few tumor cell lines of gynecological and hematological origin.<sup>67</sup> Cells undergoing apoptosis exhibit a number of characteristic morphological (nuclear condensation and fragmentation, membrane blebbing, etc.) and biochemical (DNA degradation) changes that culminate in the fragmentation of the cell, typically within 12 to



24 hours of irradiation and prior to the first postirradiation mitosis. The remains of apoptotic cells are phagocytized by neighboring cells; therefore, they do not elicit the type of inflammatory response, tissue destruction, and disorganization characteristic of necrosis. Apoptosis is an active and carefully regulated pathway that involves multiple proteins and an appropriate stimulus that activates the pathway. The molecular biology of apoptosis, the apoptosis-resistant phenotype noted for many types of tumor cells, and the role that radiation may play in the process are discussed in detail in Chapter 2. Senescence refers to a type of genetically controlled cellular growth arrest that, while not necessarily eliminating damaged cells, does halt permanently their continued movement through the cell cycle even in the presence of growth factors.<sup>68</sup> Radiation can also induce senescence, presumably due to the permanent triggering of cell cycle checkpoints. However, it might better be termed *radiation-induced permanent growth arrest* to distinguish it from the normal process of cell age-related senescence.<sup>69</sup> Autophagy is defined as the controlled lysosomal degradation of cytoplasmic organelles or other cytoplasmic components<sup>70,71</sup> in response to cellular stressors, including nutrient deprivation, hypoxia, DNA damage, or an excess of reactive oxygen species. Likewise, necrosis—characterized by cell swelling followed by membrane rupture and the release of cellular contents into the extracellular space—can occur as a somewhat passive response to nutrient deprivation but also can follow a molecular program initiated by immune cells or various toxins.<sup>72,73</sup>

Most assays of radiosensitivity of cells and tissues, including those described later, use reproductive integrity, either directly or indirectly, as an endpoint. While such assays have served the radiation oncology community well in terms of elucidating dose-response relationships for normal tissues and tumors, the interrelationships between the different modes of cell death can be quite complex. For example, Meyn<sup>67</sup> has suggested that a tumor with a high spontaneous apoptotic index may be inherently more radiosensitive because cell death might be triggered by lower doses than are usually required to cause mitotic catastrophe. Also, tumors that readily undergo apoptosis may have higher rates of cell loss, the net effect of which would be to partially offset cell production, thereby reducing the number of tumor clonogens. On the other hand, recent studies suggest that the very enzymes that orchestrate the removal of radiation-damaged cells via apoptosis also may stimulate tumor cell repopulation during and after radiotherapy.<sup>74</sup> Studies also suggest that senescent cells can produce inflammatory cytokines that further contribute to immunosuppression in the tumor microenvironment.<sup>68</sup>

### Cell Survival and Dose-Response Curve Models

Survival curve theory originated in a consideration of the physics of energy deposition in matter by ionizing radiation. Early experiments with macromolecules and prokaryotes established that dose-response relationships could be explained by the random and discrete nature of energy absorption if it was assumed that the response resulted from critical “targets” receiving random “hits.”<sup>75</sup> With an increasing number of shouldered survival and dose-response curves being described for cells irradiated both *in vitro* and *in vivo*, various equations were developed to fit these data. Target theory pioneers studied a number of different endpoints in the context of target theory, including enzyme inactivation in cell-free systems,<sup>29</sup> cellular lethality, chromosomal damage, and radiation-induced cell cycle perturbations in microorganisms.<sup>29,76</sup> Survival curves, in which the log of the “survival” of a certain biological activity was plotted as a function of the radiation dose, were found to be either exponential or sigmoid in shape, the latter usually noted for the survival of more complex organisms.<sup>29</sup>

Exponential survival curves were thought to result from the single-hit, “all or nothing” inactivation of a single target, resulting in the loss of

activity. A mathematical expression used to fit this type of dose-response relationship is

$$S = e^{-D/D_0}$$

In this equation,  $S$  is the fraction of cells that survive a given dose,  $D$ , and  $D_0$  is the dose increment that reduces the cell survival to 37% ( $1/e$ ) of some initial value on the exponential portion of the curve (i.e., a measure of the reciprocal of the slope). Target theory could also be applied to survival curves with shoulders at low doses if one assumed that either multiple targets or multiple hits in a single target were necessary for radiation inactivation. A mathematical expression based on target theory that provided a fairly good fit to survival data was

$$S = 1 - (1 - e^{-D/D_0})^n$$

with  $n$  being the back extrapolation of the exponential portion of the survival curve to zero dose. Implicit in this multitarget model was that damage had to accumulate before the overall effect was registered.

It soon became apparent that some features of this model were inadequate.<sup>77</sup> The most obvious problem was that the single-hit, multitarget equation predicted that survival curves should have initial slopes of zero, that is, that for vanishingly small doses (e.g., repeated, small doses per fraction or continuous low dose rate exposure), the probability of cell killing would approach zero. This is not what was observed in practice for either mammalian cell survival curves or as inferred from clinical studies in which highly fractionated or low dose rate treatment schedules were compared to more conventional fractionation. There was no fractionation schedule that produced essentially no cell killing, all other radiobiological factors being equal.

A somewhat different interpretation of cell survival was proposed by Kellerer and Rossi<sup>78</sup> in the late 1960s and early 1970s. The linear-quadratic or “alpha-beta” equation,

$$S = e^{-(\alpha D + \beta D^2)}$$

was shown to fit many survival data quite well, particularly in the low-dose region of the curve, and also provided for the negative initial slope that investigators had described.<sup>77</sup> In this expression,  $S$  is again the fractional cell survival following a dose  $D$ ,  $\alpha$  is the rate of cell kill by a single-hit process, and  $\beta$  is the rate of cell kill by a two-hit mechanism. The theoretical derivation of the linear-quadratic equation is based on two sets of observations. Based on microdosimetric considerations, Kellerer and Rossi<sup>78</sup> proposed that a radiation-induced lethal lesion resulted from the interaction of two sublesions. According to this interpretation, the  $\alpha D$  term is the probability of these two sublesions being produced by a single event (the “intra-track” component), whereas  $\beta D^2$  is the probability of the two sublesions being produced by two separate events (the “inter-track” component). Chadwick and Leenhouts<sup>79</sup> derived the same equation based on a different set of assumptions, namely, that a DSB in DNA was a lethal lesion and that such a lesion could be produced by either a single energy deposition involving both strands of DNA or by two separate events, each involving a single strand.

A comparison of the features and parameters of the target theory and linear-quadratic survival curve expressions is shown in Fig. 1.7.

### Clonogenic Assays In Vitro

As mentioned previously, it was not until the mid-1950s that mammalian cell culture techniques were sufficiently refined to allow quantitation of the radiation responses of single cells.<sup>61,80</sup> Puck and Marcus's acute



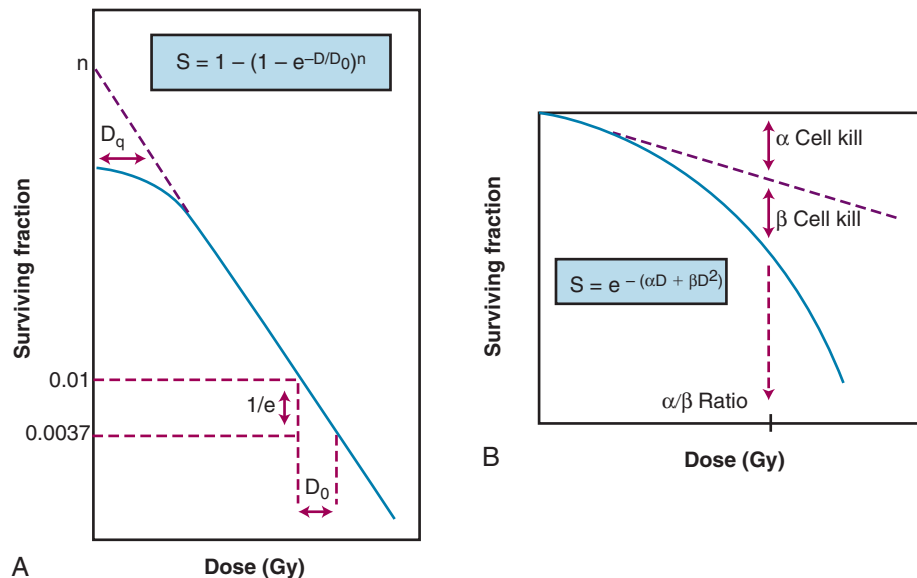


**Fig. 1.7** A comparison of two mathematical models commonly used to fit cell survival curve data. (A) The single-hit, multi-target model and its associated parameters,  $D_0$ ,  $n$ , and  $D_q$ . Although this model has since been invalidated, values for its parameters are still used for comparative purposes. (B) The linear-quadratic model and its associated parameters,  $\alpha$  and  $\beta$ . This model provided the conceptual framework for current isoeffect formulae used in radiation therapy treatment planning.

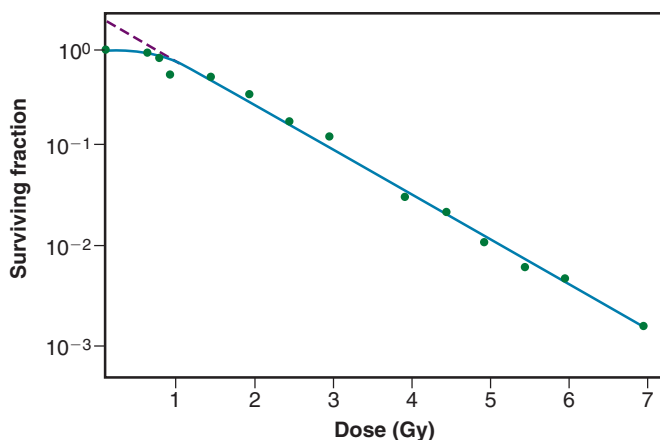


**Fig. 1.8** Clonogenic survival of HeLa cells in vitro as a function of x-ray dose. Like many mammalian cells of both tumorigenic and nontumorigenic origin, the HeLa cell survival curve is characterized by a modest initial shoulder region ( $n \approx 2.0$ ) followed by an approximately exponential final slope ( $D_0 \approx 1.0$  Gy). (Modified from Puck TT, Marcus PI. Action of x-rays on mammalian cells. *J Exp Med.* 1956;103:653.)

dose, x-ray survival curve for the human tumor cell line HeLa is shown in Fig. 1.8. Following graded x-ray doses, the reproductive integrity of single HeLa cells was measured by their ability to form macroscopic colonies of at least 50 cells (corresponding to approximately 6 successful postirradiation cell divisions) on petri dishes. Several features of this survival curve were of particular interest. First, qualitatively at least, the curve was similar in shape to those previously determined for many microorganisms, being characterized by a shoulder at low doses and a roughly exponential region at high doses. Of note, however, was the finding that the  $D_0$  for HeLa cells was only 96 R, some 10- to 100-fold less than  $D_0$ s determined for microorganisms and 1000- to 10,000-fold less than  $D_0$ s for the inactivation of isolated macromolecules.<sup>60</sup> Thus, cellular reproductive integrity was found to be a much more radiosensitive

endpoint for HeLa cells than for prokaryotes or primitive eukaryotes. The value of the extrapolation number,  $n$ , was approximately 2.0, indicating that the survival curve did have a small shoulder but, again, much smaller than typically observed for microorganisms. Puck and Marcus suggested that the  $n$  value was a reflection of the number of critical targets in the cell, each requiring a single hit before the cell would be killed, and further postulated that the targets were, in fact, the chromosomes themselves.<sup>27</sup> However, the potential pitfalls of deducing mechanisms of radiation action from parameters of a descriptive survival curve model were soon realized.<sup>81,82</sup>

Survival curves for other types of mammalian cells, regardless of whether they were derived from humans or laboratory animals, or from tumors or normal tissues, have been shown to be qualitatively similar to the original HeLa cell survival curve.

### Clonogenic Assays In Vivo

In order to bridge the gap between the radiation responses of cells grown in culture and in an animal, Hewitt and Wilson developed an ingenious method to assay single-cell survival in vivo.<sup>83</sup> Lymphocytic leukemia cells obtained from the livers of donor CBA mice were harvested, diluted, and inoculated into disease-free recipient mice. By injecting different numbers of donor cells, a standard curve was constructed that allowed a determination of the average number of injected cells necessary to cause leukemia in 50% of the recipient mice. It was determined that the endpoint of this titration, the 50% take dose ( $TD_{50}$ ), corresponded to an inoculum of a mere two leukemia cells. Using this value as a reference, Hewitt and Wilson then injected leukemia cells harvested from  $\gamma$ -irradiated donor mice into recipients and again determined the  $TD_{50}$  following different radiation exposures. In this way, the surviving fraction after a given radiation dose could be calculated from the ratio of the  $TD_{50}$  for unirradiated cells to that for the irradiated cells. Using this technique, a complete survival curve was constructed that had a  $D_0$  of 162 R and an  $n$  value close to 2.0, values quite similar to those generated for cell lines irradiated in vitro. For the most part, in vivo survival curves for a variety of cell types were also similar to corresponding in vitro curves.

A similar trend was apparent when *in vivo* survival curves for nontumorigenic cells were first produced. The first experiments by Till and McCulloch<sup>84,85</sup> using normal bone marrow stem cells were inspired by the knowledge that failure of the hematopoietic system was a major cause of death following total body irradiation and that lethally irradiated animals could be “rescued” by a bone marrow transplant. The transplanted, viable bone marrow cells were observed to form discrete nodules or colonies in the otherwise sterilized spleens of irradiated animals. Subsequently, these authors transplanted known quantities of irradiated donor bone marrow into lethally irradiated recipient mice. They were able to count the resulting splenic nodules and then calculate the surviving fraction of the injected cells in much the same way as was done for *in vitro* experiments. The  $D_0$  for mouse bone marrow was 0.95 Gy.<sup>84</sup> Other *in vivo* assay systems based on the counting of colonies or nodules included the skin epithelium assay of Withers,<sup>86</sup> the intestinal crypt assays of Withers and Elkind,<sup>87,88</sup> and the lung colony assay of Hill and Bush.<sup>89</sup> During the late 1960s and early 1970s, it also became possible to do excision assays, in which tumors irradiated *in vivo* were removed, enzymatically dissociated, and single cells plated for clonogenic survival *in vitro*. This allowed more quantitative measurement of survival, avoiding some of the pitfalls of *in vivo* assays (e.g., Rockwell and Kallman<sup>90</sup>).

### Nonclonogenic Assays In Vivo

Some normal tissues and tumors are not amenable to clonogenic assays. Thus, new assays were needed that had clinical relevance yet did not rely on reproductive integrity as an endpoint. Use of such assays required one leap of faith—namely, that the endpoints assessed would have to be a consequence of the killing of clonogenic cells, although not necessarily in a direct, one-to-one manner. Because nonclonogenic assays do not directly measure cell survival as an endpoint, data derived from them and plotted as a function of radiation dose are properly called dose-response curves rather than cell survival curves, although such data are often analyzed and interpreted similarly.

Historically, among the first nonclonogenic assays was the mean lethal dose or  $LD_{50}$  assay, in which the (whole body) radiation dose to produce lethality in approximately 50% of the test subjects is determined, usually at a fixed time after irradiation, such as 30 ( $LD_{50/30}$ ) or 60 days ( $LD_{50/60}$ ). Clearly, the  $LD_{50}$  assay is not very specific in that the cause of death can result from damage to a number of different tissues.

Another widely used nonclonogenic method to assess normal tissue radioresponse is the skin reaction assay, originally developed by Fowler et al.<sup>91</sup> Pigs were often used because their skin is similar to that of humans in several respects. An ordinate scoring system was used to compare and contrast different radiation schedules, which was derived from the average severity of the skin reaction noted during a certain time period (specific to the species and whether the endpoint occurs early or late) following irradiation. For example, for early skin reactions, a skin score of 1 might correspond to mild erythema, whereas a score of 4 might correspond to confluent moist desquamation over more than half of the irradiated area.

Finally, two common nonclonogenic assays for tumor response are the growth delay/regrowth delay assay<sup>92</sup> and the tumor control dose assay.<sup>93</sup> Both assays are simple and direct, are applicable to most solid tumors, and are clinically relevant. The growth delay assay involves measurements of a tumor's dimensions or volume as a function of time after irradiation. For tumors that regress rapidly during and after radiotherapy, the endpoint scored is typically the time in days that it takes for the tumor to regrow to its original volume at the start of irradiation. For tumors that regress more slowly, a more appropriate endpoint might be the time that it takes for the tumor to grow or regrow to a specified size, such as three times its original volume.

Dose-response curves are generated by plotting the amount of growth delay as a function of radiation dose.

The tumor control assay is a logical extension of the growth delay assay. The endpoint of this assay is the total radiation dose required to achieve a specified probability of local tumor control—usually 50% ( $TCD_{50}$ )—in a specified period of time after irradiation. The  $TCD_{50}$  value is obtained from a plot of the percentage of tumors locally controlled as a function of total dose. The slope of the resulting dose-response curve may be used for comparative purposes as a measure of the tumor's inherent “radiosensitivity” and/or its degree of heterogeneity. More heterogeneous tumors tend to have shallower dose response curves than more homogeneous ones, as do spontaneous tumors relative to experimental ones maintained in inbred strains of mice.

### Cellular “Repair”: Sublethal and Potentially Lethal Damage Recovery

Taking the cue from target theory that the shoulder region of the radiation survival curve indicated that “hits” had to accumulate prior to cell killing, Elkind and Sutton<sup>94,95</sup> sought to better characterize the nature of the damage caused by these hits and how the cell processed this damage. Even in the absence of any detailed information about DNA damage and repair at the time, a few things seemed obvious. First, those hits or damages that were registered as part of the accumulation process yet did not in and of themselves produce cell killing were, by definition, sublethal. Second, sublethal damage (SLD) became lethal only when it interacted with additional sublethal damage, that is, when the total amount of damage had accumulated to a sufficient level to cause cell killing. But what would be the result of deliberately interfering with the damage accumulation process by, for example, delivering part of the intended radiation dose, inserting a radiation-free interval, and then delivering the remainder of the dose? The results of such “split-dose” experiments turned out to be crucial to the understanding of why and how fractionated radiation therapy works as it does. The discovery and characterization of SLD, as low tech and operational the concept may be by today's standards, still stands as arguably the single most important contribution that radiation biology has made to the practice of radiation oncology.

By varying the time interval between two doses of approximately 5.0 Gy and plotting the log of the surviving fraction of cells after both doses (i.e., 10 Gy total dose) as a function of the time between the doses, the resulting split-dose recovery curve was observed to rise to a maximum after about 2 hours and then level off. In other words, the overall surviving fraction of cells following 10 Gy was higher if the dose was split into two fractions with a time interval in between than delivered as a single dose. Elkind interpreted these results as indicating that the cells that survived the initial dose fraction had “repaired” some of the damage during the radiation-free interval and, as such, this damage was no longer available to interact with the damage inflicted by the second dose. At the time, Elkind referred to this phenomenon as *sublethal damage repair* (SLDR). In retrospect, it is perhaps preferable to call it *sublethal damage recovery*, since biochemical DNA repair processes were not actually measured, only changes in cell survival.

Of additional interest was the observation that the shape of the split-dose recovery curve varied with the temperature during the radiation-free interval (Fig. 1.9). When the cells were maintained at room temperature between the split doses, the SLDR curve rose to a maximum after about 2 hours and then leveled off. When the cells were returned to a 37° C incubator for the radiation-free interval, a different pattern emerged. Initially, the split-dose recovery curve rose to a maximum after 2 hours; then, the curve exhibited a series of oscillations, dropping to a second minimum for a split of about 4 to 5 hours, and then rising again to a higher maximum for split-dose intervals of 10

hours or more. The interpretation of this pattern of SLDR was that other radiobiological phenomena operated simultaneously with cellular recovery. In this case, the fine structure of the split-dose recovery curve was not caused by an oscillating repair process but rather by a superimposed cell cycle effect: the so-called radiation “age response” through the cell cycle. This is discussed later in the “Ionizing Radiation and the Cell Cycle” section (see also Fig. 1.14).

Since Elkind and Sutton’s original work, SLDR kinetics have been described for many different types of mammalian cells in culture,<sup>60</sup> and for most normal and tumor tissues in vivo (e.g., Belli et al.<sup>96</sup> and Emery et al.<sup>97</sup>). Pertinent findings include the following:

1. The amount of SLD capable of being repaired for a given cell type varies both with the radiation quality (less for radiations of increasing

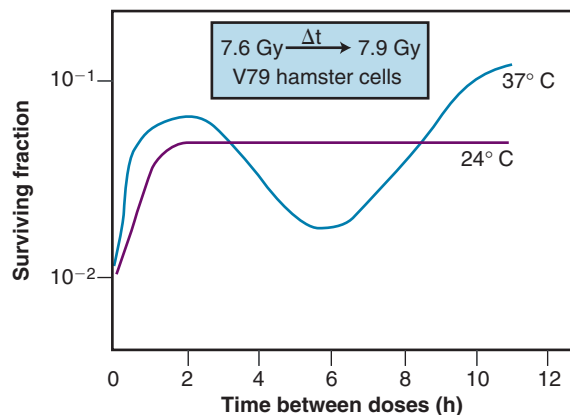


**Fig. 1.9** “Split-dose” or sublethal damage recovery demonstrated in cultured hamster V79 cells that received a first x-ray dose at time = 0, followed by a second dose after a variable radiation-free interval. Cells were maintained at either room temperature (24° C) or at 37° C during the “split” time. (Modified from Elkind M, Sutton-Gilbert H, Moses W, et al. Radiation response of mammalian cells grown in culture. V. Temperature dependence of the repair of x-ray damage in surviving cells (aerobic and hypoxic). *Radiat Res.* 1965;25:359.)

LET) and the oxygenation status of the cells (recovery reduced or absent at extremely low oxygen tensions).<sup>28</sup>

2. The half-time for SLDR in mammalian cells in culture is, on average, about 1 hour, although there is evidence that it may be somewhat longer for late-responding normal tissues in vivo.<sup>28</sup>
3. The survival increase between split doses is a manifestation of the “regeneration” of the shoulder of the radiation survival curve. After an initial radiation dose and an adequate time interval for SLDR, the response of surviving cells to graded additional doses is nearly identical to that obtained from cells without previous radiation exposure. Thus, the width of the shoulder of the survival curve came to be associated with the capacity of the cells for recovery from sublethal damage. This concept is illustrated in Fig. 1.10.
4. Cells are able to undergo repeated cycles of damage and recovery without a change in recovery capacity. As such, one would predict an equal effect per dose fraction during the course of fractionated radiotherapy. In a more practical sense, this means that a multifraction survival curve can be generated using the formula  $SF_n = (SF_1)^n$ , where  $SF_1$  is the surviving fraction of cells after a single-dose fraction (determined from a single-dose survival curve), and  $SF_n$  is the surviving fraction of cells after  $n$  dose fractions. Accordingly, multifraction survival curves are shoulderless and exponential (Fig. 1.11).
5. Sublethal damage recovery is largely responsible for the *dose rate effect* for low-LET radiation, which will be discussed in detail later in this chapter. As the dose per fraction (intermittent radiation) or dose rate (continuous irradiation) is decreased and the overall treatment time increased, the biological effectiveness of a given total dose is reduced. (Note that SLDR also occurs during continuous irradiation, i.e., that a radiation-free interval is not required per se.)

A second type of cellular recovery following irradiation is termed *potentially lethal damage repair or recovery* (PLDR), and was first described for mammalian cells by Phillips and Tolmach<sup>98</sup> in 1966. PLDR is, by definition, a spectrum of radiation damage that may or may not result in cell killing depending on the cell’s postirradiation environment. Environmental conditions that favor PLDR include maintenance of cells in overcrowded conditions (plateau phase or contact-inhibited<sup>99,100</sup>) and

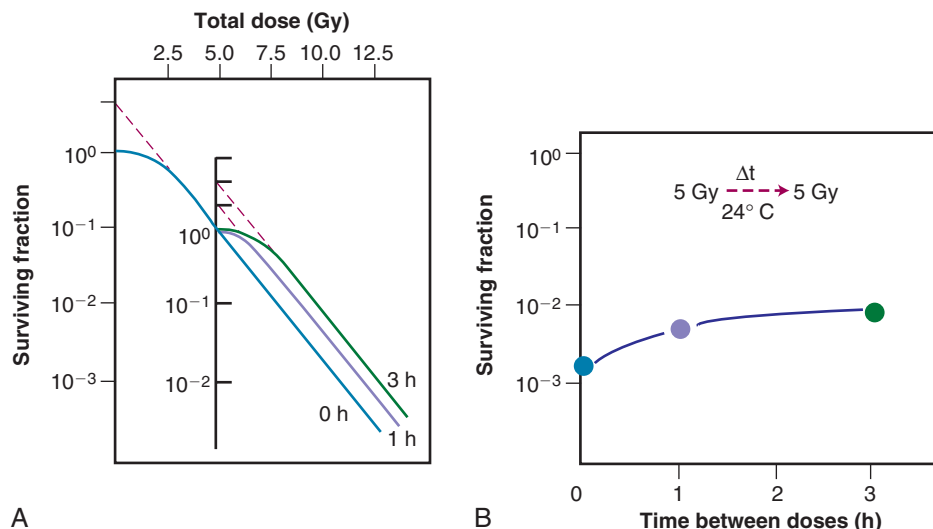


**Fig. 1.10** Sublethal damage recovery is also manifest as a return of the shoulder on the radiation survival curve when a total dose is delivered as two fractions separated by a time interval (A). If the interfraction interval is shorter than the time it takes for this recovery to occur, the shoulder will be only partially regenerated (e.g., compare the shoulder regions of the survival curves for intervals of 1 h vs. 3 h). The regeneration of the shoulder accounts for the observed survival increase in the corresponding split-dose assay (B, and Fig. 1.9).

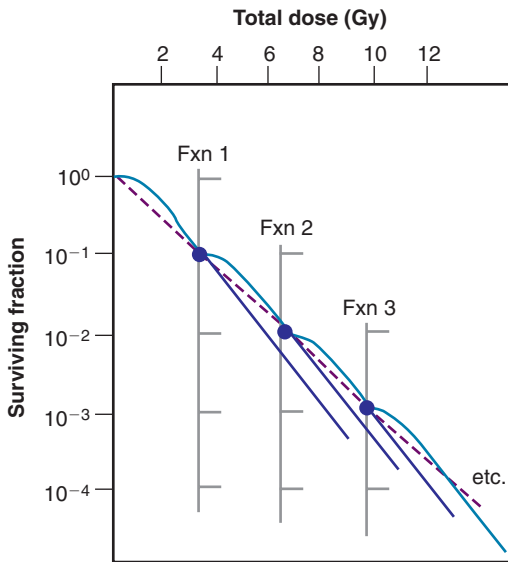
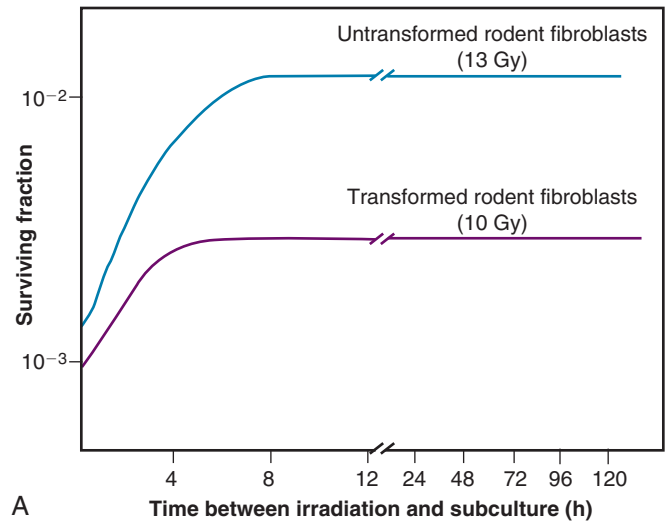


**Fig. 1.11** Hypothetical multifraction survival curve (dashed line) for repeated 3.0 Gy fractions under conditions in which sufficient time between fractions is allowed for full sublethal damage recovery, and cell cycle and proliferative effects are negligible. The multifraction survival curve is shallower than its corresponding single dose curve (solid lines) and has no shoulder, that is, surviving fraction is an exponential function of total dose.

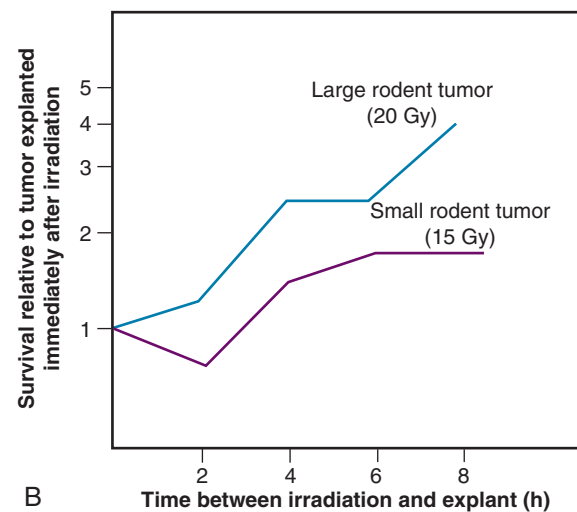
incubation following irradiation at either reduced temperature<sup>101</sup> in the presence of certain metabolic inhibitors<sup>98</sup> or in balanced salt solutions rather than complete culture medium.<sup>101</sup> What these treatment conditions have in common is that they are suboptimal for continued growth of cells. This gives resting cells more opportunity to repair DNA damage prior to cell division than cells that continue traversing the cell cycle immediately after irradiation. Phillips and Tolmach<sup>98</sup> were the first to propose this repair-fixation or competition model to explain PLDR.

While, admittedly, some of these postirradiation conditions are not likely to be encountered *in vivo*, slow growth of cells in general, with or without a large fraction of resting cells, is a common characteristic of many tissues. As might be expected, tumors (and, subsequently, select normal tissues amenable to clonogenic assay) were shown to repair PLD.<sup>100</sup> Experiments using rodent tumors were modeled after comparable studies using plateau phase cells in culture, that is, a delayed-plating assay was used. For such an experiment, irradiated cell cultures or animal tumors are left in a confluent state (either in the overcrowded cell culture or in the intact tumor in the animal) for varying lengths of time before removing them, dissociating them into single-cell suspensions and plating the cells for clonogenic survival at a low density. The longer the delay between irradiation and the clonogenic assay, the higher the resulting surviving fraction of individual cells, even though the radiation dose is the same. In general, survival rises to a maximum within 4 to 6 hours and levels off thereafter (Fig. 1.12).

The kinetics and extent of recovery from both SLD and PLD are correlated with the molecular repair of DNA and the rejoining of chromosome breaks.<sup>102,103</sup> For the purposes of radiation therapy, however, the most important consideration is that both processes have the potential to increase the surviving fraction of cells between subsequent dose fractions. Such a survival increase could be manifest clinically as either increased normal tissue tolerance or decreased tumor control. It is also important to appreciate that small differences in recovery capacity between normal and tumor cells after a single-dose fraction are magnified into large differences after 30 or more dose fractions.



A



B

**Fig. 1.12** Potentially lethal damage recovery can be demonstrated using a “delayed-plating” assay in which a variable delay time is inserted between exposure to a large single dose of radiation and the harvesting of the cells for a clonogenic assay. If cells are maintained in overcrowded and/or nutrient-deprived conditions during the delay period, the surviving fraction increases relative to that obtained when there is no delay. (A) Potentially lethal damage recovery *in vitro* in a nontumorigenic rodent fibroblast cell line and its transformed tumorigenic counterpart. (B) Potentially lethal damage recovery *in vivo* in both small and large mouse fibrosarcomas. (A, Modified from Zeman E, Bedford J. Dose-rate effects in mammalian cells. V. Dose fractionation effects in noncycling C3H 10T1/2 cells. *Int J Radiat Oncol Biol Phys.* 1984;10:2089; B, modified from Little J, Hahn G, Frindel E, et al. Repair of potentially lethal radiation damage *in vitro* and *in vivo*. *Radiology.* 1973;106:689.)

### Repair in Tissues

When considering the repair phenomenon in intact tissues, it is important to remember that both the magnitude of the repair (related both to the shape of the shoulder region of the corresponding dose-response curve and the dose delivered) and the rate of the repair can influence how the tissue behaves during a course of radiation therapy. For example, a particular tissue—normal or tumor—may be quite capable of repairing most damage produced by each dose fraction, but if the interfraction interval is so short as to not allow all the damage to be repaired prior to the next dose, the tolerance of that tissue will be less than otherwise anticipated. Second, while the sparing effect of dose fractionation for

both normal and tumor tissues can be explained largely by SLD recovery between fractions, at sufficiently small doses per fraction, the degree of sparing will reach a maximum below which no further sparing occurs, all other radiobiological factors being equal. This is a reflection of the fact that some radiation damage is necessarily lethal and not modifiable by either further fractionation or changing postirradiation conditions.

### Ionizing Radiation and the Cell Cycle

Another basic feature of the cellular response to ionizing radiation is perturbation of the cell cycle. Such effects can modify the radioresponsiveness of tissues either directly or indirectly depending on the fraction of cycling cells present in the tissue, their proliferation rates, and the kinetic organization of the tissue or tumor.

Advances in techniques for the study of cell cycle kinetics during the 1950s and 1960s paved the way for the generation of survival curves as a function of cell "age." Using a technique known as autoradiography, Howard and Pelc<sup>104</sup> were able to identify the S, or DNA synthesis, phase of the cell cycle. When combined with the other obvious cell cycle marker, mitosis, they were able to discern the four phases of the cell cycle for actively growing cells: G<sub>1</sub>, S, G<sub>2</sub>, and M.

### Methodology

Several techniques were subsequently developed for the collection of synchronized cells *in vitro*. One of the most widely used was the mitotic harvest or "shake-off" technique first described by Terasima and Tolmach.<sup>105,106</sup> By agitating cultures, mitotic cells, which tend to round up and become loosely attached to the culture vessel's surface, can be dislodged, collected along with the overlying growth medium, and inoculated into new culture flasks. By incubating these flasks at 37° C, cells begin to proceed synchronously into G<sub>1</sub> phase (and semi-synchronously thereafter). Thus, by knowing the length of the various phase durations for the cell type being studied and then delivering a radiation dose at a time of interest after the initial synchronization, the survival response of cells in different phases of the cell cycle can be determined.

A second synchronization method involved the use of DNA synthesis inhibitors such as fluorodeoxyuridine<sup>107</sup> and, later, hydroxyurea<sup>108</sup> to selectively kill S phase cells yet allow cells in other phases to continue cell cycle progression until they become blocked at the border of G<sub>1</sub> and S phases. By incubating cells in the presence of these inhibitors for times sufficient to collect nearly all cells at the block point, large numbers of cells can be synchronized. The inhibitor technique has two other advantages: that some degree of synchronization is possible *in vivo*<sup>109</sup> as well as *in vitro* and that, by inducing synchrony at the end of the G<sub>1</sub> phase, a higher degree of synchrony can be maintained for longer periods than if synchronization had been at the beginning of G<sub>1</sub>. On the other hand, the mitotic selection method does not rely on the use of drugs that could perturb the normal cell cycle kinetics of the population.

Developments in the early 1970s provided what is now considered among the most valuable tools for the study of cytokinetic effects: the flow cytometer and its offshoot, the fluorescence-activated cell sorter.<sup>110</sup> These have largely replaced the aforementioned longer and more labor-intensive cell cycle synchronization methods. Using this powerful technique, single cells are stained with a fluorescent probe that binds stoichiometrically to a specific cellular component, DNA in the case of cell cycle distribution analysis. The stained cells are then introduced into a pressurized flow cell and forced to flow single file and at a high rate of speed through a focused laser beam that excites the fluorescent dye. The resulting light emission from each cell is collected by photomultiplier tubes, recorded, and output as a frequency histogram of cell number as a function of relative fluorescence, with the amount of fluorescence directly proportional to DNA content. Accordingly, cells with

a "1X" DNA content would correspond to cells in G<sub>1</sub> phase, cells with a "2X" DNA content in G<sub>2</sub> or M phase, and cells with DNA contents between "1X" and "2X" in the S phase of the cell cycle. By performing a mathematical fit to the DNA histogram, the proportion of cells in each phase of the cell cycle can be determined, the phase durations can be derived, and differences in DNA ploidy can be identified. DNA flow cytometry is quite powerful in that a static measure of cell cycle distribution can be obtained for a cell population of interest and dynamic studies of, for example, transit through the various cell cycle phases or treatment-induced kinetic perturbations can be monitored over time (Fig. 1.13). Flow cytometers are often outfitted with a cell-sorting feature. In this case, cells analyzed for a property of interest can be collected in

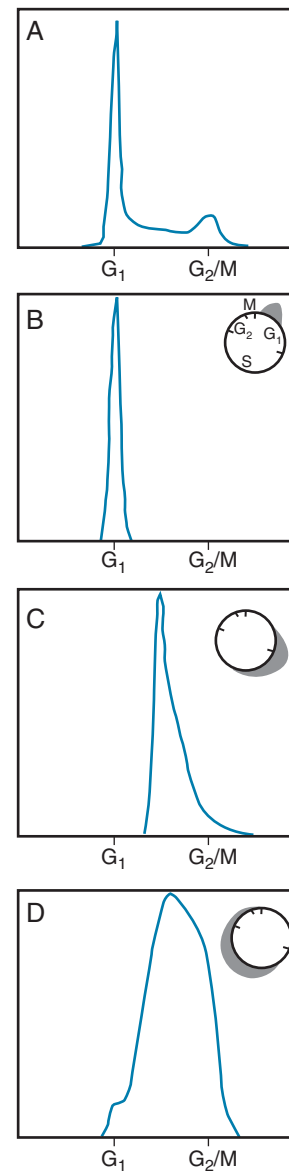


**Fig. 1.13** The analytical technique of flow cytometry has revolutionized the study of cell cycle kinetics by allowing rapid determination of DNA content in cells stained with a fluorescent dye that binds stoichiometrically to cellular DNA. (A) Frequency distribution for a population of exponentially growing cells. The large and small peaks correspond to cells with G<sub>1</sub> ("1X") and G<sub>2</sub>/M ("2X") phase DNA content, respectively; those cells in S phase have an intermediate DNA content. (B–D) DNA histograms for a cell population synchronized initially in mitosis and then allowed to progress into G<sub>1</sub> (B), S and G<sub>2</sub>/M (C and D). See text for details.



separate “bins” after they pass through the laser beam and, if possible, used for other experiments.

### Age Response Through the Cell Cycle

Results of Terasima and Tolmach's<sup>106</sup> age response experiment using synchronized HeLa cells are shown in the lower panel of Fig. 1.14.

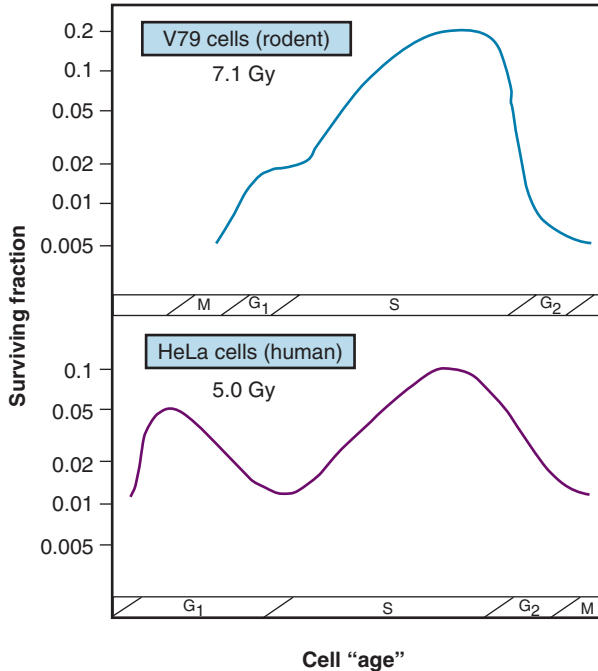


**Fig. 1.14** Cell cycle age response for sensitivity to radiation-induced cell killing in a representative rodent cell line (V79, *top*) having a short  $G_1$  phase duration, and a representative human cell line (HeLa, *bottom*), having a long  $G_1$  phase duration. Both cell lines exhibit a peak of radioresistance in late S phase and maximum radiosensitivity in late  $G_2$ /M phase. A second “trough” of radiosensitivity can be discerned near the  $G_1$ /S border for cells with long  $G_1$  phase durations. (Modified from Sinclair W. Dependence of radiosensitivity upon cell age. In: *Proceedings of the Carmel Conference on Time and Dose Relationships in Radiation Biology as Applied to Radiotherapy*. BNL Report 50203. Upton, NY: Brookhaven National Laboratory; 1969.)

Following a single dose of 5 Gy of x-rays, cells were found to be most radioresistant in late S phase. Cells in  $G_1$  were resistant at the beginning of the phase, but became sensitive toward the end of the phase, and  $G_2$  cells were increasingly sensitive as they moved toward the most sensitive M phase. In subsequent experiments by Sinclair,<sup>111,112</sup> age-response curves for synchronized Chinese hamster V79 cells showed that the peak in resistance observed in  $G_1$  HeLa cells was largely absent for V79 cells. This is also illustrated in Fig. 1.14 (upper panel). Otherwise, the shapes of the age-response curves for the two cell lines were similar. The overall length of the  $G_1$  phase determines whether the resistant peak in early  $G_1$  will be present; in general, this peak of relative radioresistance is observed only for cells with long  $G_1$  phases. For cells with short  $G_1$  phases, the entire phase is often of intermediate radiosensitivity. An analysis of the complete survival curves for synchronized cells<sup>111,113</sup> confirms that the most sensitive cells are those in the M and late  $G_2$  phases, in which survival curves are steep and largely shoulderless, and the most resistant cells are those in late S phase. The resistance of these cells is conferred by the presence of a broad survival curve shoulder rather than by a significant change in survival curve slope (Fig. 1.15). When high-LET radiations are used, the age-response variation through the cell cycle is significantly reduced or eliminated, since survival curve shoulders are either decreased or removed altogether by such exposures (see also “Relative Biological Effectiveness” section to come). Similar age-response patterns have been identified for cells synchronized *in vivo*.<sup>109</sup>

The existence of a cell cycle age response for ionizing radiation provided an explanation for the unusual pattern of SLDR observed for cells maintained at 37° C during the recovery interval (see Fig. 1.9). In Elkind and Sutton's experiments, exponentially growing cells were used, that is, cells that were asynchronously distributed across the different phases of the cell cycle. The cells that survived irradiation tended to be those most radioresistant. Thus, the remaining population became enriched with the more resistant cells. For low-LET radiation, those cells that were most resistant were in S phase at the time of the first radiation dose. However, at 37° C, cells continued to progress through the cell cycle; those surviving cells in S phase at the time of the first dose may have moved into  $G_2$  phase by the time the second dose was delivered. Thus, the observed survival nadir in the SLDR curve was not due to a loss or reversal of repair but rather because the population of cells was now enriched in  $G_2$  phase cells, which are inherently more radiosensitive. For even longer radiation-free intervals, it is possible that the cells surviving the first dose would transit from  $G_2$  to M and

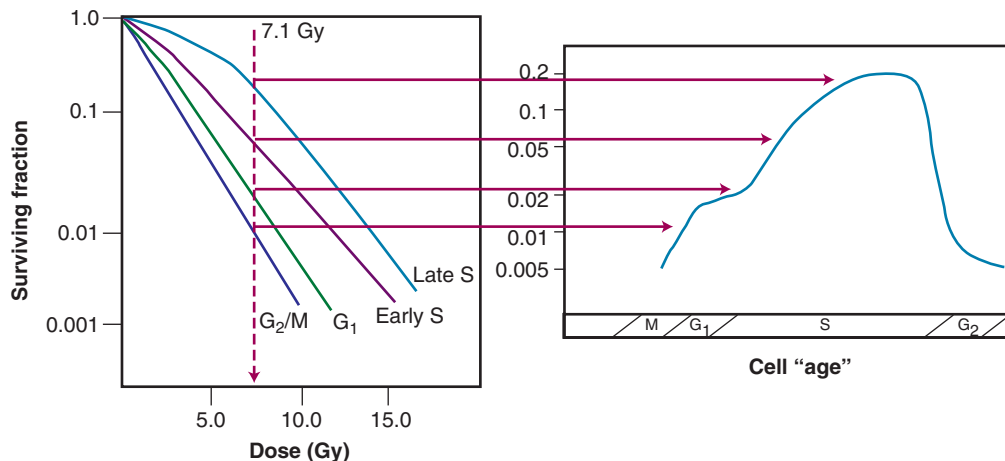


**Fig. 1.15** Cell survival curves for irradiated populations of Chinese hamster cells synchronized in different phases of the cell cycle (*left*), illustrating how these radiosensitivity differences translate into the age response patterns shown at right (and in Fig. 1.14).

back into  $G_1$  phase, dividing and doubling their numbers. In this case, the SLDR curve again shows a surviving fraction increase because the number of cells has increased. None of these cell cycle-related phenomena occur when the cells are maintained at room temperature during the radiation-free interval, because continued movement through the cell cycle is inhibited under such conditions. In that case, all that is noted is the initial survival increase due to SLDR.

### Radiation-Induced Cell Cycle Blocks and Delays

Radiation is also capable of disrupting the normal proliferation kinetics of cell populations. This was recognized by Canti and Spear in 1927<sup>114</sup> and studied in conjunction with radiation's ability to induce cellular lethality. With the advent of mammalian cell culture and synchronization techniques along with time-lapse cinemicrography, it became possible for investigators to study mitotic and division delay phenomena in greater detail.

Mitotic delay, defined as a delay in the entry of cells into mitosis, is a consequence of “upstream” blocks or delays in the movement of cells from one cell cycle phase to the next. Division delay, a delay in the time of appearance of new cells at the completion of mitosis, is caused by the combined effects of mitotic delay and any further lengthening of the mitosis process itself. Division delay increases with dose and is, on average, about 1 to 2 hours per gray<sup>106</sup> depending on the cell line.

The cell cycle blocks and delays primarily responsible for mitotic and division delay are, respectively, a block in the  $G_2$ -to-M phase transition, and a block in the  $G_1$ -to-S phase transition. The duration of the  $G_2$  delay, like the overall division delay, varies with cell type, but for a given cell type is both dose and cell cycle age dependent. In general, the length of the  $G_2$  delay increases linearly with dose. For a given dose, the  $G_2$  delay is longest for cells irradiated in S or early  $G_2$  phase, and shortest for cells irradiated in  $G_1$  phase.<sup>115</sup> Another factor contributing to mitotic and division delay is a block in the flow of cells from  $G_1$  into S phase. For x-ray doses of at least 6 Gy, there is a 50% decrease in the rate of tritiated thymidine uptake (indicative of entry into S phase) in exponentially growing cultures of mouse L cells. Little<sup>116</sup> reached a similar conclusion from  $G_1$  delay studies using human liver LICH cells maintained as confluent cultures.

A possible role for DNA damage and its repair in the etiology of division delay was bolstered by the finding that certain cell types that either did not exhibit the normal cell cycle delays associated with radiation exposure (such as AT cells<sup>42</sup>) or, conversely, were treated with chemicals that ameliorated the radiation-induced delays<sup>117</sup> tended to contain higher amounts of residual DNA damage and to show increased radiosensitivity.

It is now known that the radiation-induced perturbations in cell cycle transit are under the control of cell cycle checkpoint genes, whose products normally govern the orderly (and unidirectional) flow of cells from one phase to the next. The checkpoint genes are responsive to feedback from the cell as to its general condition and readiness to transit to the next cell cycle phase. DNA integrity is one of

the criteria used by these genes to help make the decision whether to continue traversing the cell cycle or to pause—either temporarily or, in some cases, permanently. Cell cycle checkpoint genes are discussed in Chapter 2.

### Redistribution in Tissues

Because of the age response through the cell cycle, an initially asynchronous population of cells surviving a dose of radiation becomes enriched with S phase cells. Owing to variations in the rate of further cell cycle progression, however, this partial synchrony decays rapidly. Such cells are said to have “redistributed,”<sup>118</sup> with the net effect of sensitizing the population as a whole to a subsequent dose fraction (relative to what would have been expected had the cells remained in their resistant phases). A second type of redistribution also has a net sensitizing effect, in which cells accumulate in  $G_2$  phase (in the absence of cell division) during the course of multifraction or continuous irradiation because of a buildup of radiation-induced cell cycle blocks and delays. This has been observed during continuous irradiation by several investigators.<sup>119</sup> In some of these cases, a net increase in radiosensitivity is seen at certain dose rates. This so-called “inverse dose rate effect,” where certain dose rates are more effective at cell killing than other, higher dose rates, was extensively studied by Mitchell, Bedford and associates (for a review, see Bedford et al.<sup>120</sup>). The magnitude of the sensitizing effect of redistribution varies with cell type depending on what dose rate is required to stop cell division. For dose rates below the critical range that causes redistribution, some cells can escape the  $G_2$  block and proceed on to cell division.

### Densely Ionizing Radiation

#### Linear Energy Transfer

The total amount of energy deposited in biological materials by ionizing radiation (usually expressed in units of keV, ergs or joules per g or kg) is in and of itself insufficient to describe the net biological consequences of those energy deposition events. For example, 1 Gy of x-rays, while physically equivalent in terms of total energy imparted per unit mass to 1 Gy of neutrons or  $\alpha$ -particles, does not produce equivalent biological effects. It is the microdosimetric pattern of that energy deposition, that is, the spacing or density of the ionization events, that determines biological effectiveness. This quantity—the average energy deposited locally per unit length of the ionizing particle's track—is termed its *linear energy transfer* (LET).

LET is a function both of the charge and mass of the ionizing particle. Photons set in motion fast electrons that have a net negative charge but a negligible mass. Neutrons, on the other hand, give rise to recoil protons or  $\alpha$ -particles that possess one or two positive charges, respectively, and are orders of magnitude more massive than electrons. Neutrons, therefore, have a higher LET than photons and are considered densely ionizing, whereas the x-rays or  $\gamma$ -rays are considered sparsely ionizing. The LET concept is illustrated in Fig. 1.16 for both densely

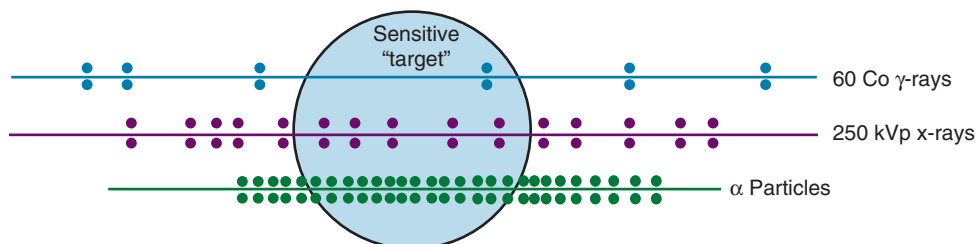


**Fig. 1.16** Variation in the density of ionizing events along an incident particle's track for radiations of differing linear energy transfer. The more closely spaced the ionizing events, the more energy will be deposited in the target volume and, to a point, the more biologically effective per unit dose the type of radiation will be.

and sparsely ionizing radiations. For a given ionizing particle, the rate of energy deposition in the absorbing medium increases as the particle slows down. Therefore, a beam of radiation can only be described as having an average value for LET.

Representative LET values for types of radiation that have been used for radiation therapy include 0.2 keV/μm for  $^{60}\text{Co}$  γ-rays; 2.0 keV/μm for 250 kVp x-rays; approximately 0.5 to 5.0 keV/μm for protons of different energies; approximately 50 to 150 keV/μm for neutrons; 100 to 150 keV/μm for α-particles; and anywhere from 100 to 2500 keV/μm for “heavy ions.”

### Relative Biological Effectiveness

Insofar as the “quality” (LET) of the type of radiation influences its biological effectiveness, two questions immediately come to mind. First, why do seemingly subtle differences in microdosimetric energy deposition patterns lead to vastly different biological consequences? Second, how is this differing biological effectiveness manifest in terms of the commonly used assays and model systems of foundational radiobiology, and how can this difference be expressed in a quantitative way?

Because high-LET radiations are more densely ionizing than their low-LET counterparts, it follows that energy deposition in a particular “micro”-target volume will be greater and therefore, more severe damage to biomolecules would be expected. In this case, the fraction of cell killing attributable to irreparable and unmodifiable DNA damage increases in relation to that caused by the accumulation of sublethal damage. Because of this, a number of radiobiological phenomena commonly associated with low-LET radiation are decreased or eliminated when high-LET radiation is used. For example, there is little, if any, sublethal<sup>60</sup> or potentially lethal damage recovery.<sup>115</sup> This is manifest as a reduction or loss of the shoulder of the acute dose survival curve, little or no sparing effect of dose fractionation or dose rate, and a corresponding reduction in the tolerance doses for normal tissue complications, particularly for late-responding tissues.<sup>121</sup> Variations in the age response through the cell cycle also are reduced or eliminated for high-LET radiation,<sup>109</sup> and the oxygen enhancement ratio (OER), a measure of the differential radiosensitivity of poorly versus well-oxygenated cells (see later discussion), decreases with increasing LET.<sup>122</sup> The dependence of OER on LET is illustrated in Fig. 1.17; at an LET of approximately 100 keV/μm, the relative radioresistance of hypoxic cells is eliminated.

In light of these differences between high- and low-LET radiations, the term *relative biological effectiveness* (RBE) has been coined to compare and contrast two radiation beams of different LET. RBE is defined as the ratio of doses of a known type of low-LET radiation (historically, 250 kVp x-rays were the standard) to that of a higher-LET radiation to yield the same biological endpoint. RBE does not increase indefinitely with increasing LET, however, but rather reaches a maximum at approximately 100 keV/μm and then decreases again, yielding an approximately bell-shaped curve.

One interpretation as to why the RBE reaches a maximum at an LET of approximately 100 keV/μm is that, at this ionization density, the average separation between ionizing events corresponds roughly to the diameter of the DNA double helix (approximately 2 nm). As such, radiations of this LET have the highest probability of producing DSBs in DNA, the putative lethal lesion, by the passage of a single charged particle. Lower-LET radiations have a smaller likelihood of producing such “two-hit” lesions from a single particle track and, therefore, are less biologically effective. Radiation beams of higher LET than the optimum are less efficient because some of the energy is wasted as more ionization events than minimally necessary to kill a cell are deposited in the same local area. This phenomenon has been termed the *overkill effect*.

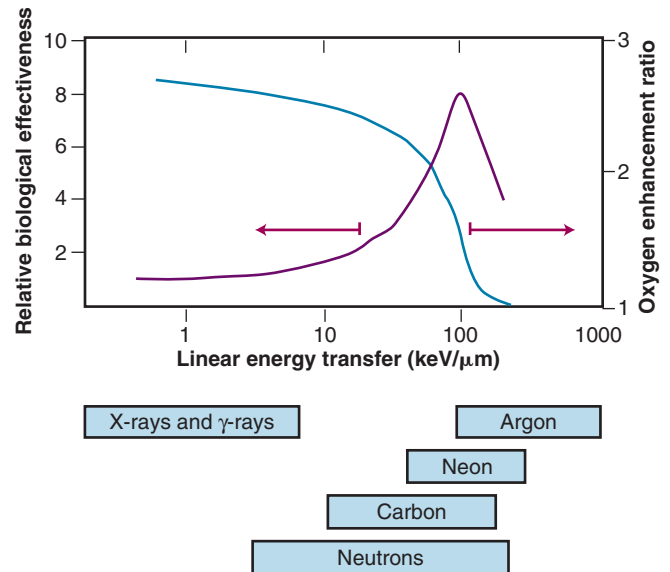


**Fig. 1.17** Relative biological effectiveness (RBE, left Y-axis) as a function of linear energy transfer (LET) for a number of biological endpoints, including production of chromosomal aberrations, cell killing, and tissue reactions. The RBE rises to a maximum corresponding to an LET of approximately 100 keV/μm and then decreases as the LET continues to rise. Shown below the X-axis are the ranges of LET for photons plus several different types of particulate radiations that have been used clinically. Also shown is the dependence of the oxygen enhancement ratio (OER, right Y-axis) on LET.

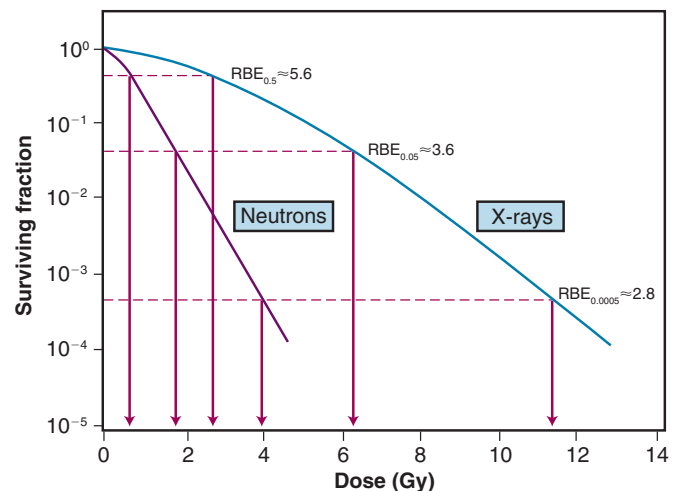


**Fig. 1.18** Theoretical cell survival curves for x-rays and neutrons, illustrating the increase in relative biological effectiveness (RBE) with decreasing dose. This occurs because higher linear energy transfer radiations preferentially decrease or eliminate the shoulder on cell survival curves. (Modified from Nias A. *Clinical Radiobiology*. 2nd ed. New York: Churchill Livingstone; 1988.)

### Factors That Influence Relative Biological Effectiveness

RBE is highly variable and depends on several parameters, including the type of radiation, total dose, dose rate, dose fractionation pattern, and the biological effect being assayed. Therefore, when quoting an RBE value, the exact experimental conditions used to measure it must be stated. Because increasing LET differentially reduces the shoulder region of the radiation survival curve compared to its exponential or near-exponential high-dose region, the single-dose RBE increases with decreasing dose (Fig. 1.18). Second, the RBE determined by comparing

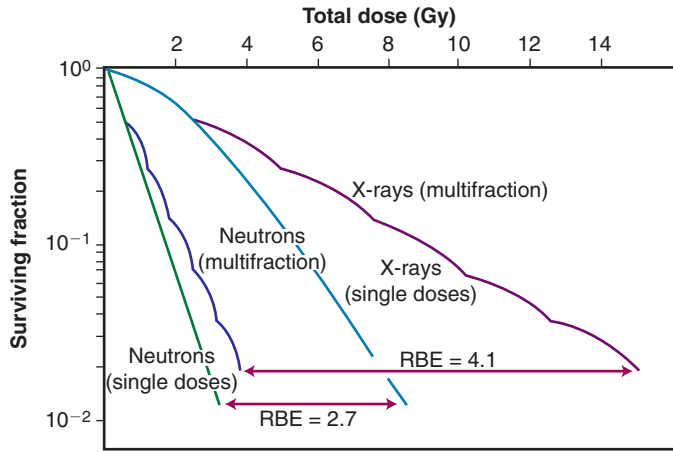


**Fig. 1.19** Increase in the relative biological effectiveness (RBE) of neutrons relative to x-rays when comparing single doses with fractionated treatment. For a given level of cell killing (or other approximately isoeffective endpoint), the more highly fractionated the treatment, the higher the RBE.

two isoeffective acute doses is less than the RBE calculated from two isoeffective (total) doses given either as multiple fractions or at a low dose rate. This occurs because the sparing effect of fractionation magnifies differences in the initial slope or shoulder region of cell survival or tissue dose-response curves (Fig. 1.19).

### The Oxygen Effect

Perhaps the best-known chemical modifier of radiation action is molecular oxygen. As early as 1909, Schwarz recognized that applying pressure to skin and thereby decreasing blood flow (and oxygen supply) caused a reduction in radiation-induced skin reactions.<sup>123</sup> For many decades thereafter, radiation oncologists and biologists continued to suspect that the presence or absence of oxygen was capable of modifying radiosensitivity. In 1955, however, Thomlinson and Gray<sup>124</sup> brought this idea to the forefront of radiation biology and therapy by proposing that tumors contain a fraction of still-clonogenic, hypoxic cells that, if persistent throughout treatment, would adversely affect clinical outcome. Although commonly considered a negative prognostic indicator for radiation therapy, hypoxia nevertheless has one particularly attractive feature: built-in specificity for tumors, to the extent that normal tissues contain few, if any, hypoxic cells.

By studying histological sections of a human bronchial carcinoma, Thomlinson and Gray noted that necrosis was always seen in the centers of cylindrical tumor cords having a radius in excess of approximately 200  $\mu\text{m}$ .<sup>124</sup> Further, regardless of how large the central necrotic region was, the sheath of apparently viable cells around the periphery of this central region never had a radius greater than about 180  $\mu\text{m}$ . The authors went on to calculate the expected maximum diffusion distance of oxygen from blood vessels and found that the value of 150 to 200  $\mu\text{m}$  agreed quite well with the radius of the sheath of viable tumor cells observed histologically. With the advent of more sophisticated and quantitative methods for measuring oxygen utilization in tissues, the average diffusion distance of oxygen has since been revised downward to approximately 70  $\mu\text{m}$ .<sup>28</sup> Thus, the inference was that the oxygenation status of tumor cells varied from fully oxic to completely anoxic depending on where the cells were located in relation to the nearest blood vessels. Accordingly, tumor cells at intermediate distances from the blood supply would be hypoxic and radioresistant, yet remain clonogenic.

The first unambiguous demonstration that a solid rodent tumor did contain clonogenic, radioresistant hypoxic cells was by Powers and

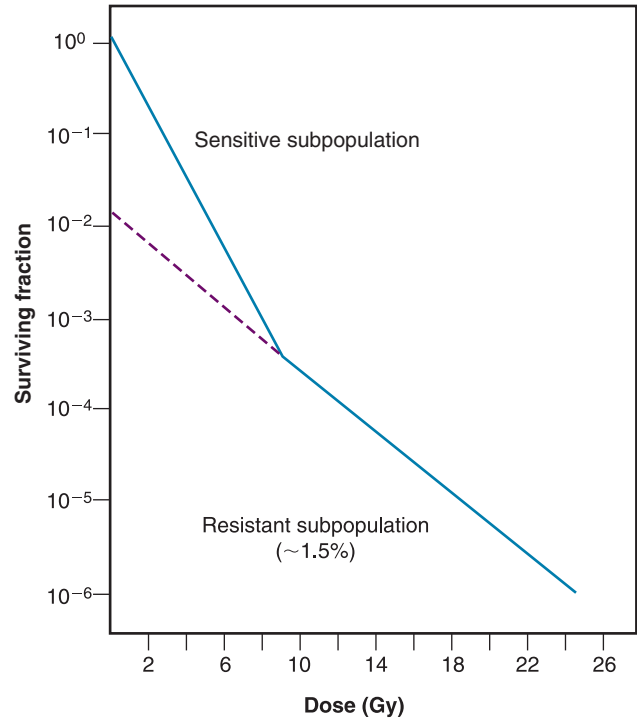


**Fig. 1.20** Cell survival curve for a murine lymphosarcoma growing subcutaneously and irradiated in vivo. The biphasic curve suggests the presence of a small but relatively radioresistant subpopulation of cells, determined in accompanying experiments to represent the tumor's clonogenic hypoxic fraction. (Modified from Powers WE, Tolmach LJ. A multicomponent x-ray survival curve for mouse lymphosarcoma cells irradiated. *Nature*. 1963;197:710.)

Tolmach<sup>125</sup> in 1963. These authors used the dilution assay to generate an in vivo survival curve for mouse lymphosarcoma cells. The survival curve for this solid tumor was biphasic, having an initial  $D_0$  of about 1.1 Gy and a final  $D_0$  of 2.6 Gy (Fig. 1.20). Since the survival curve for lymphoid cells is shoulderless, it was simple to back-extrapolate the shallower component of the curve to the surviving fraction axis and determine that the resistant fraction of cells constituted about 1.5% of the total population. This was considered compelling evidence (yet did not unambiguously prove) that this subpopulation of cells was both hypoxic and clonogenic.

The question then became how to prove that this small fraction of tumor cells was radioresistant because of hypoxia as opposed to being radioresistant for other reasons. An elegant, if somewhat macabre, method was developed to address this dilemma, called the *paired survival curve technique*.<sup>125,126</sup> In this assay, laboratory animals bearing tumors were divided into three treatment groups, one group irradiated while breathing air, a second group irradiated while breathing 100% oxygen, and a third group killed first by cervical dislocation and then irradiated. Within each group, animals received graded radiation doses so that complete survival curves were generated for each treatment condition. When completed, the paired survival curve method yielded three different tumor cell survival curves: a fully oxic curve (most radiosensitive), a fully hypoxic curve (most radioresistant), and the survival curve for air-breathing animals which, if the tumor contained viable hypoxic cells, was biphasic and positioned between the other two curves. It was then possible to mathematically strip the fully aerobic and hypoxic curves from the curve for air-breathing animals and determine the radiobiologically hypoxic fraction.



Across a variety of rodent tumors evaluated to date using the paired survival curve method, the percentage of hypoxic cells was found to vary between 0% and 50%, with an average of about 15%.<sup>126</sup>

### Mechanistic Aspects of the Oxygen Effect

A more rigorous analysis of the nature of the oxygen effect is possible with cells or bacteria grown *in vitro*. Historically, oxygen had been termed a *dose-modifying agent*, that is, that the ratio of doses to achieve a given survival level under hypoxic and aerobic conditions was constant regardless of the survival level chosen. This dose ratio to produce the same biological endpoint is termed the *oxygen enhancement ratio* (OER), and is used for comparative purposes (Fig. 1.21). The OER typically has a value of between 2.5 and 3.0 for large single doses of x-rays or  $\gamma$ -rays, 1.5 to 2.0 for radiations of intermediate LET, and 1.0 (i.e., no oxygen effect) for high-LET radiations.

Increasingly, there is evidence that oxygen is not strictly dose modifying. Several studies have shown that the OER for sparsely ionizing radiation is lower at lower doses than at higher doses. Lower OERs for doses per fraction in the range commonly used in radiotherapy have been inferred indirectly from clinical and experimental tumor data and more directly in experiments with cells in culture.<sup>127,128</sup> It has been suggested that the lower OERs result from an age response for the oxygen effect, not unlike the age responses for inherent radiosensitivity and cell cycle delay.<sup>28</sup> Assuming that cells in  $G_1$  phase of the cell cycle have a lower OER than those in S phase and since  $G_1$  cells are also more radiosensitive, they would tend to dominate the low-dose region of the cell survival curve.

While the exact mechanism(s) of the oxygen effect are obviously complex, a fairly simplistic model can be used to illustrate our current understanding of this phenomenon (Fig. 1.22). The radical competition model holds that oxygen acts as a radiosensitizer by forming peroxides in important biomolecules (including, but not necessarily limited to, DNA) already damaged by radiation exposure, thereby “fixing” the radiation damage. In the absence of oxygen, DNA can be restored to its preirradiated condition by hydrogen donation from endogenous reducing species in the cell, such as the free radical scavenger glutathione, a thiol compound. In essence, this can be considered a type of very fast chemical restitution or repair. These two processes, fixation and restitution, are considered to be in a dynamic equilibrium, such that changes in the relative amounts of either the radiosensitizer, oxygen, or the

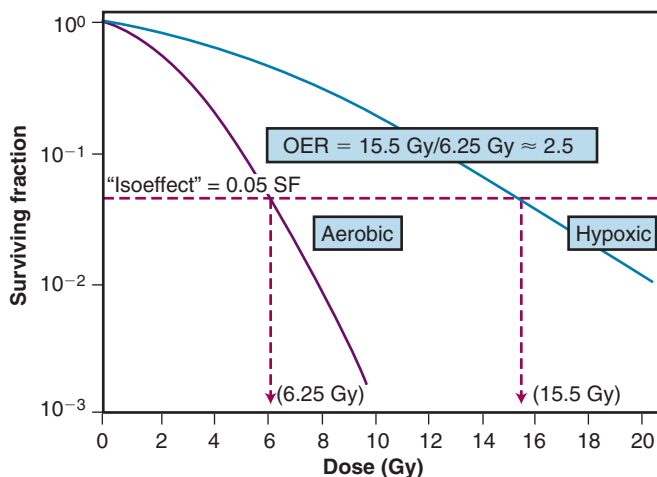


**Fig. 1.21** Representative survival curves for cells irradiated with x-rays in the presence (aerobic) or virtual absence (hypoxic) of oxygen. The oxygen enhancement ratio (OER) is defined as the ratio of doses under hypoxic:aerobic conditions to yield the same biological effect, in this case, a cell surviving fraction of 0.05.

radioprotector, glutathione, tip the scales in favor of either fixation (more damage, more cell killing, greater radiosensitivity) or restitution (less damage, less cell killing, greater radioresistance), respectively.

Consistent with this free radical-based interpretation of the oxygen effect is the finding that, for all intents and purposes, oxygen need only be present during the irradiation (or no more than a few milliseconds after irradiation) in order to produce an aerobic radioresponse.<sup>129,130</sup> The concentration of oxygen necessary to achieve maximum sensitization is quite small, evidence for the high efficiency of oxygen as a radiosensitizer. A sensitivity midway between a fully hypoxic and fully aerobic radioresponse is achieved at an oxygen tension of about 3 mm of mercury, corresponding to about 0.5% oxygen, much lower than partial pressures of oxygen usually encountered in normal tissues. This value of 0.5% has been termed oxygen's *k-value* and is obtained from an oxygen *k-curve* of relative radiosensitivity plotted as a function of oxygen tension<sup>131</sup> (Fig. 1.23).

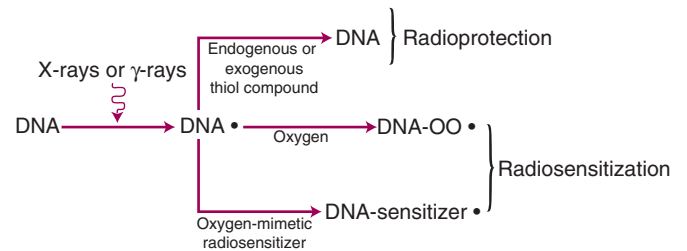


**Fig. 1.22** Schematic representation of the proposed mechanism of action for the oxygen effect. The radical competition model holds that oxygen acts as a radiosensitizer by forming peroxides in DNA already damaged by radiation, thereby “fixing” the damage. In the absence of oxygen, DNA can be restored to its preirradiated state by hydrogen donation from endogenous reducing species in the cell, such as the free radical scavenger glutathione. An oxygen-mimetic, hypoxic cell radiosensitizer may be used to substitute for oxygen in these fast free radical reactions or an exogenously supplied thiol compound may be used to act as a radioprotector.

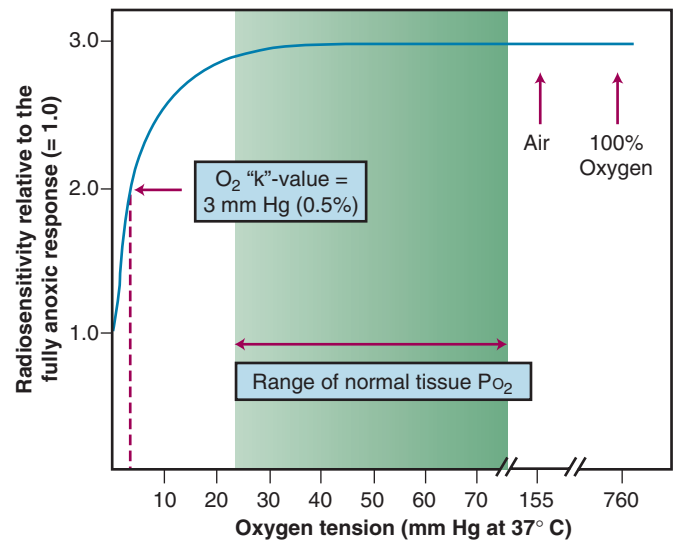


**Fig. 1.23** An oxygen “k-curve” is used to illustrate the dependence of radiosensitivity on oxygen concentration. If a fully anoxic cell culture is assigned a relative radiosensitivity of 1.0, introducing even 0.5% (3 mm Hg) oxygen into the system increases the radiosensitivity of cells to 2.0; by the time the oxygen concentration reaches about 2.0%, cells respond as if they are fully aerated (i.e., radiosensitivity  $\approx$  3.0). The shaded area represents the approximate range of oxygen concentrations encountered in human normal tissues.



## Reoxygenation in Tumors

After the convincing demonstration of hypoxic cells in a mouse tumor,<sup>125</sup> it was assumed that human tumors contained a viable hypoxic fraction as well. However, if human tumors contained even a tiny fraction of clonogenic hypoxic cells, simple calculations suggested that tumor control would be nearly impossible with radiation therapy.<sup>132</sup> Since therapeutic successes obviously do occur, some form of reoxygenation must take place during the course of multifraction irradiation. This was not an unreasonable idea since the demand for oxygen by sterilized cells would gradually decrease as they were removed from the tumor, and a decrease in tumor size, a restructuring of tumor vasculature, or intermittent changes in blood flow could make oxygen available to these previously hypoxic cells.

The reoxygenation process was extensively studied by van Putten and Kallman,<sup>133</sup> who serially determined the fraction of hypoxic cells in a mouse sarcoma during a course of clinically relevant multifraction irradiation. The fact that the hypoxic fraction was about the same at the end of treatment as at the beginning of treatment was strong evidence for a reoxygenation process because, otherwise, the hypoxic fraction would be expected to increase over time due to repeated enrichment with resistant cells after each dose fraction. Reoxygenation of hypoxic, clonogenic tumor cells during an extended multifraction treatment would increase the therapeutic ratio assuming that normal tissues remained well oxygenated. This is thought to be another major factor in the sparing of normal tissues relative to tumors during fractionated radiation therapy.

What physiological characteristics would lead to tumor reoxygenation during a course of radiotherapy, and at what rate would this be expected to occur? One possible cause of tumor hypoxia and, by extension, a possible mechanism for reoxygenation, was suggested by Thomlinson and Gray's pioneering work.<sup>124</sup> The type of hypoxia that they described is what is now called *chronic* or *diffusion-limited hypoxia*. This results from the tendency of tumors both to have high oxygen consumption rates and to outgrow their blood supply. It follows that natural gradients of oxygen tension should develop as a function of distance from blood vessels. Cells situated beyond the diffusion distance of oxygen would be expected to be dead or dying secondary to anoxia; yet, in regions of chronically low oxygen tension, clonogenic and radioresistant hypoxic cells could persist. Should the tumor shrink as a result of radiation therapy or if the cells killed by radiation cause a decreased demand for oxygen, it is likely that this would allow some of the chronically hypoxic cells to reoxygenate. However, such a reoxygenation process could be quite slow—days at minimum—depending on how quickly tumors regress during treatment. The patterns of reoxygenation in some experimental rodent tumors are consistent with this mechanism of reoxygenation, but others are not.

Other rodent tumors reoxygenate very quickly, from minutes to hours.<sup>134</sup> This occurs in the absence of any measurable tumor shrinkage or change in oxygen utilization by tumor cells. In such cases, the model of chronic, diffusion-limited hypoxia, and slow reoxygenation does not fit the experimental data. During the late 1970s, Brown<sup>135</sup> proposed that a second type of hypoxia must exist in tumors, an acute, perfusion-limited hypoxia. Based on the growing understanding of the vascular physiology of tumors, it was clear that tumor vasculature was often abnormal in both structure and function secondary to abnormal angiogenesis. If tumor vessels were to close transiently from temporary blockage, vascular spasm, or high interstitial fluid pressure in the surrounding tissue, the tumor cells in the vicinity of those vessels would become acutely hypoxic almost immediately. Then, assuming that blood flow resumed in minutes to hours, these cells would reoxygenate. However, this type of hypoxia also can occur in the absence of frank closure or blockage of tumor vessels (which is now considered a less

common cause of acute hypoxia) from, for example, vascular shunting, longitudinal oxygen gradients, decreased red cell flux or overall blood flow rate, abnormal vascular geometry, and so on.<sup>136</sup> Because of this, the name *perfusion-limited* hypoxia is perhaps misleading; a better moniker might be *fluctuant* or *intermittent* hypoxia. While intermittent hypoxia would explain the rapid reoxygenation observed for some tumors, it does not preclude the simultaneous existence of chronic, diffusion-limited hypoxia.

Intermittent hypoxia has since been demonstrated for rodent tumors by Chaplin et al.<sup>137</sup> and human tumors by Lin et al.<sup>138</sup> It is still not clear how many human tumors contain regions of hypoxia (although most do—see next section), what type(s) of hypoxia is present, whether this varies with tumor type or site, and whether and how rapidly reoxygenation occurs. However, the knowledge that tumor hypoxia is a diverse and dynamic process opens up a number of possibilities for the development of novel interventions designed to cope with, or even exploit, hypoxia.

## Measurement of Hypoxia in Human Tumors

Despite prodigious effort directed at understanding tumor hypoxia and developing strategies to combat the problem, it was not until the late 1980s that these issues could be addressed for human tumors because there was no way to measure hypoxia directly. Before that time, the only way to infer that a human tumor contained treatment-limiting hypoxic cells was by using indirect, nonquantitative methods. Some indirect evidence supporting the notion that human tumors contained clonogenic, radioresistant hypoxic cells includes the following:

1. An association between anemia and poor local control rates that, in some cases, could be mitigated by preirradiation blood transfusions<sup>139</sup>
2. Success of some clinical trials in which hyperbaric oxygen breathing was used to better oxygenate tumors<sup>140,141</sup>
3. Success of a few clinical trials of oxygen-mimetic hypoxic cell sensitizers combined with radiation therapy<sup>139,142</sup>

In 1988, one of the first studies showing a strong association between directly measured oxygenation status in tumors and clinical outcome was published by Gatenby et al.<sup>143</sup> An oxygen-sensing electrode was inserted into the patient's tumor, and multiple readings were taken at different depths along the probe's track. The electrode was also repositioned in different regions of the tumor to assess intertrack variability in oxygen tension. Both the arithmetic mean Po<sub>2</sub> value for a particular tumor and the tumor volume-weighted Po<sub>2</sub> value directly correlated with local control rate. A high tumor oxygen tension was associated with a high complete response rate, and vice versa. In a similar prospective study, Höckel et al.<sup>4,144</sup> concluded that pretreatment tumor oxygenation was a strong predictor of outcome among patients with intermediate and advanced-stage cervical carcinoma (Fig. 1.24).

The use of oxygen electrodes has its limitations. One weakness is that relative to the size of individual tumor cells, the electrode is large, averaging an outer diameter of 300 μm, a tip recess of 120 μm, and a sampling volume of about 12 μm in diameter.<sup>145</sup> Thus, not only is the oxygen tension measurement regional, but the insertions and removals of the probe no doubt perturb the oxygenation status. Another problem is that there is no way to determine whether the tumor cells are clonogenic or not. If such cells were hypoxic yet not clonogenic, they would not be expected to impact radiotherapy outcome.

A second direct technique for measuring oxygenation status takes advantage of a serendipitous finding concerning how hypoxic cell radiosensitizers are metabolized. Certain classes of radiosensitizers, including the nitroimidazoles, undergo a bioreductive metabolism in the absence of oxygen that leads to their becoming covalently bound to cellular macromolecules.<sup>146,147</sup> Assuming that the bioreductively bound drug

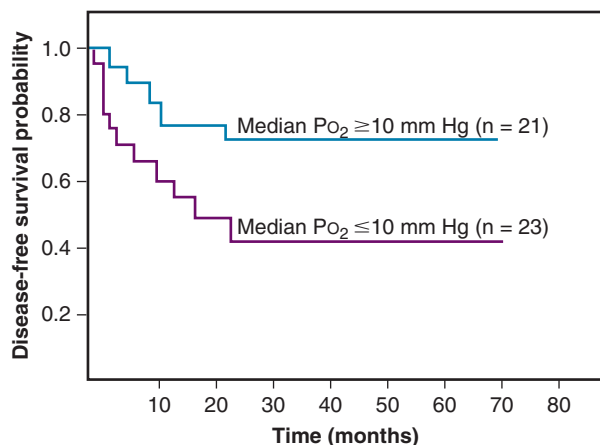


**Fig. 1.24** The disease-free survival probability of a small cohort of cervical cancer patients stratified according to pretreatment tumor oxygenation, as measured using an oxygen electrode. (Modified from Höckel M, Knoop C, Schlenger K, et al. Intratumoral pO<sub>2</sub> predicts survival in advanced cancer of the uterine cervix. *Radiother Oncol.* 1993;26:45.)

could be quantified by radioactive labeling<sup>148</sup> or tagged with an isotope amenable to detection using positron emission tomography<sup>149</sup> or magnetic resonance spectroscopy,<sup>150</sup> a direct measure of hypoxic fraction can be obtained. Another approach to detecting those cells containing bound drug was developed by the Raleigh group (e.g., Cline et al.<sup>151</sup> and Kennedy et al.<sup>152</sup>). This immunohistochemical method involved the development of antibodies specific for the bound nitroimidazole metabolites. After injecting the parent drug, allowing time for the reductive metabolism to occur, taking biopsies of the tumor, and preparing histopathology slides, the specific antibody is then applied to the slides and regions containing the bound drug are visualized directly. This immunostaining method has the distinct advantages that hypoxia can be studied at the level of individual tumor cells,<sup>153</sup> spatial relationships between regions of hypoxia and other tumor physiological parameters can be assessed,<sup>154</sup> and the drug does not perturb the tumor microenvironment. However, the method remains an invasive procedure, is labor intensive, does not address the issue of the clonogenicity of stained cells (although such cells do have to be metabolically active), and requires that multiple samples be taken because of tumor heterogeneity.

One hypoxia marker based on the immunohistological method detects reductively bound pimonidazole hydrochloride and has been used in experimental and clinical studies around the world (e.g., Bussink et al.,<sup>155</sup> Nordmark et al.<sup>156</sup>). Human tumor specimens stained with the marker were found to have a wide range of hypoxic fractions (similar to that for experimental rodent tumors), with a mean value of approximately 15%.<sup>152,157</sup> This marker can also be used to probe disease states other than cancer that may have the induction of tissue hypoxia as part of their etiology, such as cirrhosis of the liver<sup>158,159</sup> and ischemia-reperfusion injury in the kidney.<sup>160</sup>

There is also considerable interest in endogenous markers of tissue hypoxia<sup>161,162</sup> that could reduce to some extent the procedural steps involved in, and the invasive aspects of, detecting hypoxia using exogenous agents. Among the endogenous cellular proteins being investigated in this regard are the hypoxia-inducible factor 1- $\alpha$  (HIF-1 $\alpha$ , which acts as a transcription factor for hypoxia-regulated genes<sup>163</sup>), the enzyme carbonic anhydrase IX (CA-9 or CAIX, involved in respiration and maintenance of the proper acid–base balance in tissues<sup>164,165</sup>), glucose transporter-1 (GLUT-1, which facilitates glucose transport into cells and glycolysis<sup>166–168</sup>), lysyl oxidase (LOX, which oxidizes lysine residues in extracellular matrix proteins that can enhance

the processes of tumor invasion and metastasis<sup>169,170</sup>), and osteopontin (OPN, a glycoprotein that facilitates tumor invasion and metastasis<sup>171–173</sup>).

Clearly, although aberrant expression of some individual hypoxia markers has been associated with poor clinical outcome, no one marker is likely to be sufficiently robust or reproducible to either be diagnostic for the presence of a malignancy (or, at least, the presence of hypoxia in an already diagnosed tumor) or prognostic of treatment outcome. Thus, there has been increasing interest in the study of patterns of hypoxia-associated gene or protein expression for multiple markers simultaneously, for example, Le et al.,<sup>5</sup> Erpolat et al.,<sup>173</sup> and Toustrup et al.<sup>174</sup>

## Radiosensitizers, Radioprotectors, and Bioreductive Drugs

The perceived threat that tumor hypoxia posed spawned much research into ways of overcoming the hypoxia problem. One of the earliest proposed solutions was the use of high-LET radiations,<sup>175</sup> which were less dependent on oxygen for their biological effectiveness. Other agents enlisted to deal with the hypoxia problem included hyperbaric oxygen breathing<sup>140</sup>; artificial blood substitutes with increased oxygen-carrying capacity<sup>176</sup>; oxygen-mimetic hypoxic cell radiosensitizers, such as misonidazole or etanidazole<sup>139</sup>; hyperthermia<sup>177</sup>; normal tissue radioprotectors, such as amifostine<sup>178</sup>; vasoactive agents that modify tumor blood flow, such as nicotinamide<sup>179</sup>; agents that modify the oxygen-hemoglobin dissociation curve, such as pentoxifylline<sup>180</sup>; and bioreductive drugs designed to be selectively toxic to hypoxic cells, such as tirapazamine.<sup>181,182</sup>

### Radiosensitizers

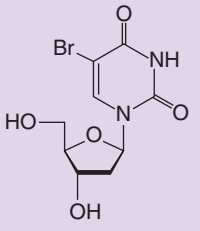
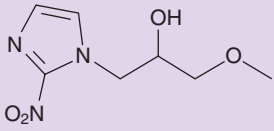
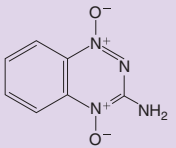
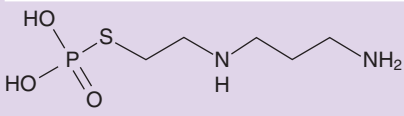
Radiosensitizers are loosely defined as chemical or pharmacological agents that increase the cytotoxicity of ionizing radiation. “True” radiosensitizers meet the stricter criterion of being relatively nontoxic in and of themselves, acting only as potentiators of radiation toxicity. “Apparent” radiosensitizers still produce the net effect of making the tumor more radioresponsive, yet the mechanism is not necessarily synergistic nor is the agent necessarily nontoxic when given alone. Ideally, a radiosensitizer is only as good as it is selective for tumors. Agents that show little or no differential effect between tumors and normal tissues do not improve the therapeutic ratio and, therefore, may not be of much clinical utility. Table 1.2 summarizes some of the classes of radiosensitizers (and radioprotectors—see later discussion) that have been used in the clinic.

**Hypoxic cell radiosensitizers.** The increased radiosensitivity of cells in the presence of oxygen is believed to be due to oxygen’s affinity for the electrons produced by the ionization of biomolecules. Molecules other than oxygen also have this chemical property, known as *electron affinity*,<sup>183</sup> including some agents that are not otherwise consumed by the cell. Assuming that such an electron-affinic compound is not used by the cell, it should diffuse further from capillaries and reach hypoxic regions of a tumor and, acting in an oxygen-mimetic fashion, sensitize hypoxic cells to radiation.

One class of compounds that represented a realistic trade-off between sensitizer efficiency and diffusion effectiveness was the nitroimidazoles, which include such drugs as metronidazole, misonidazole, etanidazole, pimonidazole, and nimorazole. The nitroimidazoles consist of a nitroaromatic imidazole ring, a hydrocarbon side chain that determines the drug’s lipophilicity, and a nitro group that determines the drug’s electron affinity. Misonidazole was extensively characterized in cellular and animal model systems, culminating in its use in clinical trials. Clinical experiences with misonidazole and some of its successor compounds are discussed in Chapter 3.

The relative efficacy of a particular hypoxic cell radiosensitizer is most often described in terms of its sensitizer enhancement ratio (SER),

TABLE 1.2 Selected Chemical Modifiers of Radiation Therapy

Chemical Structure	Name (Type of Compound)	Mechanism of Action	Clinic Status
	5-Bromodeoxyuridine (halogenated pyrimidine)	Radiosensitizer of rapidly proliferating cells through incorporation into DNA during S phase. Uptake results in decrease or removal of the shoulder of the radiation survival curve.	No clear evidence of clinical efficacy has been established to date. The drug continues to be used in a research setting.
	Misonidazole (2-nitroimidazole)	Radiosensitizer of hypoxic cells. Principal mechanism of action is mimicry of oxygen's ability to "fix" free radical damage caused by exposure to radiation and some toxic chemicals.	Clinical trial results were disappointing overall except in selected sites, most notably, head and neck cancer. The drug's failure largely has been ascribed to a dose-limiting toxicity, peripheral neuropathy.
	Tirapazamine (organic nitroxide)	Bioreductive drug selectively toxic to hypoxic cells. The drug is reduced to a toxic intermediate capable of producing DNA strand breaks only in the relative absence of oxygen.	Phase II and Phase III clinical trials to date have been disappointing overall, except in select subsets of patients with head and neck or lung cancer. Some trials are still ongoing for the drug combined with radiotherapy and cis-platinum.
	Amifostine (thiol free radical scavenger)	Radioprotector capable of "restituting" free radical damage caused by exposure to radiation and some toxic chemicals.	FDA-approved indications for amifostine include protection against the nephro- and ototoxicity of platinum drugs and to reduce the incidence and severity of xerostomia in patients receiving radiotherapy for head and neck cancer.

FDA, U.S. Food and Drug Administration.

a parameter similar in concept to the OER. Whereas the OER is the ratio of doses to produce the same biological endpoint under hypoxic versus aerobic conditions, the SER is the dose ratio for an isoeffect under hypoxic conditions alone versus hypoxic conditions in the presence of the hypoxic cell sensitizer. If a dose of a sensitizer produces an SER of 2.5 to 3.0 for large single doses of low-LET radiation, it can be considered to a first approximation "as effective as oxygen." This statement can be very misleading, however, in that the dose of the sensitizer required to produce the SER of 3.0 would be higher than the comparable "dose" of oxygen, high enough in some cases to preclude its use clinically. Finally, since the primary mechanism of action of the nitroimidazoles is substitution for oxygen in radiation-induced free-radical reactions, these drugs need only be present in hypoxic regions of the tumor at the time of irradiation.

The nitroimidazoles also have characteristics that decrease their clinical usefulness. The hydrocarbon side chain of the molecule determines its lipophilicity; this chemical property affects the drug's pharmacokinetics, which is a primary determinant of drug-induced side effects.<sup>184</sup> The dose-limiting toxicity of the fairly lipophilic agent misonidazole is peripheral neuropathy, an unanticipated and serious side effect.<sup>139,185</sup> Etanidazole was specifically designed to be less lipophilic<sup>186</sup> in hopes of decreasing neurological toxicity. Although this goal was accomplished as a proof of concept, clinical results with etanidazole were otherwise disappointing<sup>187</sup> (see also Chapter 3).

Finally, in considering the prodigious amount of research and clinical effort that has gone into the investigation of hypoxic cell radiosensitizers over the past 50 years, it is difficult not to be discouraged by the predominantly negative results of the clinical trials. However, these negative

results have prompted a rethinking of the hypoxia problem and novel approaches to dealing with it as well as consideration of other factors that may have contributed to the lack of success of the nitroimidazole radiosensitizers.<sup>185</sup> Among the more obvious questions raised are the following:

1. Did the patients entered in the various clinical trials actually have tumors that contained clonogenic hypoxic cells? At the time of most of these studies, hypoxia markers were not yet available; thus, it was not possible to triage patients into subgroups in advance of treatment.
2. Do hypoxic cells really matter to the outcome of radiotherapy? If reoxygenation is fairly rapid and complete during radiotherapy, the presence of hypoxic cells prior to the start of treatment may be of little consequence.
3. Given that the OER is lower for small doses versus large doses, it follows that the SER would be reduced as well. If so, a benefit in a subgroup of patients might not be readily observed, at least not at a level of statistical significance.

**Bioreductive drugs.** In the wake of the failure of most hypoxic cell radiosensitizers to live up to their clinical potential, a new approach to combating hypoxia emerged: the use of bioreductive drugs that are selectively toxic to hypoxic cells. While these agents kill rather than sensitize hypoxic cells, the net effect of combining them with radiation therapy is an apparent sensitization of the tumor due to the elimination of an otherwise radioresistant subpopulation. Such drugs have been shown to outperform the nitroimidazole radiosensitizers in experimental studies with clinically relevant fractionated radiotherapy.<sup>188</sup> To the extent that hypoxic cells are also resistant to chemotherapy because of tumor

microenvironmental differences in drug delivery, pH, or the cell's proliferative status, complementary tumor-cell killing might be anticipated for combinations of bioreductive agents and anticancer drugs as well.<sup>189</sup>

Most hypoxia-specific cytotoxic drugs fall into three categories: the nitroheterocyclics, the quinone antibiotics, and the organic nitroxides.<sup>190</sup> All require bioreductive activation by nitroreductase enzymes such as cytochrome P450, DT-diaphorase, and nitric oxide synthase to reduce the parent compound to its cytotoxic intermediate, typically an oxidizing free radical capable of damaging DNA and other cellular macromolecules. The active species is either not formed or immediately back-oxidized to the parent compound in the presence of oxygen, which accounts for its preferential toxicity under hypoxic conditions. Examples of nitroheterocyclic drugs with bioreductive activity include misonidazole and etanidazole<sup>191,192</sup> and dual-function agents such as RSU 1069.<sup>193</sup> The latter drug is termed "dual function" because its bioreduction also activates a bifunctional alkylating moiety capable of introducing cross-links into DNA. Mitomycin C and several of its analogs (including porfiromycin and EO9) are quinones with bioreductive activity that have been tested in randomized clinical trials in head and neck tumors (e.g., Haffty et al.<sup>194</sup>).

The lead compound for the third class of bioreductive drugs, the organic nitroxides, is tirapazamine (SR 4233, Table 1.2).<sup>181,182,188</sup> The dose-limiting toxicity for single doses of tirapazamine is a reversible hearing loss; other effects observed include nausea and vomiting, and muscle cramps.<sup>195</sup>

Tirapazamine is particularly attractive because it both retains its hypoxia-selective toxicity over a broader range of (low) oxygen concentrations than the quinones and nitroheterocyclic compounds<sup>196</sup> and its "hypoxic cytotoxicity ratio," the ratio of drug doses under hypoxic versus aerobic conditions to yield the same amount of cell killing, averages an order of magnitude higher than for the other classes of bioreductive drugs.<sup>189</sup> Laboratory and clinical data also support a tumor-sensitizing role for tirapazamine in combination with cisplatin.<sup>195</sup>

To date, clinical trials with tirapazamine combined with radiotherapy and/or chemotherapy have yielded mixed results,<sup>195,197,198</sup> although it has improved outcomes for some standard treatments. While it is disappointing that tirapazamine has not made a more significant impact on clinical practice, the search for more effective agents from the same or similar chemical class continues.<sup>199</sup>

**Proliferating cell radiosensitizers.** Another source of apparent radioresistance is the presence of rapidly proliferating cells. Such cells may not be inherently radioresistant but rather have the effect of making the tumor seem refractory to treatment because the production of new cells outpaces the cytotoxic action of the therapy.

Analogues of the DNA precursor thymidine, such as bromodeoxyuridine (BrdUdR) or iododeoxyuridine (IdUdR), can be incorporated into the DNA of actively proliferating cells in place of thymidine because of close structural similarities between the compounds. Cells containing DNA substituted with these halogenated pyrimidines are more radiosensitive than normal cells, with the amount of sensitization directly proportional to the fraction of thymidine replaced.<sup>200</sup> In general, the radiosensitization takes the form of a decrease in or elimination of the shoulder region of the radiation survival curve. To be maximally effective, the drug must be present for at least several rounds of DNA replication prior to irradiation. Although the mechanism by which BrdUdR and IdUdR exert their radiosensitizing effect remains somewhat unclear, it is likely that both the formation of more complex radiation-induced lesions in the vicinity of the halogenated pyrimidine molecules and interference with DNA damage sensing or repair are involved.<sup>201</sup>

The clinical use of halogenated pyrimidines began in the late 1960s with a major clinical trial in head and neck cancer.<sup>202</sup> In retrospect, the

choice of head and neck tumors for this study was far from ideal, because the oral mucosa is also a rapidly proliferating tissue and was similarly radiosensitized, causing severe mucositis and a poor therapeutic ratio overall. In later years, tumors selected for therapy with halogenated pyrimidines were chosen in the hopes of better exploiting the differential radiosensitization between tumors and normal tissues.<sup>203</sup> Aggressively growing tumors surrounded by slowly growing or nonproliferating normal tissues, such as high-grade brain tumors or some sarcomas, have been targeted, for example.<sup>204,205</sup> Later strategies for further improving radiosensitization by BrdUdR and IdUdR involved changing the schedule of drug delivery: giving the drug as a long, continuous infusion both before and during radiotherapy<sup>206</sup>; and administering the drug as a series of short, repeated exposures.<sup>207</sup> Overall, however, the use of halogenated pyrimidines in the clinic has remained experimental and has not become mainstream.

**Chemotherapy drugs as radiosensitizers.** Several chemotherapy agents have long been known to increase the effectiveness of radiotherapy despite not being "true" radiosensitizers, like the nitroimidazoles. This has driven the clinical practice of treating many more patients today than in the past with chemotherapy and radiation therapy concurrently. Two drugs in particular used for chemoradiotherapy are 5-fluorouracil (5-FU, effective against gastrointestinal malignancies<sup>208</sup>) and cisplatin (effective against head and neck<sup>209</sup> and cervix cancers<sup>210</sup>).

Based on these clinical successes in combining radiation with concurrent chemotherapy, and with ever-increasing numbers of molecularly targeted drugs and biologics available today, it is naturally of interest whether any of these novel compounds could also act as radiosensitizers. Two classes of such drugs already have entered the clinical mainstream as sensitizers: the antiepidermal growth factor receptor (EGFR) inhibitors and the antivascular endothelial growth factor (VEGF) inhibitors. Cetuximab is a monoclonal antibody raised against the EGFR that has been shown to improve outcomes in advanced head and neck cancers when combined with radiation therapy<sup>211</sup> and bevacizumab is a humanized monoclonal antibody raised against VEGF that prolongs overall and progression-free survival in patients with advanced colorectal cancer when combined with standard chemotherapy.<sup>212</sup> It is hoped that these and other targeted agents will play greater roles in cancer therapy in the future.

### Normal Tissue Radioprotectors

Amifostine (WR 2721, see Table 1.2), is a phosphorothioate compound developed by the US Army for use as a radiation protector. Modeled after naturally occurring radioprotective sulfhydryl compounds such as cysteine, cysteamine, and glutathione,<sup>213</sup> amifostine's mechanism of action involves the scavenging of free radicals produced by ionizing radiation, radicals that otherwise could react with oxygen and "fix" the chemical damage. Amifostine can also detoxify other reactive species through the formation of thioether conjugates; in part because of this, the drug can also be used as a chemoprotective agent.<sup>214</sup> Amifostine is a prodrug that is dephosphorylated by plasma membrane alkaline phosphatase to the free thiol WR 1065, the active metabolite. As is the case with the hypoxic cell radiosensitizers, amifostine need only be present at the time of irradiation to exert its radioprotective effect.

In theory, if normal tissues could be made to tolerate higher total doses of radiation through the use of radioprotectors, then the relative radioresistance of hypoxic tumor cells would be less likely to limit radiation therapy. However, encouraging preclinical studies demonstrating radioprotection of a variety of cells and tissues notwithstanding,<sup>215,216</sup> radioprotectors such as amifostine would not be expected to increase the therapeutic ratio unless they could be introduced selectively into normal tissues but not tumors. The pioneering studies of Yuhas et al.<sup>178,217,218</sup> addressed this issue by showing that the drug's active



metabolite reached a higher concentration in most normal tissues than in tumors and that this mirrored the extent of radio- or chemoprotection. The selective protection of normal tissues results from slower tumor uptake of the drug and tumor cells being both less able to convert amifostine to WR 1065 (owing to lower concentrations of the required phosphatases) and less able to transport this active metabolite throughout the cell.

*Dose-reduction factors* (DRFs; the ratio of radiation doses to produce an isoeffect in the presence vs. absence of the radioprotector) in the range of 1.5 to 3.5 are achieved for normal tissues, whereas the corresponding DRFs for tumors seldom exceed 1.2. Those normal tissues exhibiting the highest DRFs include bone marrow, gastrointestinal tract, liver, testes, and salivary glands.<sup>178</sup> The brain and spinal cord are not protected by amifostine, and oral mucosa only marginally so.<sup>178</sup> Comparable protection factors are obtained for some chemotherapy agents, including cyclophosphamide and cisplatin.<sup>219,220</sup> The dose-limiting toxicities associated with the use of amifostine include hypotension, emesis, and generalized weakness or fatigue.<sup>221</sup>

Amifostine is currently indicated for the reduction of renal toxicity associated with repeated cycles of cisplatin chemotherapy in patients with advanced ovarian and non-small cell lung cancer. It is also approved for use in patients receiving radiotherapy for head and neck cancer in the hopes of reducing xerostomia secondary to exposure of the parotid glands.

Finally, just as there are apparent radiosensitizers, there are also apparent radioprotectors that have the net effect of allowing normal tissues to better tolerate higher doses of radiation and chemotherapy but through mechanisms of action not directly related to the scavenging of free radicals. Various biological response modifiers, including cytokines, prostaglandins (such as misoprostol<sup>222,223</sup>), anticoagulants (such as pentoxifylline<sup>224,225</sup>), and protease inhibitors are apparent radioprotectors because they can interfere with the chain of events that normally follows the killing of cells in tissues by, for example, stimulating compensatory repopulation or preventing the development of fibrosis. Finally, there is also growing interest in the use of biologics that inhibit apoptosis as normal tissue radioprotectors.<sup>226,227</sup> Such agents should have little or no effect on tumor cells, most of which are already apoptosis resistant.

## CLINICAL RADIOBIOLOGY

### Growth Kinetics of Normal Tissues and Tumors

In the simplest sense, normal tissues are normal because the net production of new cells, if it occurs at all, exactly balances the loss of old cells from the tissue. In tumors, the production of new cells exceeds cell loss, even if only by a modest amount. Although the underlying radiobiology of cells in vitro applies equally to the radiobiology of tissues, the imposition by growth kinetics of this higher level of organizational behavior makes the latter far more complex systems.

### Descriptive Classification Systems

Two qualitative classification systems based loosely on the proliferation kinetics of normal tissues are in use. Borrowing heavily from the pioneering work of Bergonié and Tribondeau,<sup>13</sup> Rubin and Casarett's<sup>228</sup> classification system for tissue "radiosensitivity" consists of four main categories:

Type I or vegetative intermitotic cells (VIMs) are considered the most radiosensitive, consisting of regularly dividing, undifferentiated stem cells such as are found in the bone marrow, intestinal crypts, and the basal layer of the epidermis of the skin.

Type II or differentiating intermitotic cells (DIMs) are somewhat less radiosensitive, consisting of progenitor cells that are in the process of developing differentiated characteristics yet are still capable of a

limited number of cell divisions. Myelocytes of the bone marrow and spermatocytes of the testis are examples of Type II cells.

Type III or reverting postmitotic cells (RPMs) are relatively radioresistant, consisting of those few types of cells that are fully differentiated and do not divide regularly yet under certain conditions can revert to a stem cell–like state and divide as needed. Examples of Type III cells include hepatocytes and lymphocytes, although the latter are unique in that they are a notable exception to the Rubin and Casarett classification system—an RPM cell type that is exquisitely radiosensitive.

Type IV or fixed postmitotic cells (FPMs) are the most radioresistant, consisting of the terminally differentiated, irreversibly postmitotic cells characteristic of most normal tissue parenchyma, such as neurons and muscle cells. Should such cells be killed by radiation, they typically cannot be replaced.

A second, simpler classification system, based on anatomical and histological considerations, has been proposed by Michalowski.<sup>229</sup> Using this system, tissues are categorized on the basis of whether the tissue stem cells, if any, and the functional cells are compartmentalized (so-called Type H or hierarchical tissues, such as skin, gut epithelium, testis, etc.) or intermixed (Type F or flexible tissues, such as lung, liver, kidney, and spinal cord).

### Growth Kinetic Parameters and Methodologies

In order to predict the response of an intact tissue to radiation therapy in a more quantitative way, a number of kinetic parameters have been described that provide a better picture of the proliferative organization of tumors and normal tissues (Table 1.3).

**Growth fraction.** Among the first kinetic characteristics described was the growth fraction (GF). The presence of a fraction of slowly cycling or noncycling cells in experimental animal tumors was first noted by Mendelsohn et al.<sup>230,231</sup> and, subsequently, in human tumors by other investigators. While normal tissues do not grow and therefore do not have a GF per se, many are composed of noncycling cells that have differentiated in order to carry out tissue-specific functions. Some normal tissues do contain a small fraction of actively proliferating stem cells. Others contain apparently dormant or "resting" cells that are temporarily out of the traditional four-phase cell cycle but are capable of renewed proliferation in response to appropriate stimuli. Lajtha gave these resting but recruitable cells of normal tissues the designation  $G_0$ .<sup>232</sup> While a tumor counterpart of the  $G_0$  cell may or may not exist, the majority of slowly cycling or noncycling tumor cells are thought to be in such a state because of nutrient deprivation, not because of a normal cell cycle regulatory mechanism. Thus, Dethlefsen<sup>233</sup> has suggested that the term *Q cell* be reserved for quiescent cells in tumors to distinguish them from the  $G_0$  cell of normal tissues.

Measurement of a tumor's GF is problematic,<sup>234,235</sup> but an estimate can be obtained with a technique known as *continuous thymidine labeling*. Using this method, the tumor receives a continuous infusion of radio-labeled thymidine for a period of time long enough for all proliferating cells to have gone through at least one round of DNA synthesis and incorporated the radioactive label. Then, a biopsy of the tumor is obtained and tissue sections prepared for autoradiography. Once the slides are processed and scored, the continuous labeling index, that fraction of the total population of tumor cells containing tritiated thymidine, is calculated. This value is a rough estimate of the tumor's GF.

**Cell cycle and volume doubling times.** The percent labeled mitosis (PLM) technique of Quastler and Sherman<sup>236</sup> was a key development in the study of the cell cycle in vivo because it provided a unique window into the behavior of that fraction of cells within a tissue that was actively proliferating. By focusing on cells in mitosis, the assay allowed both the overall cell cycle time ( $T_c$ ) and the durations of the individual cell



TABLE 1.3 Estimated Cell Cycle Kinetic Parameters for Human Tumors

Parameter	Definition	How Measured	Representative Values for Human Solid Tumors	Notes
$T_c$	(Average) Cell cycle time	Percent labeled mitosis technique; flow cytometry	0.5–6.5 days (median $\approx$ 2.5)	$T_c$ in vivo usually longer than for comparable cells cultured in vitro.
GF	Growth fraction	Estimated from continuous labeling technique	0.05–0.90 days (median $\approx$ 0.40?)	Difficult to measure directly; not much data available.
$T_{pot}$	Potential doubling time	Flow cytometry (relative movement method: $T_{pot} = \lambda T_s / LI$ )	2–19 days (median $\approx$ 5)	$T_{pot} \approx T_c$ as GF approaches 1.0.
$\phi$	Cell loss factor	$1 - T_{pot}/T_d$	0.30–0.95 days (median $\approx$ 0.90?)	Thought to be the major cause of long $T_d$ s for human tumors; particularly high in carcinomas.
$T_d$	Volume doubling time	Direct measurement of tumor dimensions over time	5–650 days (median $\approx$ 90)	Increases with increasing tumor size, often because of increases in $T_c$ and $\phi$ , and a decrease in GF.
$T_{eff}/T_p$	Effective clonogen doubling time	Estimated from clinical data on the loss of local control with increasing overall treatment time	4–8 days	$T_p$ approaches $T_{pot}$ toward the end of a course of fractionated radiotherapy.

Data from Steel GG. *Growth Kinetics of Tumours*. Oxford: Clarendon Press; 1977, and Joiner M, van der Kogel A. *Basic Clinical Radiobiology*. 4th ed. London: Hodder Arnold; 2009.

cycle phases to be determined without the uncertainties introduced by the presence of noncycling cells in the population. Today, flow cytometric methods have largely replaced the arduous and time-consuming PLM assay.

Briefly, the PLM technique involves tracking over time a cohort of proliferating cells that initially was in S phase (and exposed briefly to tritiated thymidine) and then proceeded through subsequent mitoses. Serial biopsy samples from the tissue of interest are obtained at regular intervals following labeling, and the fraction of cells both in mitosis (identified cytologically) and carrying the radioactive label is determined. A first peak of labeled mitoses is observed within 24 hours after labeling, and as cells pass through their second division, a second wave of labeled mitoses is noted. The average  $T_c$  for the population of proliferating cells corresponds to the peak-to-peak interval of the resulting PLM curve, a plot of the fraction of labeled mitoses as a function of time following the radioactive pulse. With sufficiently robust data, the durations of the individual cell cycle phases can be obtained as well. The PLM technique is illustrated schematically in Fig. 1.25.

Historically, the interpretation of PLM curves was sometimes hampered by technical artifacts and by the fact that proliferating cell populations have distributed cell cycle times.<sup>234,235,237</sup> Despite these limitations, it is clear that most cells in vivo proliferate more slowly than their in vitro counterparts. Although the variation in intermitotic times is quite large, a median value for  $T_c$  of 2 to 3 days is a reasonable estimate.<sup>234</sup>

While the cycle times of proliferating cells in vivo are long by cell culture standards, they are quite short when compared with the corresponding volume doubling times ( $T_d$ ) for human tumors. Although highly variable from tumor type to tumor type and somewhat difficult to measure, the  $T_d$  for human solid tumors averages about 3 to 4 months.<sup>234</sup> In many cases, sample calculations further suggest that the discrepancy between  $T_c$  for proliferating tumor cells and  $T_d$  for the tumor as a whole cannot be accounted for solely by the tumor having a low GF.

**Cell loss factor.** Cell kineticists initially adhered to the notion that the continued growth of tumors over time reflected abnormalities in

cell production. Pathologists and tumor biologists, meanwhile, had ample evidence that tumors routinely lost large numbers of cells, the result of cell death, maturation, and/or emigration.<sup>234,238,239</sup> It is now clear that the overall rate of tumor growth, as reflected by its  $T_d$ , is governed by the competing processes of cell production and cell loss. In fact, the cell loss factor,  $\phi$ , the rate of cell loss expressed as a fraction of the cell production rate, is surprisingly high for both experimental and human tumors, as high as 0.9 or more for carcinomas and lower, on average, for sarcomas.<sup>234</sup> Cell loss is usually the most important factor governing the overall volume  $T_d$  of solid tumors.

The clinical implications of tumors having high rates of cell loss are obvious. First, any attempts at making long-term predictions of treatment outcome based on short-term regression rates of tumors during treatment are misleading. Second, although regression rate may not correlate well with eventual outcome, it may be a reasonable indicator of when best to schedule subsequent therapy on the assumption that a smaller tumor will be more radio- and chemosensitive, as well as easier to remove surgically.

**Potential doubling time and "effective" doubling time.** With the recognition that cell loss plays a major role in the overall growth rate of tumors and can mask a high cell production rate, a better measure of the potential repopulation rate of normal tissues and tumors was needed.<sup>240</sup> One indicator of regenerative capacity is the potential doubling time ( $T_{pot}$ ).<sup>234,241</sup> By definition,  $T_{pot}$  is an estimate of the time that would be required to double the number of clonogenic cells in a tumor in the absence of cell loss. It follows that  $T_d$  will usually be much longer than  $T_{pot}$  because of cell loss, and  $T_c$  will be shorter than  $T_{pot}$  because of the presence of nonproliferating cells.<sup>237</sup>

$T_{pot}$  can be estimated from a comparison of the S phase pulse labeling index (LI) and the duration of S phase ( $T_s$ ) by using the following equation:

$$T_{pot} = \lambda T_s / LI$$

where  $\lambda$  is a correction factor related to the nonuniform distribution of cell "ages" in a growing population (usually,  $\lambda \approx 0.8$ ).  $T_s$  and LI can

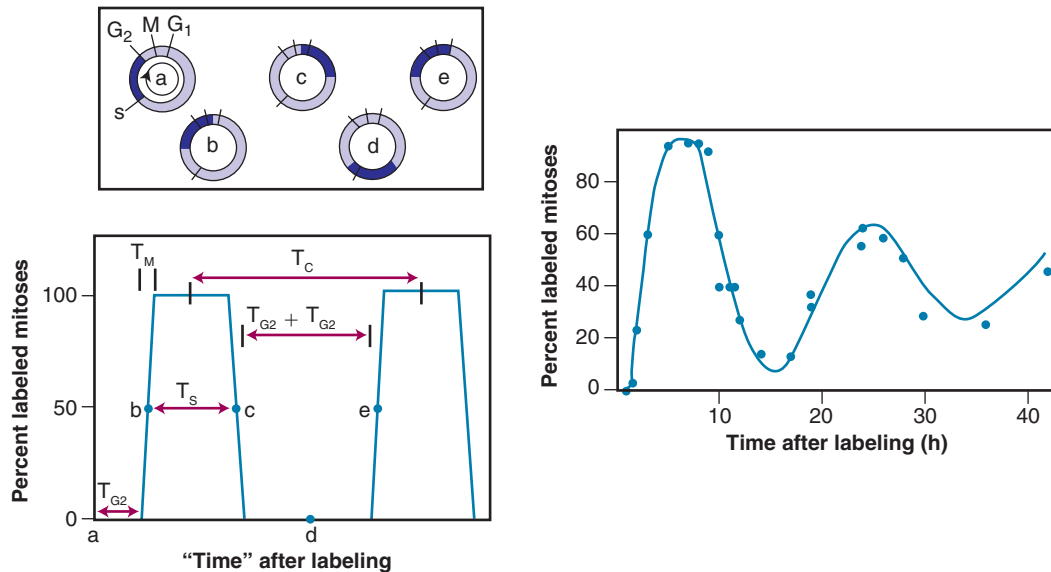


**Fig. 1.25** The technique of labeled mitoses (PLM) for an idealized cell population with identical cell cycle times (*left panels*) and for a representative normal tissue or tumor with a dispersion in cell cycle times (*right panel*). *Top left*: Following a brief exposure to tritiated thymidine or equivalent at time = “a,” the labeled cohort of S phase cells continues (dark shading) around the cell cycle and is sampled at times = “b,” “c,” “d,” and “e,” respectively. *Bottom left panel*: For each sample, the percentage of cells both in mitosis and containing the thymidine label is determined and plotted as a function of time; from such a graph, individual cell cycle phase durations can be derived. *Right panel*: In this more realistic example, a mathematical fit to the PLM data would be needed to calculate the (average) cell cycle phase durations.

be determined by the relative movement method.<sup>241,242</sup> This technique involves an injection of a thymidine analog, usually BrdUrd, which is promptly incorporated into newly synthesized DNA and whose presence can be detected using flow cytometry. The labeled cohort of cells is then allowed to continue movement through the cell cycle and a biopsy of the tumor is taken several hours later, at which point the majority of the BrdUrd-containing cells have progressed into G<sub>2</sub> phase or beyond. A value for LI is determined from the fraction of the total cell population that contains BrdUrd, and  $T_S$  is calculated from the rate of movement of the labeled cohort during the interim between injection of the tracer and biopsy.

Values for  $T_{pot}$  for human tumors have been measured and, although quite variable, typically range between 2 and 20 days.<sup>234,240,243</sup> These findings lend support to the important notion that slowly growing tumors can contain subpopulations of rapidly proliferating cells. To the extent that these cells retain unlimited reproductive potential, they may be considered the tumor’s stem cells (in a generic sense, at least) capable of causing recurrences after treatment. These cells represent a serious threat to local control of the tumor by conventional therapies, especially protracted treatments (that provide them additional time to proliferate).

The use of a cell kinetic parameter such as  $T_{pot}$  as either a predictor of a tumor’s response to therapy or as a means of identifying subsets of patients particularly at risk for recurrence has been attempted, with some positive, but mostly negative, results.<sup>6,141,244</sup> Lest these negative findings suggest that proliferation in tumors is unimportant, bear in mind that it is unlikely that a pretreatment estimate of  $T_{pot}$ —or any other single cell kinetic parameter (e.g., LI) for that matter—would be relevant once treatment commences and the growth kinetics of the tumor are perturbed.

One approach to dealing with this problem is to measure proliferative activity during treatment. Although not without other limitations, the use of an “effective clonogen doubling time” ( $T_{eff}$  or  $T_p$ ) has been

advocated.<sup>245–247</sup> Estimates of  $T_p$  can be obtained from two types of experiments. In an experimental setting,  $T_p$  can be inferred from the additional dose necessary to keep a certain level of tissue reaction constant as the overall treatment time is increased. (When expressed in terms of dose rather than time, the proper term would be  $D_{eff}$ , although the underlying concept is the same.) For example, acute skin reactions usually both develop and begin to resolve during the course of radiation therapy, suggesting that the production of new cells in response to injury gradually surpasses the killing of existing cells by each subsequent dose fraction. By intensifying treatment once this repopulation begins, it theoretically should be possible to reach a steady state wherein the tissue reaction remains constant. In a clinical setting,  $T_p$  can be estimated from a comparison of tumor control rates for treatment schedules in which the dose per fraction and total dose used were held approximately constant but the overall treatment time varied. In some cases, the loss of local control with increasing overall treatment time provides an estimate not only of  $T_p$  but also of the delay time before the repopulation begins, sometimes referred to as  $T_k$ , the repopulation “kickoff” time.<sup>248–250</sup>

**Repopulation in tumors and normal tissues.** As discussed earlier, both normal tissues and tumors are capable of increasing their cell production rate in response to radiation-induced cell killing, a process known as regeneration or repopulation. The time of onset of the regenerative response varies with the turnover rate of the tissue or tumor since cell death (and depopulation) following irradiation is usually linked to cell division. Generally, tissues that naturally turn over fairly rapidly repopulate earlier and more vigorously than tissues that turn over slowly. However, it has been shown that the repopulation patterns of normal tissues and tumors following the start of irradiation tend to be characterized by a delay (of at least several weeks in many cases; see  $T_k$  discussed earlier) prior to the rapid proliferative response.<sup>248–250</sup> Once this proliferative response begins, however, it can be quite vigorous. While this is clearly desirable for early-responding normal tissues attempting to recover from radiation injury, rapid proliferation in tumors

is obviously undesirable.<sup>251</sup> For example, clinical studies of local control of head and neck tumors indicate that an average of about 0.6 Gy per day is lost to repopulation.<sup>245</sup> Attempts to counteract this accelerated proliferation by dose intensification during the latter part of a treatment course can be problematic because late-responding normal tissues do not benefit from accelerated repopulation during treatment and risk incurring complications.

## EARLY AND LATE EFFECTS IN NORMAL TISSUES

### “Early” Versus “Late”

Normal tissue complications observed following radiation therapy are the result, either directly or indirectly, of the killing of critical target cells within the tissue that are crucial to the tissue's continued functional and/or structural integrity. The loss of these cells can occur either as a direct consequence of the cytotoxic action of the radiation or indirectly due to the radiation injury or killing of other cells. In some cases, the tissue's response to the depletion of its component cells can exacerbate the injury, for example, when a hyperproliferation of fibroblasts and the resulting collagen deposition replace a tissue's parenchymal cells, resulting in fibrosis.

It is important to realize that a particular tissue or organ may contain more than one type of target cell, each with its own radiosensitivity. One tissue may manifest more than one complication following radiation therapy, with the severity of each determined by the radiosensitivity of the particular target cell and the time-dose-fractionation schedule employed. It follows from this that the severity of one complication does not necessarily predict the severity of another complication, even within the same tissue (although “consequential” late effects secondary to severe early reactions are possible in some cases<sup>252</sup>). For example, dry or moist desquamation of the skin results from the depletion of the basal cells of the epidermis, fibrosis results from damage to dermal fibroblasts, and telangiectasia results from damage to small blood vessels in the dermis. For many tissues, however, the cell(s) whose death is (are) responsible for a particular normal tissue injury remain(s) unclear.

While the radiosensitivity of the putative target cells determines the severity of an early or late effect in a normal tissue, the “earliness” or “lateness” of the clinical manifestation of that injury is related to the tissue's proliferative organization (discussed above). The distinction between the radiosensitivity of a tissue's cells and the radioresponsiveness of the tissue as a whole can be a source of confusion. Bergonié and Tribondeau's “laws,”<sup>213</sup> for example, confused the concepts of radiosensitivity and radioresponsiveness to some extent, referring to tissues that responded to damage early as “radiosensitive,” when this is not necessarily the case.

### Whole Body Radiation Syndromes

Many human beings have been exposed to total body irradiation, including the survivors of Hiroshima and Nagasaki, Polynesian Islanders and military personnel present during above ground nuclear tests during the 1950s, and victims of accidental exposures in the workplace (e.g., Chernobyl). Of the latter, about 100 fatalities due to radiation accidents have been documented since the mid-1940s.<sup>253–255</sup>

The whole body radiation syndromes described here only occur when most or all of the body is irradiated. Also, although total body irradiation (TBI) is a prerequisite for the manifestation of these syndromes, neither the dose received nor its biological consequences are necessarily uniform. The radiosensitivities of the respective target cells determine the effective threshold dose below which the syndrome does not occur, whereas the onset time of individual symptoms is governed more by the proliferative organization of the tissue.

The mean lethal dose ( $LD_{50}$ ) is defined as the (whole body) dose that results in mortality for 50% of an irradiated population. The  $LD_{50}$  value is often expressed in terms of the time scale over which the deaths occur, such as at either 30 or 60 days postirradiation. For humans, the single-dose  $LD_{50/60}$  for x-rays or  $\gamma$ -rays is approximately 3.5 Gy in the absence of medical intervention and about twice that with careful medical management.<sup>28,255</sup> The  $LD_{50}$  increases with decreasing dose rate of low-LET radiation and decreases for radiations of higher LET.

**The prodromal syndrome.** The prodromal syndrome consists of one or more transient, neuromuscular, and gastrointestinal symptoms that begin soon after irradiation and persist for up to several hours. The symptoms, which can include anorexia, nausea, vomiting, diarrhea, fatigue, disorientation, and hypotension, and their severity and duration, increase with increasing dose. Because in most radiation accident situations the dose that victims received is unknown initially, careful attention to the prodromal syndrome can be used as a crude dosimeter.

**The cerebrovascular syndrome.** The cerebrovascular syndrome occurs for total body doses in excess of 50 Gy. The onset of signs and symptoms is almost immediate following exposure, consisting of severe gastrointestinal and neuromuscular disturbances—including nausea and vomiting, disorientation, ataxia, and convulsions.<sup>28,255</sup> The cerebrovascular syndrome is invariably fatal; survival time is seldom longer than about 48 hours. Only a few instances of accidental exposure to such high doses have occurred, two of which (a nuclear criticality accident at Los Alamos National Laboratory in 1958 and a <sup>235</sup>U reprocessing plant accident in Rhode Island in 1964) have been extensively documented in the medical literature.<sup>256,257</sup>

The immediate cause of death for the cerebrovascular syndrome is likely vascular damage leading to progressive brain edema, hemorrhage, and/or cardiovascular shock.<sup>255</sup> Following such high doses delivered acutely, even cells traditionally considered radioresistant, such as neurons and the parenchymal cells of other tissues and organs, will be killed along with the more radiosensitive vascular endothelial cells and the various glial cells of the central nervous system.

**The gastrointestinal syndrome.** For doses upwards of about 8 Gy, the gastrointestinal syndrome predominates, characterized by lethargy, vomiting and diarrhea, dehydration, electrolyte imbalance, malabsorption, weight loss, and, ultimately, sepsis. These symptoms begin to appear within a few days of irradiation and are progressive in nature, culminating in death after 5 to 10 days. The target cells for the gastrointestinal syndrome are principally the crypt stem cells of the gut epithelium. As mature cells of the villi are lost over a several-day period, no new cells are available to replace them; thus, the villi begin to shorten and eventually become completely denuded. This greatly increases the risk of bleeding and sepsis, both of which are aggravated by declining blood counts.

Prior to the Chernobyl accident, in which approximately a dozen firefighters received total doses sufficient to succumb to the gastrointestinal syndrome, there was only one other documented case of a human dying of gastrointestinal injury.<sup>28,255</sup> To date, no human has survived a documented whole body dose of 10 Gy of low-LET radiation.

**The hematopoietic syndrome.** Acute doses of approximately 2.5 Gy or more are sufficient to cause the hematopoietic syndrome, a consequence of the killing of bone marrow stem cells and lymphocytes. This syndrome is characterized by a precipitous (within 1–2 days) reduction in the peripheral blood lymphocyte count, followed by a more gradual reduction (over a period of 2–3 weeks) in the numbers of circulating leukocytes, platelets, and erythrocytes. The granulocytopenia and thrombocytopenia reach a maximum within 30 days after exposure; death, if it is to occur, is usually a result of infection and/or hemorrhage.<sup>28,255</sup> Theoretically, the use of antibiotics, blood transfusions, and bone marrow transplantation can save the lives of individuals who receive doses at or near the  $LD_{50}$ . In practice, however, the exact dose

is seldom known, and should it be high enough to reach the threshold for the gastrointestinal syndrome, such heroic measures would be in vain. This was the case for all but 2 of the 13 Chernobyl accident victims who received bone marrow transplants.<sup>28</sup> Of the two survivors, only one technically had his life saved by the transplant; the other survivor showed autologous bone marrow repopulation.

### Teratogenesis

One of the most anxiety-provoking risks of irradiation in the eyes of the general public is prenatal exposure of the developing embryo or fetus.<sup>254,255</sup> In part, such concern is warranted because teratogenic effects are quite sensitive to induction by ionizing radiation, with readily measurable neurological abnormalities noted in individuals exposed prenatally to doses as low as approximately 0.06 Gy.<sup>28</sup> The radiation-induced excess relative risk of teratogenesis during the most sensitive phase of gestation is approximately 40% per Gy.<sup>28</sup> By comparison, the spontaneous incidence of a congenital abnormality occurring during an otherwise normal pregnancy is about 5% to 10%.<sup>255</sup>

Information on the teratogenic effects of radiation in humans come from two major sources, the Japanese atomic bomb survivors and patients who received diagnostic or therapeutic irradiation either prior to the establishment of modern radiation protection standards or in clinical emergency situations. While a range of abnormalities have been identified in individuals irradiated in utero (including anecdotal reports of miscarriages and stillbirths, cataracts and other ocular defects, gross malformations, sterility, etc.), the most commonly reported are microcephaly, intellectual/cognitive impairment, and growth retardation.<sup>28,254,255</sup> Each of these teratogenic effects has a temporal relationship to the stage of gestation at the time of irradiation as well as a radiation dose and dose rate dependency. Lethality is the most common consequence of irradiation during the preimplantation stage (within 10 days of conception), growth retardation has been noted for irradiation during the implantation stage (10–14 days after conception), and during the organogenesis period (about 15–50 days after conception), the embryo is sensitive to both lethal, teratogenic, and growth retarding effects.<sup>255</sup> Radiation-induced gross abnormalities of the major organ systems do not occur during the fetal period (more than 50 days postconception), although generalized growth retardation and some neurological defects have been noted for radiation doses in excess of 1 Gy.

### Radiation-Induced Cataracts

Late effects resulting from irradiation of the eye were noted within a few years of the discovery of x-rays,<sup>228,255</sup> with cataracts being the most frequent pathological finding. From a clinical perspective, the induction of a cataract following radiotherapy is a normal tissue complication that can be corrected surgically and, as such, is not considered quite as dire as other late effects. From a radiobiological perspective, however, cataracts are unique among the somatic effects of radiation in several respects. First, although the lens of the eye is a self-renewing tissue complete with a stem cell compartment of epithelial cells that divide and gradually differentiate into mature lens fibers, there is no clear mechanism of cell loss.<sup>28</sup> As such, the stem cells damaged by radiation (which manifest themselves as abnormal, opaque lens fibers) persist, eventually leading to a cataract. Second, cataracts are among the few radiation-induced lesions that can be distinguished pathologically from their spontaneously occurring counterparts; radiation cataracts first appear in the posterior pole of the lens, whereas spontaneous cataracts usually begin in the anterior pole.<sup>258,259</sup> Third, radiogenic cataracts exhibit a variable latency period (anywhere from about a year to several decades, averaging 5–8 years) that decreases with increasing radiation dose. Finally, cataract formation is a nonstochastic (deterministic) process; that is, there is a threshold dose below which no cataracts occur, but above the

threshold, the frequency and severity of cataracts increases with increasing dose.<sup>258,259</sup> For low-LET radiation, the single-dose threshold for a cataract in humans is approximately 2 Gy, which increases to about 4 Gy for fractionated exposures. These dose thresholds apply to any detectable cataract, although not necessarily a symptomatic one, which generally requires a fractionated dose of at least 10 Gy. Neutrons are also known to be quite effective at inducing cataracts, with RBEs of about 5 to 10 commonly observed in laboratory rodents.<sup>255</sup>

### Radiation Carcinogenesis

Unrepaired or misrejoined DNA damage caused by radiation exposure is usually lethal to the cell, although this is not invariably the case, particularly when the genetic material is simply rearranged rather than deleted. Whether such changes have further implications for the cell bearing them depends on the location of the damage in the genome, the nature and extent of the mutational event, whether working copies of proteins can still be produced from the gene or genes involved, what function these proteins normally have, and the type of cell. There is compelling evidence that some of these radiation-induced genetic rearrangements—particularly ones that activate oncogenes or inactivate tumor suppressor genes—either alone or in combination with other such changes predispose a cell to neoplastic transformation, a necessary early step in the process of tumor induction.<sup>254,260</sup>

**Laboratory studies.** Although ionizing radiation is one of the most studied and best understood carcinogens, it is not a particularly potent one. This fact hampers studies of radiation carcinogenesis in humans, because investigators must identify a modest radiogenic increment of excess risk with a long latency period against a high background spontaneous cancer rate and multiple confounding factors. Nevertheless, from a public health perspective, carcinogenesis is the most important somatic effect of radiation for doses of 1.5 Gy or less.<sup>28</sup>

The use of cell cultures and laboratory rodents to study carcinogenesis avoids some of the pitfalls of human epidemiological studies but have their own inherent limitations. Cell culture systems employ neoplastic transformation as the endpoint, which is a prerequisite for, but by no means equal to, carcinogenesis *in vivo*. Neoplastic transformation is defined as the acquisition of one or more phenotypic traits in nontumorigenic cells that are usually associated with malignancy, such as immortalization, reduced contact inhibition of growth, increased anchorage-independent growth, reduced need for exogenously supplied nutrients and growth factors, various morphological and biochemical changes, and, in nearly all cases, the ability to form tumors in histocompatible animals.<sup>237</sup> Such systems can be used to study relatively early events in the carcinogenesis process, have much greater sensitivity and statistical resolution than *in vivo* assays, and can be used to measure dose-response relationships. Laboratory animal studies, however, are considered more relevant in that tumor formation is the endpoint, latency periods are shorter, statistical variability is reduced, and the carcinogen exposure conditions can be carefully controlled.

Pertinent results from laboratory studies of radiation carcinogenesis include the following:

1. Carcinogenesis is a stochastic effect, that is, a probabilistic function of the dose received, with no evidence of a dose threshold. Increasing the radiation dose increases the probability of the effect, but not its severity.<sup>254,260</sup>
2. The neoplastic transformation frequency increases linearly with dose, at least over the low-dose range (about 1.5 Gy or less).
3. There is a dose rate effect for transformation and carcinogenesis (for low-LET radiations); protracted exposures carry a reduced risk relative to acute exposures.
4. The processes of neoplastic transformation and carcinogenesis are necessarily in competition with the cell-killing effects of ionizing



radiation.<sup>28</sup> As such, dose-response curves for tumor formation in vivo tend to be bell shaped as a function of dose (e.g., Upton<sup>261</sup>). In vitro, where cytotoxicity can be assessed separately from transformation and appropriate corrections made, dose-response curves tend to be linear.

**Epidemiological studies in humans.** In humans, most of the information useful for risk estimation is derived from epidemiological studies, with the dose almost always exceeding 0.1 Gy and often exceeding 1.0 Gy. However, most of the controversy concerns doses less than 0.1 Gy, delivered over protracted, rather than acute, time periods. Therefore, in order to infer low-dose effects from high-dose data, epidemiologists make extrapolations and assumptions about dose-response relationships that may or may not be valid in all cases.

Many sources of error can also plague epidemiological data, including selection bias, small sample size, heterogeneous population characteristics, and dose uncertainties.<sup>255</sup> The human populations that have been and continue to be evaluated for radiation-induced excess cancers are Japanese atomic bomb survivors; persons exposed to fallout from nuclear tests or accidents; radiation workers receiving occupational exposure; populations living in areas characterized by above average natural background radiation or in proximity to man-made sources of radiation; and patients exposed to repeated diagnostic or therapeutic radiation. Pertinent findings from these studies include the following.

1. Within the limits of statistical resolution, the shape of the dose-response curve is not inconsistent with a linear, no-threshold model.<sup>254,260</sup>
2. Different tissues have different sensitivities to radiation-induced carcinogenesis, with bone marrow (leukemias other than chronic lymphocytic), breast (female), salivary glands, and thyroid especially susceptible.<sup>255</sup>
3. The latency period between irradiation and the clinical presentation of a solid tumor averages 20 years or more, and about half that for hematological malignancies. However, the latency period varies with the age of the individual, generally increasing with decreasing age at exposure. Latency periods tend to be shorter for radiation-induced second malignancies, in which patients had received much higher doses.
4. Two risk projection models have been used to predict the risk of radiation carcinogenesis in the human population: the absolute risk model, and the relative risk model. Using the absolute risk model, excess risk in an irradiated population begins after the latency period has passed and is added to the age-adjusted spontaneous cancer risk. After a period of time, the cancer risk returns to spontaneous levels. The relative risk model predicts that the excess cancer risk is a multiple of the spontaneous incidence. At present, the epidemiological data tend to support the relative risk model for most solid tumors and the absolute risk model for leukemia.
5. The current recommendations of the International Commission on Radiological Protection (ICRP) state that the nominal probability of radiation-induced cancer death is approximately 4% per Sievert (Sv) for working adults and about 5% per Sv for the whole population under conditions of frequent, low-dose exposure over extended periods.<sup>262</sup> These risk estimates double for acute, high-dose exposures.

The Sievert is a unit of dose equivalent used for radiation protection purposes and is equal to the radiation dose (in Gy) multiplied by a radiation weighting ( $W_R$ ) factor specific for the type of radiation (with  $W_R$  roughly equivalent to the radiation's RBE). As warranted, a second correction to the equivalent dose can be made to account for the differing radiosensitivities of the different tissues exposed, termed the *tissue weighting factor* ( $W_T$ ). Once this correction is applied, equivalent dose becomes effective dose, also expressed in units of Sv.

**Carcinogenic risk from prenatal irradiation.** The risk of carcinogenesis as a result of prenatal radiation exposure is made even more controversial by conflicting results of epidemiological studies. One major study cohort consisted of several thousand children (plus a demographically similar population of unirradiated children) who received prenatal exposure from diagnostic procedures during the 1950s and 1960s. The Oxford Survey of Childhood Cancer<sup>263</sup> reported nearly twice the incidence of leukemia in children who had received prenatal irradiation. Although other epidemiological studies lend credence to the Oxford Survey's findings,<sup>254,260</sup> it is still possible that factors other than the x-ray exposure may have caused, or at least contributed to, the excess cancer risk. On the other hand, children of the Japanese atomic bomb survivors who were pregnant at the time of the bombing did not support the Oxford Survey's findings of increased risk of *childhood* malignancy; however, they did support an increased risk of malignancy later in life.<sup>28</sup>

On the assumption that it is preferable to overestimate rather than underestimate risk, it is prudent to assume that the carcinogenic risk of radiation exposure to an embryo or fetus is about twice that for postnatal exposure.

**Carcinogenic risk from medical imaging procedures.** Recent data gleaned from the Japanese atomic bomb survivors indicate a small but statistically significant excess cancer risk even for doses as low as 35 to 150 mSv.<sup>264,265</sup> That this is in the range of doses delivered during a computed tomography (CT) scan—in particular, a pediatric CT scan<sup>266,267</sup>—has made headlines and both sparked controversy<sup>268</sup> as well as increased awareness<sup>269</sup> of radiation's risks. Estimates are that an abdominal helical CT scan of a pediatric patient results in a risk of a fatal cancer later in life of approximately one in a thousand.<sup>265</sup>

A very small risk of radiation carcinogenesis from a CT scan may seem trivial, especially to the radiation oncologist who typically delivers more than 10 times that dose to a patient each day (albeit not to the whole body). Nevertheless, the finding of a radiation-induced excess cancer risk associated with a medical imaging procedure whose use has skyrocketed over the past 35 years<sup>265</sup> has the makings of a public health issue. Currently, over 70 million CT scans are performed annually in the United States.<sup>265</sup> That, disproportionately, this increase in CT scanning has been in a pediatric population both inherently more sensitive to ionizing radiation and with the longest lifespan in which to express those radiation-induced malignancies is all that much more concerning.

Because of this, radiation oncologists, as de facto experts on the health and medical effects of ionizing radiation, should be willing to serve as educators of the public as to both the benefits and risks associated with the common procedures that they employ.

### Early and Late Effects Following Radiotherapy

It is not the intent of this section to provide an exhaustive review of the various histopathological changes observed in the irradiated normal tissues of radiation therapy patients; the reader is referred to several textbooks and pertinent review articles on the subject (e.g., Rubin and Casarett,<sup>228</sup> Mettler and Upton,<sup>255</sup> and Fajardo<sup>270</sup>). This section will focus instead on more recent developments that promise to increase our understanding of the etiology of normal tissue injury and, hopefully, provide clues as to how to decrease or even prevent their occurrence.

**Cytokines, reactive oxygen species, and inflammation.** As mentioned previously, the early and late effects that occur in irradiated normal tissues result directly or indirectly from the killing of critical target cells. Although this statement is true in a general sense, it is clearly a gross oversimplification of what is now known to be a highly complex and dynamic process of signaling cascades, radiation-induced gene expression, cell death (by any of several possible mechanisms), and compensatory proliferative responses. Cytokines, chemokines, and growth factors, inducible proteins released by irradiated cells that stimulate



other cells to produce a biological response, participate in many of these processes. Although produced locally within the irradiated volume and chiefly intended to influence the behavior of cells in the local microenvironment, some cytokines do enter the circulation and can mobilize cells distant from the irradiated site. In addition to cytokines, another important player in an irradiated tissue's microenvironment and that also contributes to the development of the complication, is persistent, sometimes cyclic, oxidative stress and inflammation that, after the initial radiation insult, can become self-perpetuating.<sup>271</sup>

By way of example, lung irradiation causes the release of, among others, cytokines transforming growth factor  $\beta$  (TGF- $\beta$ ), basic fibroblast growth factor (bFGF), and interleukin-6 (IL-6), all of which participate in the etiology of radiation pneumonitis and fibrosis. Of these, TGF- $\beta$ 's role in promoting lung fibrosis is perhaps the best understood, as is its potential to serve as an early biomarker of radiation-induced lung injury.<sup>272</sup> It drives fibrosis development by affecting the survival, proliferation, differentiation, and extracellular matrix production by fibroblasts, while at the same time producing reactive oxygen species that further contribute to oxidative stress and inflammation in the tissue's microenvironment.<sup>271,273</sup>

**Functional subunits and volume effects.** Radiation oncologists traditionally reduce the total dose when the irradiation field involves a large volume of normal tissue. Although this practice evolved empirically, the biological basis for decreasing normal tissue tolerance with increasing irradiation volume remains unclear. Withers<sup>240,274</sup> proposed a descriptive model for the pathogenesis of radiation injury in normal tissues based on the structural and functional organization of the tissue at risk for a complication. Conceptually, tissues are considered to be organized into functional subunits (FSUs), which can be inactivated by radiation exposure secondary to the killing of their constituent target cell(s). These FSUs may be anatomically defined, such as an alveolar sac of the lung, a nephron of the kidney, or lobule of the liver, or anatomically undefined (skin, gut, nervous system).<sup>28</sup> The main difference between the two is that surviving cells from surrounding FSUs can migrate and help repopulate anatomically undefined FSUs but not anatomically defined ones, presumably due to the lack of any structural demarcation. This could have the net effect of making anatomically undefined FSUs able to tolerate higher radiation doses.

Whether the inactivation of one or more FSUs impacts the overall tissue function (in the form of a radiation-induced complication) depends on how many of the tissue's FSUs are in the irradiation field and their spatial arrangement. The spinal cord responds to changing irradiation volume as if its corresponding FSUs are arranged "in series." There is a steep reduction in the tolerance dose for white matter necrosis of the rat spinal cord with increasing treatment volume for small radiation fields (up to about 2 cm exposed cord length), but little or no volume dependence for larger treatment fields, presumably because inactivation of one FSU inactivates the entire cord.<sup>141</sup> The lung, on the other hand, seems to have a large functional reserve; it is only when much larger volumes are irradiated, and correspondingly large numbers of FSUs inactivated, that a functional deficit develops. This is more in keeping with a tissue whose functional subunits operate relatively independently and are arranged "in parallel." Some other organs are believed to behave as if they have both serial and parallel components.

One immediate clinical implication for tissues with parallel versus serially arranged FSUs is that a small dosimetric hotspot would be relatively innocuous for a parallel tissue but potentially catastrophic for a serial tissue.

**Reirradiation tolerance.** A common problem that radiation oncologists face is whether or not to risk reirradiation of a previously treated site. If a decision is made to retreat, even in the most ideal case in which

the previous treatment course is well documented and the treatment fields still identifiable, the clinician is nevertheless left with the uncertainty of what time, dose, and fractionation pattern to use.

Radiobiology research in this area has been slow in coming (given the very nature of studies involving late effects), but some progress has been made and some of the factors thought to be important in normal tissue tolerance to retreatment have been identified. These include whether the initial treatment course was to "full tolerance" or not, the likelihood that residual damage from the first treatment course has persisted, the amount of time that has elapsed between the first course and the second, the target volume to be reirradiated compared to the original target volume, and the structural and functional makeup of the tissue at risk.

A few general concepts are beginning to emerge from studies with laboratory rodents (for reviews, see Thames and Hendry,<sup>275</sup> Travis and Terry,<sup>276</sup> and Joiner and van der Kogel<sup>141</sup>):

1. For rapidly proliferating tissues such as skin, bone marrow, or testis, recovery following the first course of treatment is rapid such that the tissue can be reirradiated to near the full tolerance dose within about 2 to 3 months. However, it must be borne in mind that these tissues do not exist in isolation; thus, damage to nearby tissues that they depend on could affect tolerance.
2. Some slowly proliferating tissues, such as spinal cord and lung, are capable of long-term recovery after the first course of treatment and can be retreated to a partial (25%–70%) tolerance dose, with the dose generally increasing the longer the time between the two treatments (3–6 months minimum).
3. Other slowly dividing tissues, such as bladder, seem to show permanent residual injury from the first treatment such that the total dose for a second course must be reduced by at least half regardless of how much time has elapsed between treatments. In addition, there is evidence that complications arising from retreatment tend to occur much earlier (relative to the second treatment) than they would have from a single treatment.
4. One apparent exception to this type of classification system is the kidney, for which retreatment tolerance decreases with time between the first and second treatment courses.

A model that is consistent with these observations suggests that target cells that survive the initial treatment course have three possible fates. Some may regenerate their numbers over time, making the tissue as a whole better able to tolerate a second treatment, with the rate of regeneration determining how much time should elapse between the two treatments and what total dose can be delivered safely during the second course. Other target cells may maintain a steady-state number of survivors after the first treatment; therefore, the tissue would appear to harbor "residual damage" and never be able to tolerate a full second course of radiation therapy. Finally, some target cells may undergo continued depletion after the first treatment such that tolerance to a second treatment course will actually decrease the longer the time between treatments. This may be related to a progressive expression of otherwise subclinical residual damage from the initial treatment.

**Radiation-induced second malignancies.** With increasing numbers of long-term cancer survivors, the risk of second malignancies arising as a consequence of prior treatment becomes significant. Leukemia is thought to account for about 20% of second malignancies, with the remainder usually presenting as solid tumors in and around the previously irradiated site.<sup>277,278</sup> Certain subpopulations of previously treated patients are at an even higher risk than the majority and deserve special attention, including children and young adults, those with a known genetic predisposition to cancer, immunocompromised individuals, and those with known exposure to other carcinogens (including chemotherapy).

For example, large epidemiological studies have assessed the breast and lung cancer risk in Hodgkin lymphoma survivors,<sup>279,280</sup> leukemia and sarcomas in cervical cancer survivors,<sup>281</sup> and sarcomas in long-term survivors of childhood retinoblastoma.<sup>282</sup>

### Dose Rate and Dose Fractionation Effects

While the sparing effects of fractionated, external beam radiotherapy and brachytherapy are assumed to be a result of the repair of SLD, other factors may be involved as well, most notably, repopulation. In the isoeffect relationship derived by Strandqvist,<sup>24</sup> however, the “time factor” included both the effects of dose fractionation (presumably, the result of SLDR) and overall treatment time (presumably, repopulation). It was not until 1963 that Fowler and colleagues<sup>91,132,283</sup> attempted to separate the contributions of these two factors by performing fractionation experiments with pig skin. In their experiments, 5 equal dose fractions were given in overall treatment times of either 4 or 28 days. In changing from an overall time of 4 days to 28 days, an additional 6 Gy was required to reach the same level of skin response. This was thought to reflect the contribution of overall time (i.e., repopulation) to the isoeffect total dose since the size and number of fractions were kept constant. In a parallel series of experiments in which the overall time was kept constant (28 days) but the number of fractions was increased from 5 to 21, it was found that an additional 13 Gy was required to reach the skin isoeffect level. This increase was almost as great as the 16-Gy additional dose required when changing from a single-dose treatment to a treatment protocol of 5 fractions in 4 days, implying that the change in fraction number was more important than the change in the overall treatment time.

During the 1960s and 1970s, dose rate effects were studied extensively. The clinical community was also becoming more attuned to the biological underpinnings of radiation therapy, especially the “Four Rs of Radiotherapy”: repair, reoxygenation, redistribution, and repopulation.<sup>284</sup> These are considered key radiobiological phenomena that influence the outcome of multifraction radiotherapy. (In later years, a fifth R was added, radiosensitivity.<sup>285</sup>)

Bedford and Hall<sup>286,287</sup> generated *in vitro* survival curves for HeLa cells irradiated at various dose rates between about 0.1 Gy per hour and 7.3 Gy per minute. The killing effectiveness per unit dose decreased as the dose rate was reduced; however, a limit to this dose rate or dose fractionation effect was reached under conditions in which cell cycle and proliferative effects were eliminated by the use of lower temperatures<sup>288</sup> or by growing cells to plateau phase prior to irradiation<sup>289–291</sup> (Fig. 1.26).

Similar conclusions about the nature of dose rate and dose fractionation effects were reached from clinical studies. Dutreix et al.<sup>292</sup> studied dose fractionation effects in human skin under conditions in which cell cycle and proliferative effects were minimized (i.e., short interfraction intervals and overall treatment times). Their data indicated that the incremental dose recovered due to SLDR when a single dose was replaced by two equal fractions became very small when the size of the dose per fraction dropped below approximately 2 Gy (Table 1.4). This finding is consistent with the hypothesis that survival curves have negative (rather than zero) initial slopes and, therefore, that a limit to the repair-dependent dose fractionation effect should be reached for increasingly smaller-sized dose fractions or dose rates. Accordingly, these authors cautioned that isoeffect equations in common clinical use at the time (the NSD model—see discussion to come) would be inaccurate for predicting tolerances when doses per fraction were quite small. Further, small differences in the initial slopes of survival curves for different cell types could be magnified into large differences in the limiting slopes for continuous or multifraction survival curves.

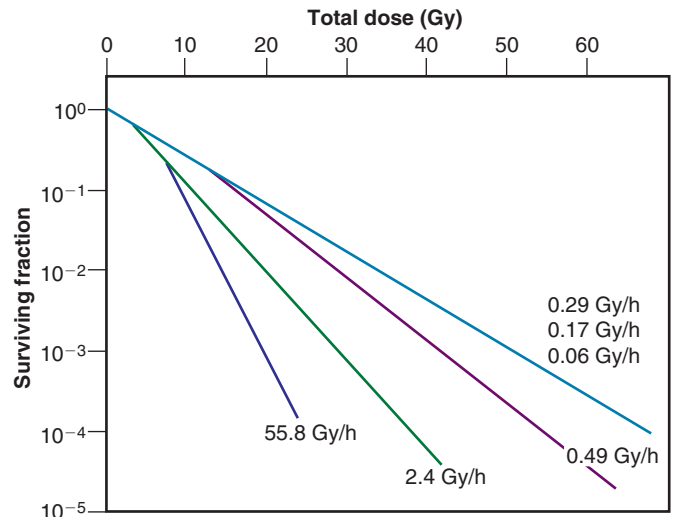


**Fig. 1.26** The dose rate effect for nonproliferating C3H 10T1/2 mouse cells maintained *in vitro*. As the dose rate decreases from about 56 to 0.3 Gy/h, survival curves become progressively shallower, reflecting the repair of radiation damage during the continuous irradiation interval. However, for dose rates less than about 0.3 Gy/h, no further sparing effect of dose protraction is observed, suggesting that there is an effective limit to the repair-dependent dose rate effect. This is considered compelling evidence that cell survival curves have nonzero initial slopes. (Modified from Wells R, Bedford J. Dose-rate effects in mammalian cells. IV. Repairable and nonrepairable damage in non-cycling C3H 10T1/2 cells. *Radiat Res.* 1983;94:105.)

**TABLE 1.4 “Recovered Dose” as a Function of Dose per Fraction for Skin Reactions in Human Radiotherapy Patients**

Single Dose ( $D_s$ )	Split Dose ( $2 D_i$ ) <sup>a</sup>	Recovered Dose ( $D_r = 2D_i - D_s$ )
15 Gy	$2 \times 8.5$ Gy	2 Gy
13 Gy	$2 \times 7.5$ Gy	2 Gy
8 Gy	$2 \times 5.5$ Gy	3 Gy
6 Gy	$2 \times 4$ Gy	2 Gy
3.5 Gy	$2 \times 2$ Gy	$\leq 0.5$ Gy

<sup>a</sup>Interfraction interval (i) was 6 h.

Data from Dutreix J, Wambersie A, Bounik C. Cellular recovery in human skin reactions: application to dose fraction number overall time relationship in radiotherapy. *Eur J Cancer.* 1973;9:159–167.

### Time-Dose-Fractionation Relationships

#### The NSD Model

Based on Strandqvist’s isoeffect curves,<sup>24</sup> Fowler and Stern’s pig skin experiments,<sup>91,283</sup> and other laboratory and clinical findings,<sup>23</sup> Ellis<sup>293,294</sup> formulated the NSD concept in 1969. The NSD equation,

$$D = (\text{NSD}) N^{0.24} T^{0.11}$$

where  $D$  is the total dose delivered,  $N$  the number of fractions used,  $T$  the overall treatment time, and NSD the nominal standard dose (a proportionality constant thought to be related to the tolerance of the tissue being irradiated), became widely used for the design of biologically equivalent treatment schedules, particularly when its more mathematically

convenient derivatives, such as the TDF<sup>295</sup> or CRE<sup>296</sup> equations became available.

The introduction of the NSD equation theoretically allowed radiotherapy prescriptions worldwide to be compared and contrasted with respect to “biological equivalence.” It also permitted the calculation of dose equivalents for split-course treatments and brachytherapy, and provided a means of revising treatment prescriptions in the event of unforeseen treatment interruptions. Because the NSD formula was based on observations of early-onset radiation effects, it was quite useful as a predictor of some tissue tolerances, as long as it was not used for treatments involving extremes of fraction number or overall time.

On the other hand, the NSD formula was ill equipped to deal with some clinical problems, particularly the prediction of late effects in normal tissues (especially at nonstandard doses per fraction) and the patterns of repopulation in normal tissues and tumors.<sup>243</sup> The use of a fixed exponent for the overall time component, T, gave the false impression that an extra dose to counteract proliferation would be needed from the outset of treatment, rather than after a delay of several weeks, which is what is observed in practice (e.g., Denekamp<sup>297</sup>).

In light of the growing frustration with the NSD model and research at the time focusing on the shape of the shoulder region of cell survival curves and the nature of dose rate and dose fractionation effects, new radiobiology-based approaches to isoeffect modeling were developed during the late 1970s and early 1980s.

### The Linear-Quadratic Isoeffect Model

In ambitious multifraction experiments using mice in which a broad range of fraction sizes and interfraction intervals was used, Douglas and Fowler<sup>298</sup> developed a novel method of data analysis in which they assumed that their resulting isoeffect curves for skin damage in the mouse foot were a reflection of the shape of the underlying tissue dose-response curve for the effect. The shape of this dose-response curve was assumed to be linear-quadratic, effectively “repurposing” the cell survival curve expression for in vivo use. Because overall treatment times were kept quite short, proliferative effects were assumed to be negligible, such that inherent radiosensitivity and repair were the main factors governing the tissue’s response.

The underlying dose-response curves were deduced by plotting  $1/D$ , where  $D$  was the total dose delivered ( $D = n \times d$ ), as a function of  $d$ , the dose per fraction. This was termed a *reciprocal dose plot* and was used to derive values for the  $\alpha/\beta$  ratio, a novel metric proposed to express a tissue’s fractionation sensitivity.<sup>298</sup> A representative reciprocal dose plot is shown in Fig. 1.27.

This new approach to isoeffect analysis, in which attention was focused on repair parameters and dose-response curve shapes, emphasized that the critical parameter in radiotherapy is the size of the dose per fraction, more so than the overall treatment time. During the course of experimental and clinical fractionation studies, it became clear that there was a systematic difference between early- and late-responding normal tissues and tumors in their responses to different fractionation patterns. Isoeffect curves for the slowly or nonproliferating normal tissues—kidney and spinal cord, for example—are steeper in general than those for more rapidly proliferating, early-responding tissues, such as skin and gut epithelium and, significantly, most tumors (Fig. 1.28).<sup>299,300</sup> A steep isoeffect curve implies that late effects were more sensitive to changes in the size of the dose per fraction, experiencing greater sparing with decreasing fraction size than their early-effects counterparts (Fig. 1.29). This difference is also reflected in the  $\alpha/\beta$  ratios derived for these tissues, which are usually low for late-responding tissues (on the order of 1–6 Gy, with an average of about 3 Gy), and high for early-responding tissues and tumors (typically 7–20 Gy, with an average of about 10 Gy; Tables 1.5 and 1.6). There are exceptions, however.

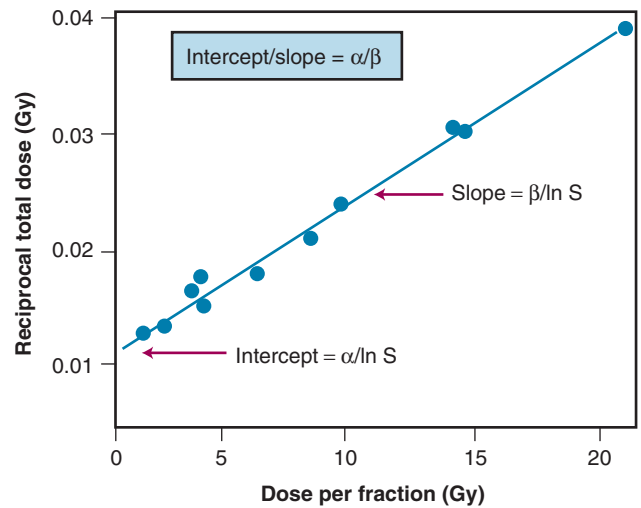


**Fig. 1.27** The reciprocal dose or “Fe” plot technique of Douglas and Fowler,<sup>298</sup> used to determine a normal tissue or tumor’s  $\alpha/\beta$  ratio. Using this method, the reciprocal of the total dose necessary to reach a given isoeffect is plotted as a function of the dose per fraction. Assuming that the killing of target cells responsible for the tissue effect can be modeled using the linear-quadratic expression,  $S = e^{-(\alpha D + \beta D^2)}$ , the  $\alpha/\beta$  ratio can be obtained from the ratio of the isoeffect curve’s intercept:slope. See text for details. (Modified from Douglas B, Fowler J. The effect of multiple small doses of x rays on skin reactions in the mouse and a basic interpretation. *Radiat Res.* 1976;66:401.)

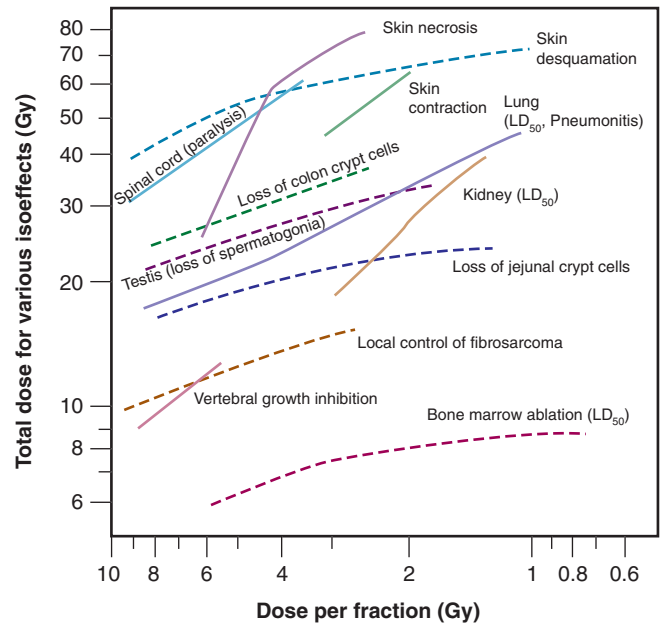


**Fig. 1.28** Isoeffect curves in which the total dose necessary to produce a certain normal tissue or tumor endpoint (as indicated) is plotted as a function of the dose per fraction under conditions in which cell proliferation is negligible. Isoeffect curves for late-responding normal tissues (*solid lines*) tend to be steeper than those for early-responding normal tissues and tumors (*dashed lines*). This suggests that, for the same total dose, late reactions may be spared by decreasing the size of the dose per fraction used. It also follows that by using smaller-sized dose fractions, a somewhat higher total dose could be given for the same probability of a late reaction but, hopefully, with a higher tumor control probability. (Modified from Withers H, Thames H, Peters L, et al. Normal tissue radioresistance in clinical radiotherapy. In: Withers H, Thames H, Peters L, eds. *Biological Basis and Clinical Implications of Tumor Radioresistance*. New York: Masson; 1983:139.)

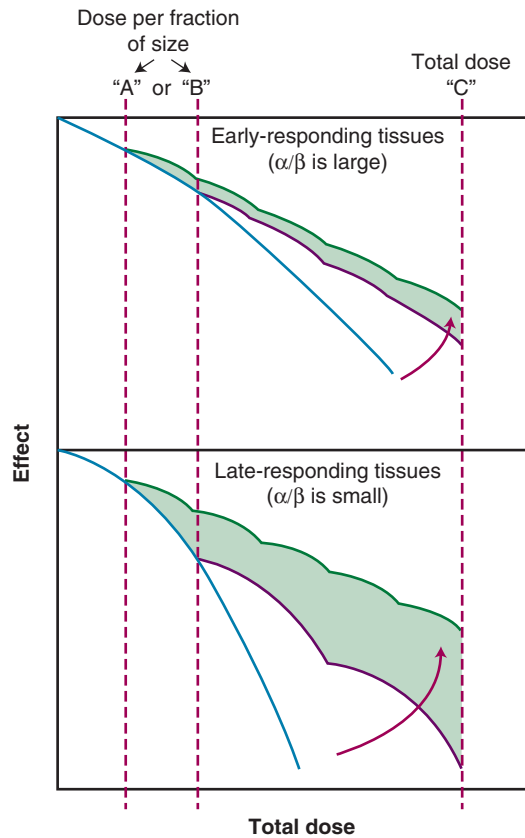


**Fig. 1.29** Hypothetical dose response curves for either an acute (*top*) or late (*bottom*) effect in an irradiated normal tissue, depending on whether the total dose “C” is delivered using dose fractions of size “A” or “B.” Because of the difference in the initial slopes of the corresponding single-dose survival curves for these cell types, reducing the fraction size from “B” to “A” preferentially spares late-responding normal tissues (*shaded areas*). (Modified from Withers H, Thames H, Peters L. Differences in the fractionation response of acutely responding and late-responding tissues. In: Karcher K, Kogelnik H, Reinartz G, eds. *Progress in Radio-Oncology II*, New York: Raven Press; 1982:287.)

### Clinical Applications of the Linear-Quadratic Isoeffect Model

The shapes of tissue and tumor isoeffect curves and their calculated  $\alpha/\beta$  ratios have a number of clinical applications. It is possible using  $\alpha/\beta$  ratios to equate treatment schedules employing different-sized doses per fraction in order to match the probability of causing a tissue injury, assuming that the overall treatment times are similar in both schedules or the tissue at risk of a complication is relatively insensitive to treatment duration.<sup>249</sup> The equation

$$D_2/D_1 = (\alpha/\beta + d_1)/(\alpha/\beta + d_2)$$

can be used for this purpose, where  $D_1$  and  $d_1$  are, respectively, the total dose and dose per fraction (in Gy) of one radiotherapy treatment plan,  $D_2$  and  $d_2$  are the total dose and dose per fraction for an alternate treatment plan designed to be biologically equivalent for a particular tissue effect, and with the fractionation sensitivity of that tissue defined by its unique  $\alpha/\beta$  ratio. Of course, avoiding a normal tissue complication is not the sole criterion used in treatment planning; in considering a particular time, dose, and fraction size combination, the responses of the tumor and all incidentally irradiated normal tissues should be taken into account simultaneously.

**TABLE 1.5 Representative  $\alpha/\beta$  Ratios for Human Normal Tissues and Tumors**

Tissue Type (and Endpoint)	$\alpha/\beta$ Ratio ( $\pm 95\%$ Confidence Interval)
<b>Early-Responding Normal Tissues</b>	
Skin: erythema	10.6 (1.8; 22.8) Gy
Desquamation	11.2 (8.5; 17.6) Gy
Lung: pneumonitis $\leq 90$ days after radiotherapy	$> 8.8$ Gy
Oral Mucosa: mucositis	8–15 Gy
<b>Late-Responding Normal Tissues</b>	
Skin: telangiectasia	$\sim 2.7$ (–0.1; 8.1) Gy
Fibrosis	1.7 (0.6; 3.0) Gy
Breast: cosmesis	3.4 (2.3; 4.5) Gy
Fibrosis	3.1 (1.8; 4.4) Gy
Lung: pneumonitis $> 90$ days after radiotherapy	4.0 (2.2; 5.8) Gy
Fibrosis	3.1 (–0.2; 8.5) Gy
Bowel: perforation/stricture	3.9 (2.5; 5.3) Gy
Various other	4.3 (2.2; 9.6) Gy
Spinal cord: myelopathy	$< 3.3$ Gy
Muscle, vasculature or cartilage: impaired movement	3.5 (0.7; 6.2) Gy
Nerve: brachial plexopathy	2.0–3.5 Gy
Optic neuropathy	1.6 (–7; 10) Gy
Head and neck: various	3.5–4 Gy
<b>Tumors</b>	
Head and neck: nasopharynx	16 (–11; 43) Gy
Vocal cord	$\sim 13$ Gy
Buccal mucosa	$\sim 6.6$ (2.9; $\infty$ ) Gy
Tonsil	7.2 (3.6; $\infty$ ) Gy
Larynx	14.5 (4.9; 24) Gy
Lung: squamous cell carcinoma	$\sim 50$ –90 Gy
Cervix: squamous cell carcinoma	$> 13.9$ Gy
Skin: squamous cell carcinoma	8.5 (4.5; 11.3) Gy
Melanoma	0.6 (–1.1; 2.5) Gy
Prostate	1.1 (–3.3; 5.6) Gy
Breast (early-stage invasive ductal, lobular, and mixed)	4.6 (1.1; 8.1) Gy
Esophagus	4.9 (1.5; 17) Gy
Liposarcoma	0.4 (–1.4; 5.4) Gy

Data from Joiner M, van der Kogel A. *Basic Clinical Radiobiology*. 4th ed. London: Hodder Arnold; 2009.

An important implication of the steeper isoeffect curves for late-responding tissues compared to those for tumors is that it might be possible to increase the therapeutic ratio by using larger numbers of smaller fractions to a somewhat higher total dose than traditionally used.<sup>248,249,301</sup> Although such treatments could exacerbate acute effects in normal tissues, late effects would be spared preferentially and tumor control could be improved, thereby increasing the therapeutic ratio. The use of multiple fractions per day of smaller than conventional size (less than about 1.6 Gy) but to a somewhat higher total dose, with little or no change in overall treatment time, is called *hyperfractionation*.



TABLE 1.6 Summary of the Linear-Quadratic Isoeffect Model Parameters and Concepts

Tissue Type	$\alpha/\beta$ Ratio <sup>a</sup>	Dose-Response Curve Shape <sup>b</sup>	Isoeffect Curve Shape <sup>c</sup>
Early-responding normal tissues and most tumors	High (6–30 Gy)	Steep initial slope ( $\alpha$ is large)	Shallow
Late-responding normal tissues	Low (1–6 Gy)	Shallow initial slope ( $\alpha$ is small)	Steep

<sup>a</sup>Determined from the reciprocal dose plot technique of Douglas and Fowler.<sup>298</sup>

<sup>b</sup>Based on the assumption that differences in the calculated  $\alpha/\beta$  ratio are usually caused by differences in the  $\alpha$  component.

<sup>c</sup>Using the Thames et al.<sup>299</sup> isoeffect curve plot (see Fig. 1.28).

With particularly aggressive tumors that proliferate rapidly, multiple treatments per day might also be useful in order to decrease the overall treatment time, thereby allowing less time for repopulation of clonogenic tumor cells.<sup>302,303</sup> Treatment with multiple daily fractions of approximately standard size and number (and to about the same total dose), but in shorter overall times, is termed *accelerated fractionation*. In practice, however, a combination of accelerated and hyperfractionated treatment is often used, as purely accelerated treatment tends to be poorly tolerated.<sup>275</sup> Finally, *hypofractionation*, the use of one or a few large dose fractions delivered over short periods of time—for example, stereotactic radiosurgery (SRS), stereotactic body radiation therapy (SBRT), or intraoperative radiation therapy (IORT)—is also an option. Indications for such include cases in which the frank ablation of a small primary tumor or metastasis is the goal or in the relatively unusual circumstance in which the tumor is suspected of having a low, rather than high,  $\alpha/\beta$  ratio. Prostate cancer and melanoma are tumor types that meets these criteria, as does, to a lesser extent, breast cancer. It is clear that hypofractionation has been quite successful for the treatment of multiple types of (small) tumors, while at the same time causing no worse normal tissue complications.<sup>304–306</sup> However, the biological underpinnings associated with its use remain poorly defined and the subject of considerable controversy.<sup>307–310</sup> Regardless, today's use of hypofractionation would not be possible were it not for innovations in physics and imaging that now allow nearly all normal tissue to be excluded from the radiation field because, otherwise, complications in late-responding normal tissues would be dose limiting. This was amply demonstrated during the early days of radiotherapy.

The decision to opt for one of these fractionation protocols would depend not only on the  $\alpha/\beta$  ratios for the tissues being irradiated but also on their relative repair rates and proliferative responses before, during, and after exposure. At present, while  $\alpha/\beta$  ratios for human normal tissues and tumors are fairly well characterized, data on proliferative behavior and repair rates, especially for tumors, are less robust.<sup>243,303</sup>

With “non-standard” fractionation now the standard, radiation oncologists find themselves confronted with the same problem faced by their 1930s counterparts, that is, how to compare and contrast different treatment schedules for presumptive isoeffectiveness. The “biologically effective dose,” or BED method,<sup>250,311</sup> another derivative of the LQ model, attempts to address this issue. Knowing that cell survival and dose-response curves have negative initial slopes and that, for a sufficiently low dose per fraction or dose rate, a limit to the repair-dependent dose fractionation effect occurs that “traces” this initial slope, this question may be asked: “In the limit, for an infinite number of infinitely small dose fractions, what total radiation dose will correspond to normal tissue tolerance, tumor control, or any other endpoint of interest?” Clearly, this theoretical dose will be quite large for a tissue characterized by a dose-response curve with a shallow initial slope (like many late-responding normal tissues) and appreciably smaller for a tissue characterized by a dose-response curve with a steep initial slope (like most tumors and early-responding normal tissues). It is also important to bear in mind that BEDs are not real doses but rather extrapolates based on the

$\alpha/\beta$  ratios for the tissues at risk. For this reason, the units used to describe these extrapolated doses are, for example, Gy<sub>3</sub> and Gy<sub>10</sub> rather than Gy, in which the subscripts 3 and 10 refer to the assumed  $\alpha/\beta$  ratio of the tissue at risk. A second caveat is that, while two different radiotherapy treatment schedules can be compared qualitatively on the basis of their respective Gy<sub>3</sub> or Gy<sub>10</sub> doses, Gy<sub>3</sub> and Gy<sub>10</sub> cannot be intercompared.

A mathematical rearrangement of the linear-quadratic expression  $S = e^{-(\alpha D + \beta D^2)}$  yields

$$BED = E/\alpha = nd(1 + d/\alpha/\beta)$$

where E is the (iso)effect being measured (E is divided by  $\alpha$  to obtain the BED value in units of dose), n is the number of fractions, d is the dose per fraction, and the  $\alpha/\beta$  ratio is specific for the tissue being irradiated. The factor  $(1 + d/\alpha/\beta)$  has been called the *relative effectiveness term* because, in essence, it is a correction for the fact that treatment is not really given as an infinite number of infinitely small dose fractions but rather as a finite number of fractions of a finite size.

Perhaps the best way to illustrate the use of the BED equation is by example. Suppose that a radiation oncologist is developing a clinical protocol in head and neck cancer comparing standard fractionation (30 fractions of 2 Gy to a total dose of 60 Gy in an overall treatment time of about 6 weeks) to a schedule of 50 fractions of 1.4 Gy to a total dose of 70 Gy in approximately the same overall treatment time. The tissues of most concern for radiation injury are the tumor, the oral mucosa, and the spinal cord, that is, two early-responding tissues and one late-responding tissue. Finally, assume that an  $\alpha/\beta$  ratio of 10 Gy is appropriate for the tumor and oral mucosa and an  $\alpha/\beta$  ratio of 3 Gy is appropriate for the spinal cord. For calculation purposes, an  $\alpha/\beta$  ratio of 10 Gy can be used for most early-responding normal tissues and tumors and 3 Gy for most late-responding normal tissues unless more robust, better vetted values are available. For example, an  $\alpha/\beta$  ratio of 4 Gy may be more appropriate for breast cancer; 20 Gy for non-small cell lung cancer; approximately 2 Gy for CNS, kidney, and prostate cancer; and approximately 0.6 Gy for melanoma.<sup>247</sup>

For the standard fractionation schedule, therefore:

For tumor and mucosa:

$$E/\alpha = 60 \text{ Gy} (1 + 2 \text{ Gy}/10 \text{ Gy}) = 72 \text{ Gy}_{10}$$

For the spinal cord:

$$E/\alpha = 60 \text{ Gy} (1 + 2 \text{ Gy}/3 \text{ Gy}) = 100 \text{ Gy}_3$$

For the more highly fractionated schedule (rounded off to the nearest whole number):

For tumor and mucosa:

$$E/\alpha = 70 \text{ Gy} (1 + 1.4 \text{ Gy}/10 \text{ Gy}) = 80 \text{ Gy}_{10}$$



**TABLE 1.7 Current Status of Existing and Proposed Parameters of the Linear-Quadratic Isoeffect Model for Human Normal Tissues and Tumors**

Parameter	Property Governed	AVAILABILITY OF DATA WITH RESPECT TO		
		Early Effects	Late Effects	Tumors
$\alpha/\beta$ Ratio	Fractionation sensitivity	Can assume 10 Gy for most	Can assume 3 Gy for most	Can assume 10 Gy for most
$T_{1/2}$ (repair half-time)	Repair kinetics	Poor/fair	Poor	None/poor
$T_p$ (effective clonogen doubling time) and/or $T_k$ ("kickoff" time—time proliferation begins relative to the start of treatment)	Dose lost to accelerated proliferation during radiotherapy	Fair	Poor/NA	Poor/fair
Volume effect	Variation in tissue tolerance with increasing target volume	Poor	Poor	None/poor
$\gamma$ (normalized dose-response gradient)	Steepness of dose-response curve for effect; can be used to estimate the normal tissue complication probability	Fair	Fair	Fair

Modified from Bentzen SM. Estimation of radiobiological parameters from clinical data. In: Hagen U, Jung H, Streffer C, eds. *Radiation Research 1895-1995*. Volume 2, Congress Lectures. Würzburg: Universitätsdruckerei H. Sturtz AG; 1995:833-838.

For the spinal cord:

$$E/\alpha = 70 \text{ Gy} (1 + 1.4 \text{ Gy}/3 \text{ Gy}) = 103 \text{ Gy}_3$$

Although little quantitative information can be gleaned from this exercise, a few qualitative statements can be made. First, a comparison of the  $Gy_{10}$  values for the two treatment schedules suggests that the more highly fractionated schedule should result in somewhat better tumor control, albeit at the expense of more vigorous mucosal reactions (i.e., 72  $Gy_{10}$  compared with 80  $Gy_{10}$ , an 11% increase in "biodose"). However, the comparison of the  $Gy_3$  values for the two schedules suggests that the spinal cord tolerance would be essentially unchanged (i.e., 100  $Gy_3$  compared to 103  $Gy_3$ , a 3% increase).

Even with the BED concept being only semi-quantitative at best, its use for treatment planning purposes over the past 3 decades has provided a wealth of clinical data that has allowed a better definition of what is or is not tolerable for particular normal tissues in terms of  $Gy_3$  or  $Gy_{10}$ . Using head and neck cancer as an example, Fowler et al.<sup>247,312,313</sup> have suggested that the tolerance dose for acute mucosal reactions is in the range of 59 to 63  $Gy_{10}$  and for late reactions in the range of 110 to 117  $Gy_3$ .

It would be remiss to conclude any discussion of the LQ isoeffect model, or any biologically based model with potential clinical application, without a few words of warning. First, this model, although certainly more robust than the NSD model and much better grounded in biological principles, is still a theoretical model. Some limitations of the basic model are obvious: an overly simplistic assumption that an isoeffect in a tissue corresponds to an isosurvival of a particular cell type; no provision for the influence of cell cycle, proliferative or microenvironmental effects in the overall dose-response relationship; no way to account for differences in repair rates between different tissues; no consideration of volume effects; uncertainty surrounding the model's applicability for extremes of fractionation; and a limited understanding of how to apply the model in patients receiving multimodality therapy.

Various add-ons to the LQ model have been proposed,<sup>314-316</sup> especially with respect to compensating for tumor cell repopulation and correcting for differing tissue repair rates when multiple fractions per day or

brachytherapy are used. However, the lack of robust values at present for the parameters introduced in such calculations (e.g., potential doubling times, repopulation "kick-off" times, and half-times for repair) can limit their usefulness. The current status of some of the existing and proposed parameters of the LQ model for human tumors and normal tissues is summarized in Table 1.7.

## RADIATION BIOLOGY IN THE 21ST CENTURY

Since the mid-1980s, most graduate students pursuing careers in oncology necessarily trained as molecular, cellular, or tumor biologists and not as radiation biologists per se, although some may have worked with ionizing radiation as a tool for probing fundamental cellular processes or as part of translational research designed to develop new cancer therapies. Even fewer have taken a formal course in radiation biology, let alone in its more clinical aspects. This shift in focus and training that effectively has blurred the line between "radiation biologist" and "cancer biologist" is part of the natural evolution of the oncologic sciences over the years and surely not an unexpected or unwarranted one. However, the fact remains that the field of radiation biology as a distinct entity, with its rich 120-year history that has made major contributions to fields as diverse as carcinogenesis, epidemiology, toxicology, DNA damage and repair, genetics and cytogenetics, cell cycle biology and radiation oncology, to name but a few, is threatened with extinction. In many respects, the extinction is in name only, as the radiation-related research enterprise continues regardless of the backgrounds of its investigators and how they self-identify. What is being lost, and at an increasingly rapid rate, is competent radiation biology educators. This is especially troubling, as there remains a need for all radiological science professionals to be at least reasonably well versed in the basic principles of radiation biology. Radiation oncologists, in particular, need to be familiar both with the foundational and modern aspects of the field and, since the events of September 11, 2001, a new mandate has emerged: the need to provide expertise in the basics of radiation biology and radiation protection to emergency responders, civic leaders, and the general public in the event of a radiological or nuclear terrorist attack.

From a research perspective, fundamental studies of genomic instability,<sup>317,318</sup> epigenetics,<sup>319,320</sup> and cell signaling as it applies to radiation response<sup>321,322</sup> continue to be active areas of investigation. Our growing understanding of the complex roles played by cytokines in the etiology of normal tissue complications following radiation exposure<sup>323,324</sup> promises to someday deliver novel, molecularly based radioprotectors that may benefit radiation accident victims, first responders during radiation emergencies, and astronauts on deep-space missions. Radiation scientists also have been important contributors to the fields of genomics and proteomics, functional and molecular imaging, and molecularly targeted cancer therapy, and to the search for tumor-specific biomarkers that can aid in cancer diagnosis, staging, and the monitoring of treatment progress.

In early 2018, a new agenda was proposed<sup>325</sup> that provides an ambitious roadmap for the next 10 to 20 years of radiation biology research. New priority areas for research include combining radiotherapy (especially hypofractionation) with immunotherapy; targeting DNA repair, cancer metabolism, tumor stem cells, and the tumor microenvironment; and developing novel high-throughput in vitro screening systems and animal models.

## CRITICAL REFERENCES

15. Regaud C, Ferroux R. Discordance des effets de rayons X, d'une part dans le testicule, par le peau, d'autre part dans la fractionnement de la dose. *C R Soc Biol*. 1927;97:431–434.
17. Coutard H. Roentgen therapy of epitheliomas of the tonsillar region, hypopharynx and larynx from 1920 to 1926. *Am J Roentgenol Radium Ther Nucl Med*. 1932;28:313–331.
27. Puck TT, Marcus PI. Action of X-rays on mammalian cells. *J Exp Med*. 1956;103:653–666.
78. Kellerer AM, Rossi HH. The theory of dual radiation action. *Curr Top Radiat Res Q*. 1972;8:85–158.
84. Till JE, McCulloch EA. A direct measurement of the radiation sensitivity of normal mouse bone marrow cells. *Radiat Res*. 1961;14:213–221.
94. Elkind MM, Sutton H. X-ray damage and recovery in mammalian cells. *Nature*. 1959;184:1293–11295.
105. Terasima T, Tolmach LJ. Changes in X-ray sensitivity of HeLa cells during the division cycle. *Nature*. 1961;190:1210–1211.
122. Barendsen GW. Responses of cultured cells, tumors and normal tissues to radiations of different linear energy transfer. *Curr Top Radiat Res Q*. 1968;4:293–356.
124. Thomlinson RH, Gray LH. The histological structure of some human lung cancers and the possible implications for radiotherapy. *Br J Cancer*. 1955;9:539–549.
125. Powers WE, Tolmach LJ. A multicomponent X-ray survival curve for mouse lymphosarcoma cells irradiated in vivo. *Nature*. 1963;197:710–711.
126. Moulder JE, Rockwell S. Hypoxic fractions of solid tumors: experimental techniques, methods of analysis and a survey of existing data. *Int J Radiat Oncol Biol Phys*. 1984;10:695–712.
134. Kallman RF. The phenomenon of reoxygenation and its implications for fractionated radiotherapy. *Radiology*. 1972;105:135–142.
135. Brown JM. Evidence for acutely hypoxic cells in mouse tumours, and a possible mechanism of reoxygenation. *Br J Radiol*. 1979;52:650–656.
136. Dewhirst MW. Relationships between cycling hypoxia, HIF-1, angiogenesis and oxidative stress. *Radiat Res*. 2009;172:653–665.
143. Gatenby RA, Kessler HB, Rosenblum JS, et al. Oxygen distribution in squamous cell carcinoma metastases and its relationship to outcome of radiation therapy. *Int J Radiat Oncol Biol Phys*. 1988;14:831–838.
178. Yuhas JM, Spellman JM, Culo F. The role of WR 2721 in radiotherapy and/or chemotherapy. In: Brady L, ed. *Radiation Sensitizers*. New York: Masson; 1980:303–308.
182. Brown JM. SR 4233 (tirapazamine): a new anticancer drug exploiting hypoxia in solid tumors. *Br J Cancer*. 1993;67:1163–1170.
245. Withers HR, Taylor JMG, Maciejewski B. The hazard of accelerated tumor clonogen repopulation during radiotherapy. *Acta Oncol*. 1988;27:131–146.
247. Fowler JF. 21 years of biologically effective dose. *Br J Radiol*. 2010;83:554–568.
274. Withers HR, Taylor JMG, Maciejewski B. Treatment volume and tissue tolerance. *Int J Radiat Oncol Biol Phys*. 1988;14:751.
284. Withers HR. The four R's of radiotherapy. In: Adler H, Lett JT, Zelle M, eds. *Advances in Radiation Biology*. Vol. 5. New York: Academic Press; 1975:241–271.
294. Ellis F. Dose, time and fractionation: a clinical hypothesis. *Clin Radiol*. 1969;20:1–8.
297. Denekamp J. Changes in the rate of proliferation in normal tissues after irradiation. In: Nygaard O, Adler HI, Sinclair WK, eds. *Radiation Research: Biomedical, Chemical and Physical Perspectives*. New York: Academic Press, Inc.; 1975:810–825.
299. Thames HD, Withers HR, Peters LJ, et al. Changes in early and late radiation responses with altered dose fractionation: implications for dose-survival relationships. *Int J Radiat Oncol Biol Phys*. 1982;8:219–226.
325. Kirsch DG, Diehn M, Kesarwala AH, et al. The future of radiobiology. *J Natl Cancer Inst*. 2018;110:329–340.

A complete reference list can be found online at [ExpertConsult.com](https://www.expertconsult.com).